Science of Climate Change

Volume 2.1
2022

https://scienceofclimatechange.org

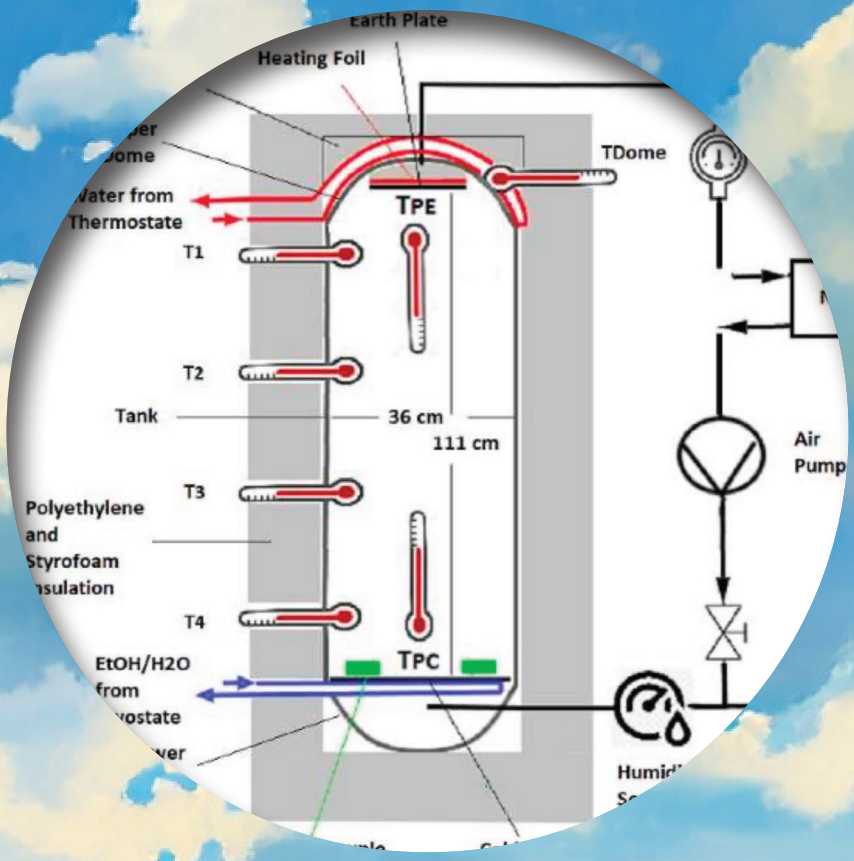

Published by: Klimarealistene (Org. no. 995 314 592)

ISSN 2703-9080 (print) ISNN 2703-9072 (online)

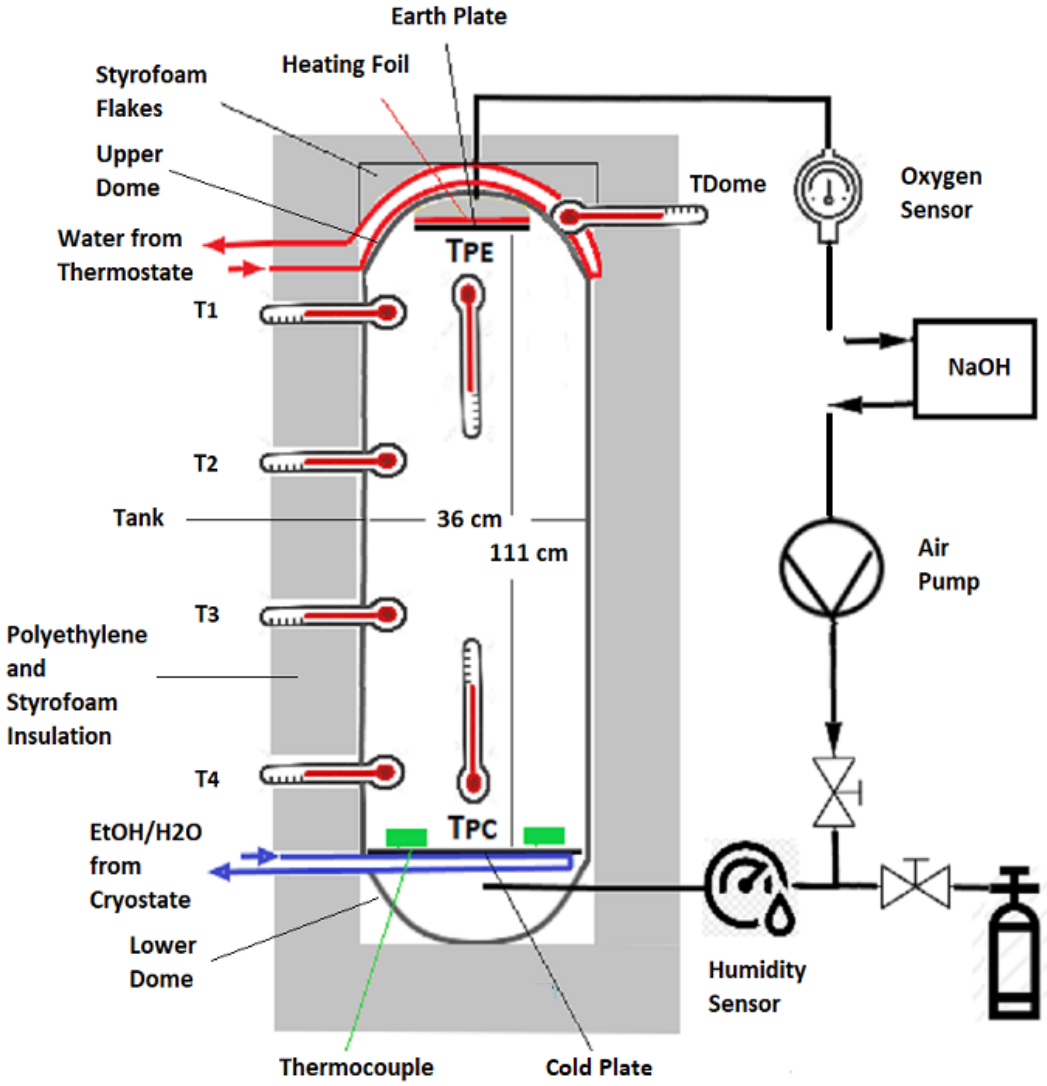

Schematics of a laboratory experiment to verify the greenhouse effect. Different from other similar experiments, no light source from visible to mid infrared is used. Instead the only radiation is from two plates: the warmer at the top and a cold at the bottom, to avoid convection.

From an article by Hermann Harde and Michael Schnell: *Verification of the Greenhouse Effect in the Laboratory.*

Figure 1, page 3.

SCIENCE OF CLIMATE CHANGE

Volume 2.1

March 2022

ISSN 2703-9072

Klimarealistene, P.O. Box 33, 3901 Porsgrunn, Norway

Table of Content

Editorial

Finally, we have been able to publish a volume with the Proceedings from the *Conference on Natural Variability and Tolerance,* held in Oslo 18-19 October 2019. The conference attracted 170 participants and was a joint effort between The Climate Realists in Norway, Sweden and Denmark. Chairman of the Organizing Committee was Morten Jødal, who also was chairman of the Norwegian Climate Realists. Jødal's main message was that the Earth's nature is resilient. Life is not dying. The number of species are growing. The polar bears and the Great Barrier Reef are doing fine in a warmer climate. And food production, using less area, is increasing more than the Earths population. Only limited by poor management.

Unfortunately, Morten Jødal died in September 2021, right after the first issue of this Journal was published and was not able to take care of the proceedings. That became my job. Luckily, we had filmed all the talks, so I was able to transcribe missing contributions from the recordings.

Finally, we have an article about a laboratory experiment which demonstrate warming due to back-radiation from greenhouse gases carbon dioxide, methane and nitrous oxide. It is shown that the effect is small and is confirmed by radiation transfer calculations. The authors conclude there is no climate emergency.

Good reading

Jan-Erik Solheim
Editor

A digital version of this volume can be found here: https://doi.org/10.53234/scc202308/14

SCC

Correspondence to harde@hsu-hh.de

Vol. 2.1 (2022)

pp. 1-33

Verification of the Greenhouse Effect in the Laboratory

Hermann Harde[1], *Michael Schnell*[2]

[1]*Helmut-Schmidt-University, Hamburg, Germany*

[2]*Ex Academy of Science of GDR, Berlin, Germany*

Abstract

The existence or non-existence of the so-called atmospheric greenhouse effect continuously dominates the extremely emotional discussion about a human impact on global warming. Most scientists agree with the fundamental greenhouse theory, but like their opponents they are missing a reliable experimental verification of this effect. Measurements at the open atmosphere are too strongly affected by perturbations to quantify the relatively small contribution of greenhouse gases to local heating of the air or the Earth's surface. Therefore, we have developed an advanced laboratory set-up, which allows to largely eliminate convection or heat conduction and to reproducibly study the direct influence of greenhouse gases under similar conditions as in the lower troposphere. We measure the additional warming of a pre-heated plate due to back-radiation of the greenhouse gases carbon dioxide, methane and nitrous oxide as a function of the gas concentration, and we derive from the observed warming the radiative forcing of these gases. The measurements are well confirmed by radiation transfer calculations and underline that there exists no climate emergency.

Keywords: Greenhouse effect; infrared-active gases; radiative forcing; carbon dioxide, methane; nitrous oxide.

Submitted 01-11-2021, Accepted 16-12-2021. https://doi.org/10.53234/scc202203/10

1. Introduction

The very first explanation of the atmospheric greenhouse effect (GHE) goes back to Jean-Baptiste Joseph Fourier in 1824 [1], who was studying the Earth's energy budget to explain the surface temperature. He was inspired by the hot box of Horace-Bénédict de Saussure consisting of an isolated compartment with several glass windows, which in the inside is strongly heated up by the transmitted solar radiation. Fourier assumed that the atmosphere is acting similar to the glass windows, transparent for the solar radiation but blocking the infrared (IR)-radiation emitted from the ground. Heat exchange with the environment by convection or heat conduction was largely neglected in this model.

First quantitative measurements with IR absorbing gases like water vapor or carbon dioxide (CO_2) go back to Tyndall (1861) [2]. He described the GHE by comparing the atmosphere with a *dam built across a river and causing a local deepening of the stream*; in a similar way should the atmosphere act as a barrier to radiation from the Earth, thus, producing a heightening of the temperature at the Earth's surface. Although he could study the absorptive and emitting behavior of these gases, he had no direct evidence for a GHE.

Within the second half of the 19th century fundamental relations for the interaction of radiation with matter were formulated, e.g., Kirchhoff's law of thermal radiation (1859) [3], the Stefan-Boltzmann law (1879) [4, 5] or Planck's radiation law (1900) [6], which form the theoretical basis of the GHE. First calculations with a still strongly simplified climate model go back to S.

Arrhenius (1898) [7], who already considered ice-albedo feedback in his model and found a CO_2 climate sensitivity (temperature increase at doubled CO_2 concentration) of 5 - 6°C. Since this time there existed continuous trials to confirm or to refute the GHE by more or less simple laboratory experiments. Direct measurements at the atmosphere are too strongly affected by convection, turbulence or scattering effects to quantify the relatively small contribution of greenhouse molecules to any local warming of the air or the Earth's surface.

One of the frontier experimental investigations was performed by R. W. Wood (1909) [8], who used two boxes containing regular air. One box was covered with a glass window transparent for sun light, but blocking IR-radiation, the other covered with a NaCl window transparent also for IR. His measurements showed significant warming of the interior but no or only a negligible temperature difference between the boxes. From this Wood and other author repeating his experiment (e.g., Nahle 2011 [9]) concluded that infrared radiation, which can escape through the NaCl window, will not contribute to heating or only with an insignificant amount, while the observed temperature increase in both boxes - different to Fourier's interpretation - is exclusively explained due to the blockage of convective heat transfer with the environment and not related to any kind of trapped radiation.

But experiments recording the temperature at the floor and ceiling of the interior, rather than looking only to a single temperature for each box, measure a 5°C larger floor to ceiling decline for the salt rock box than the glass box, while the bottom of the boxes have almost identical temperatures (V. R. Pratt 2020 [10]). These results are principally confirmed with a slightly different set-up using an internal electric heating instead of external light sources (E. Loock 2008 [11]). Such heating avoids differences in the incident radiation, which otherwise has to transmit windows of different materials and losses. A higher temperature of 2.5 - 3°C could be found for the glass box, and replacing the glass by a polished aluminum foil the temperature even rises by additional ≈ 3°C.

While the Wood-type experiments can answer the question, if and how far a reduced IR-transmissivity can contribute to warming of a compartment, respectively the troposphere, it gives no information about the interaction of greenhouse gases with IR-radiation. Thus, it still remained the question, to which extent such gases at least partially can withhold IR-radiation and how far simple absorption by GH-gases or the highly disputed back-radiation might contribute to additional warming of the floor. Such studies require to fill one compartment with the gas to be investigated and to compare this with a reference measurement using air or a noble gas.

Meanwhile different approaches have been carried out, partly with external irradiation or with internal heating (see, e.g., Loock [11]), partly measuring the gas temperature or the IR radiation in forward and backward direction (Seim & Olsen 2020 [12]). But either no warming was detected or, after closer inspection, the observed temperature increase could not be attributed to an IR-radiation effect.

Unfortunately, some fake demonstrations with apparent temperature differences of more than 10°C are presented in the internet, which allegedly reveal the strong impact of the greenhouse gases (see, e.g., Ditfurth 1978 [13). However, closer inspection shows that the higher temperature is mainly caused by a stratification effect combined with an increased isolation, when heavier CO_2 is filled from the bottom into the compartment (M. Schnell 2020 [14]). And really problematic is, when the co-recipient of the 2007 Nobel Peace Prize initiates a web-based campaign with multiple advertisements on television, focused on spreading awareness for a climate crisis and as "evidence" presents a completely unrealistic and unreproducible video experiment of the GHE (Al Gore's Climate 101 video experiment, 2001 [15]), which meanwhile has been falsified by several revisions (A. Watts 2011 [16]; J.-E. Solheim 2016 [17]). It is a dirty propaganda using such a manipulated experiment to spread fear around the word and to indoctrinate our society with the message that we can only rescue our Earth by stopping all future emissions of greenhouse gases. This undermines any serious attempts to discuss and analyze the expected influence of GH-gases on our climate. Political imaginations, speculations or religious faith are no serious

consultants to ensure a prosperous future, our knowledge and technical progress is based on scientific principles.

Therefore, it is time to stop the endless speculations about the disastrous implications of an atmospheric GHE and to concentrate on reliable investigations, which allow to quantify the size and limiting impact of GH-gases on global warming caused by anthropogenic emissions of fossil fuels.

In this contribution we present an advanced experimental set-up, which to a large extent allows to eliminate convection or heat conduction and to reproducibly study the direct influence of greenhouse gases under similar conditions as in the lower troposphere. In Section 2 we present the set-up, which different to other experiments uses a heated plate as radiation source and simultaneously as sensitive detector for the back-radiation from GH-gases. We measure the increasing temperature of this plate or, alternatively at stabilized temperature, the energy saving due to the back-radiation. Section 3 describes the theoretical concept for analyzing and evaluating the experiments. Section 4 contains some preliminary studies for the validation and calibration of the measuring system, and Section 5 presents our measurements together with an evaluation of the data, from which the radiative forcing of the gases CO_2, CH_4 and N_2O can be derived. Our results are discussed in Section 6 and Section 7 gives a summary with future perspectives.

2. Experimental Set-Up

For our studies we use an experimental set-up, which consists of two plates in a closed housing, one plate heated to 30°C, the other cooled to -11.4°C (Fig. 1). The plates have a distance of 1.11 m to each other, and the tank can be filled with different gases to study the radiation transfer between the plates in the presence of the GH-gases.

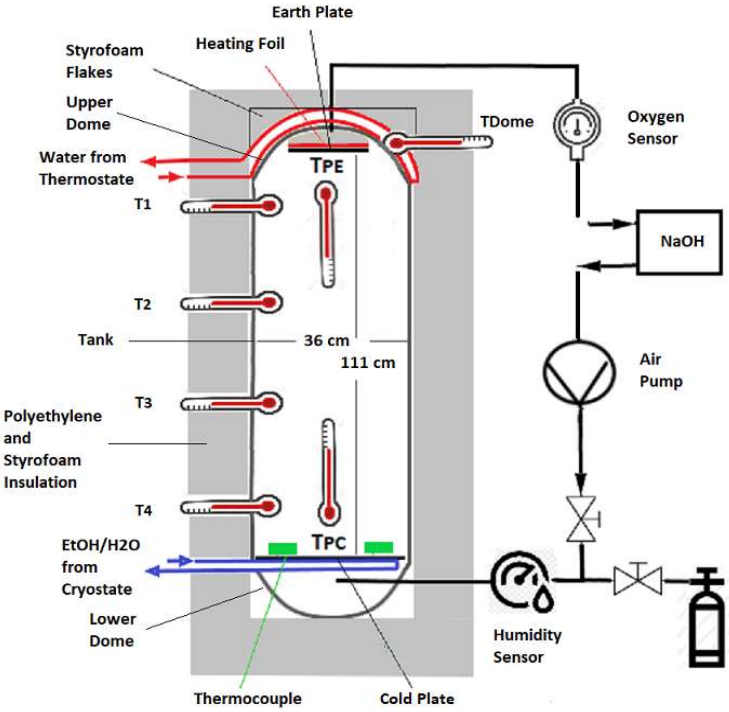

Figure 1: Schematic of the experiment set-up.

Different to other experiments, no light sources from visible to mid IR are used, only the radiation emitted by the two plates and interacting with the gases is considered. This simulates conditions for the radiation exchange similar to the Earth-Atmosphere-System (EASy) with the warmer Earth's surface and the colder atmosphere. It also avoids any problems caused by an inappropriate

spectral range of an external source, which produces a lot of waste heat in the compartment and the windows, but is not well matched to the absorption bands of the GH-gases, and thus significantly reduces the measurement sensitivity (see also Section 3).

With increasing concentration of the GH-gases the radiation balance between the plates is changing and can sensitively be measured as a further increasing temperature of the warmer plate and/or a further cooling of the cold plate. Here we restrict our investigations on recording the temperature variation of the heated plate as a function of the GH-gas concentration in the tank, or alternatively controlling the electric power required to stabilize the temperature of this plate to 30°. In analogy to a presumed warming of the Earth's surface by the atmospheric GHE we designate the warmer plate as the earth plate, which simultaneously is acting as source and sensor for IR-radiation.

Any flows, which are not part of the radiation exchange must be prevented or minimized by appropriate measures. Fig. 1 shows the schematic set-up and the most important components; for further details, see Appendix 1. Their vertical installation, with the earth plate in the top position, ensures a stable gas stratification during gas injection and prevents vertical heat exchange by convection.

Heat conduction, both along the compartment walls or by the gas, cannot be prevented but minimized. The earth plate is fixed in isolation and located in a hemispheric cover (dome) with almost identical temperature. The dome is wrapped with a vinyl tube on the outside (Appendix 1) and water at a constant temperature of 30.0 ± 0.1°C, controlled by an electric heating, flows through this hose. This arrangement is essential for our investigations and ensures that there is almost no heat conduction in this section. The heated dome guarantees good thermal insulation of the earth plate, but is also an important orientation aid for the evaluation of the experiments. It has a polished stainless-steel surface, which makes it largely insensitive to thermal radiation.

When adding a GH-gas the back-radiation of the gas is measured as increasing temperature of the black colored earth plate relative to the dome temperature, or as reduced electrical power for heating the plate. For the calibration of the different temperature sensors, see Appendix 2.

From the outset, the earth plate together with the dome has the highest temperature. This results in a small, unavoidable heat flow from the earth plate to the tank walls and the cold plate, supported by the gases. Any impact of this heat conduction, which inherently is very small, is checked by control measurements with noble gases of comparable heat conductivity (Appendix 3). The preparation and realization of a measurement together with the data registration system is described in Appendix 1.

3. Theoretical Basis of the Greenhouse-Effect and Data Analysis

In this section we summarize the physical background of IR-radiation interacting with the GH-gases. As example we consider the interaction with CO_2 molecules, this with particular emphasis to the radiation transfer in the gas and the back-radiation to the earth plate. The presented theoretical concept allows to precisely simulate the GHE under the given experimental conditions, and it forms the basis for a quantitative analysis of the measurements.

3.1 Spectral Properties of CO_2

The spectral range relevant for the interaction of longwave (lw) radiation with infrared-active molecules is determined by the Earth's surface temperature, or here, the temperature T_E of the earth plate. The spectral intensity of a black body at temperature T_E (in units of Kelvin) is given by Planck's radiation law [5] as a function of the wavelength λ (in µm):

$$I_\lambda = \frac{2\pi \cdot h \cdot c^2}{(\lambda \cdot 10^{-6})^5} \frac{1}{e^{h \cdot c \cdot 10^6/(k_B \cdot T_E \cdot \lambda)} - 1} \cdot 10^{-6} \left[\mathrm{W/m^2/\mu m}\right], \qquad (1a)$$

with $h = 6.626 \cdot 10^{-34}$ Ws^2 as Planck's constant, $c = 2.998 \cdot 10^8$ m/s as vacuum speed of light and

$k_B = 1.381 \cdot 10^{-23}$ J/K as Boltzmann's constant.

In wide areas of spectroscopy, it is more common to present spectroscopic data in reciprocal wavelengths $\tilde{\nu} = 1/\lambda$ and in units of cm^{-1}. This corresponds to a frequency scale $\nu = c/\lambda$, divided by c and is designated as wavenumbers. The respective Planck distribution then takes the form:

$$I_{\tilde{\nu}} = 2\pi \cdot h \cdot c^2 \cdot \tilde{\nu}^3 \frac{1}{e^{h \cdot c \cdot \tilde{\nu} \cdot 100/(k_B \cdot T_E)} - 1} \cdot 10^8 \left[\mathrm{W/m^2/cm^{-1}}\right]. \qquad (1b)$$

Fig. 2 shows the emitted spectral intensity (Blue Line) of the earth plate at $T_E = 30$°C (303.15 K). Within this spectral range CO_2 with its different isotopologues possesses more than 30,000 lines with a spectral line intensity larger 10^{-26} cm/molecule (for definition, see e.g., Rothman et al. 2008 [18]; Harde 2013, Subsec. 2.2.2 [19]), and even the most frequent isotopologue $^{12}C^{16}O_2$ with an abundance of 98.89 % holds 12,400 lines.

By far the strongest absorption band with spectral line intensities up to $3.3 \cdot 10^{-18}$ cm/molecule is centered around 2,400 cm^{-1} ($\lambda \approx 4.25$ µm). But at these wavenumbers the emitted spectral intensity of the earth plate is hundred times smaller than at its maximum. So, this absorption band cannot contribute more than 0.75% to the total absorption. The dominant interaction with rovibronic transitions of the CO_2 bending oscillation happens around $\tilde{\nu} = 670\,\mathrm{cm^{-1}}$ ($\lambda \approx 15$ µm), although the spectral line intensities and thus the respective absorption coefficients are roughly 30x smaller than the stronger lines at 2,400 cm^{-1}. Plotted in Fig. 2 is the calculated spectral intensity transmitting a gas sample of 20% CO_2 in dry air at a constant temperature of 20°C and over a distance of 111 cm (Plum colored). The semi-transparent wings of this absorption band (Gray) together with the weak bands around 1,000 cm^{-1} and 2,100 cm^{-1} are only partly contributing to a further slowly increasing absorption with inclining CO_2 concentration (all concentration specifications in this contribution are relating to the volume).

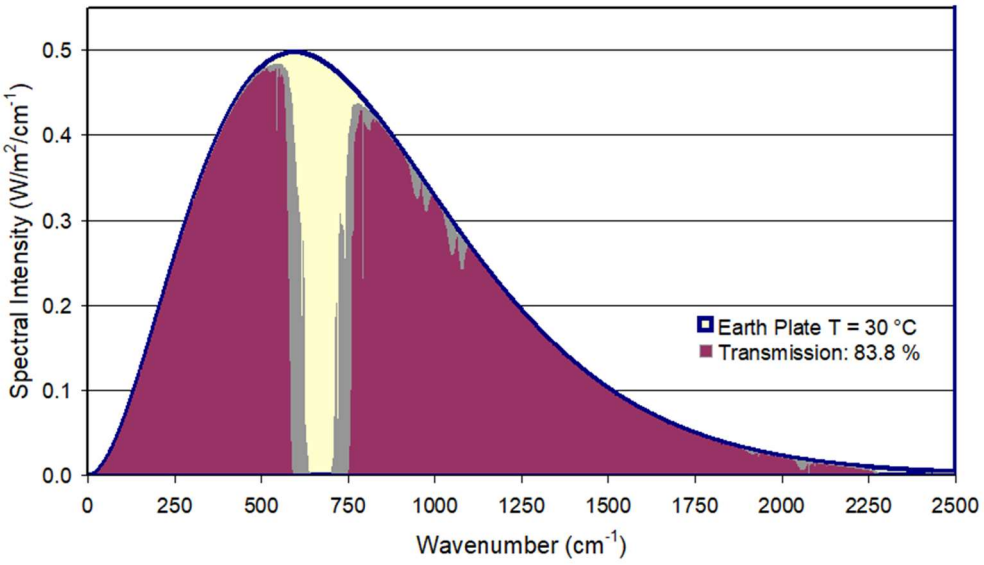

Figure 2: Spectral intensity radiated by the earth plate at T_E =30°C (Blue Graph) as a function of wavenumbers. Transmission of initial radiation through 20% CO_2 in dry air at a temperature of 20°C and over a pathlength of 111 cm is shown in Plum color.

For these calculations we use the program-platform MolExplorer (Harde & Pfuhl, 2012 [20]) with access to the HITRAN-database (Rothmann et al., 2009 [18]) and applying Lambert-Beer's law with an exponential decline of a spectral component $I_{\tilde{\nu}}(0)$ over a layer thickness z:

$$I_{\tilde{\nu}}(z) = I_{\tilde{\nu}}(0) \cdot e^{-2 \cdot \overline{\alpha}(\tilde{\nu}) \cdot z}, \qquad (2)$$

where $\overline{\alpha}(\tilde{\nu}) = \sum_i \overline{\alpha}^i_{nm}(\tilde{\nu})$ represents the effective spectral absorption coefficient, expressing the

difference between induced absorption and induced emission processes and summed over all lines *i* with transitions n → m at wavenumber $\tilde{\nu}$. We note that different to the spectral radiance $I_{\tilde{\nu},\Omega}(z)$ for the spectral intensity $I_{\tilde{\nu}}(z) = \int I_{\tilde{\nu},\Omega} d\Omega = \pi \cdot I_{\tilde{\nu},\Omega}$ as integral over all propagation directions within one hemisphere, the mean pathlength of radiation to cross a layer-thickness *L* in *z*-direction (perpendicular to the emitter surface) is twice this depth (see Harde [19], Subsec. 3.2). This is the case for atmospheric layers, and this also holds in good approximation for a set-up as used here, where the radiation suffers from multiple reflections at the walls, before it is absorbed at the cold plate.

Under these conditions the total absorption by the gas sample is 16.2%. In the atmosphere with a CO_2-concentration of 400 ppmv and neglecting interference with water vapor lines this corresponds to an atmospheric layer thickness of 555 m. But to make this clear, in both these cases the forgoing considerations and the graph in Fig. 2 only describe the fraction of incident radiation which is absorbed and released as heat in the gas, but it does not consider any eigen-radiation of the gas, which is superimposing the incident radiation and modifying the observed radiation and energy balance.

A complete and realistic simulation of measurements with a set-up as described in Section 2 requires to include this emission, which appears in the same spectral range as the earth plate radiation and which can significantly reduce the effective absorption losses, can modify the spectral distribution and is the origin of new up- or down-welling radiation. A first consideration of such Radiation Transfer (RT) - although dealing with radiation in the solar atmosphere - goes back to Schwarzschild (1906) [21].

3.2 Radiation Transfer

3.2.1 Thermal Emission of a Gas

Atoms and molecules are not only absorbing on their resonance transitions, they also emit on these transitions, well known as spontaneous emission. While the mean lifetime of an electronically excited state typically lies in the nanosecond regime before such an emission on a visible or ultraviolet transition to a lower lying state takes place, the lifetime of ro-vibronic states with transitions in the IR or far-IR range easily attains milliseconds to seconds. At regular atmospheric conditions then de-excitation due to collisions with buffer gases (N_2 and O_2 - superelastic collisions of 2nd type) at collision rates in the GHz-range is much more probable, and the absorbed energy of the incident radiation is no longer re-emitted but transferred into kinetic energy and released as heat in the gas. Fig. 2 was calculated for such conditions.

Indeed, can this behavior be observed and is quite successfully used for one of the most sensitive detection methods for trace gases in the atmosphere, the photo-acoustic effect (Wolff & Harde 2003 [22]; Harde et al. 2010 [23]): *The incident radiation resonantly interacting with the molecules, is modulated and the periodically generated heat is detected as acoustic wave by a microphone.* But often is such heat transfer misinterpreted in a way that any radiation of GH-gases in the troposphere, particularly back-radiation, is completely quenched. This is by far not the case.

Different to electronic states the lower lying ro-vibronic levels can also be populated by inelastic collisions (collisions of 1st type) with an excitation rate (from lower level *n* to upper level *m*):

$$C_{nm} = \frac{g_m}{g_n} e^{-\frac{h \cdot c \cdot \tilde{\nu}_{mn} \cdot 100}{k_B T_G}} C_{mn}, \tag{3}$$

which is proportional to the transition rate C_{mn} due to superelastic collisions and proportional to the Boltzmann-distribution with T_G as the gas temperature, $\tilde{\nu}_{mn}$ as the transition wavenumber and g_i as statistical weights of the involved states (see also, Harde 2013 [19], eq. 36). This continuous re-population of an excited state by inelastic collisions also ensures radiative transitions, which occur independently from any collision induced transitions (see, Harde [19], Subsec. 2.5). This

spontaneous emission of molecules defines the thermal radiation of a gas. Because of its origin this radiation only exists on discrete frequencies, given by the transition frequencies and the linewidths of the transitions. But on these frequencies and over longer paths the radiation strength is the same as that of a blackbody radiator, and at thermal equilibrium it is only controlled by the gas temperature T_G.

Such thermal or background radiation in the atmosphere has been observed as upwelling radiation by satellites (Tobin 1986 [24]) and as downwelling radiation at ground-stations (Arnott 2008 [25]; Feldmann et al. 2015 [26]). This excludes any doubts on the existence of this radiation also under conditions as found in the lower troposphere (see also Harde 2013 [19], Figs 21 and 22).

3.2.2 Schwarzschild-Equation

As the emission on a spectral line is directly related to the absorption strength on this transition, the spontaneous or thermal emission of the gas can be shown to be proportional to the absorption coefficient $\overline{\alpha}_{nm}(\tilde{\nu})$ on this line and the Kirchhoff-Planck function $B_{\tilde{\nu}}(T_G(z))$, which is of the same type as (1b), but describes the spectral intensity of the gas at temperature T_G and position z. Over shorter distances *dz* then changes in the spectral intensity $I_{\tilde{\nu}}(z)$ of the incident radiation can be expressed as a modification of Lambert-Beer's law (in differential form) with an absorption and emission term:

$$\frac{dI_{\tilde{\nu}}(z)}{dz} = 2\cdot\overline{\alpha}(\tilde{\nu},z)\Big(-I_{\tilde{\nu}}(z,T_E)+B_{\tilde{\nu}}(T_G(z))\Big). \qquad (4)$$

This is the Schwarzschild-equation for the spectral intensity, derived under conditions of a local thermal equilibrium in the gas (cf. Harde [19], eq. (92)). It describes the radiation transfer in the gas in the presence of absorption and thermal emission. The factor 2 again accounts for the mean pathlength of radiation to cross the layer thickness *dz*.

In general, the density of the gas, the total pressure and the temperature are changing over the propagation path. Thus, (4) has to be solved stepwise for thin layers of thickness Δz, over which, $\overline{\alpha}(\tilde{\nu},z)$ and $B_{\tilde{\nu}}(T_G(z))$ can be assumed to be constant (see Fig. 3).

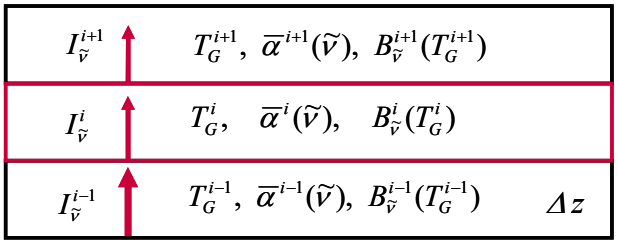

Figure 3: Stepwise calculation of the spectral intensity for the radiation transfer in a gas.

Integration of (4) for the *i*-th layer with initial conditions from layer *i*-1 then gives:

$$I_{\tilde{\nu}}^{i}(\Delta z) = I_{\tilde{\nu}}^{i-1}e^{-2\overline{\alpha}^{i}(\tilde{\nu})\Delta z} + B_{\tilde{\nu}}^{i}(T_G^{i})\cdot(1-e^{-2\overline{\alpha}^{i}(\tilde{\nu})\Delta z}). \qquad (5)$$

The first term in (5) describes the transmission of the incident spectral intensity over the layer thickness, while the second term represents the self-absorption of the thermal background radiation in forward direction and is given by the spontaneous emission of the layer into one hemisphere.

3.2.3 Some First Consequences

A special case of RT is given, when the gas has the same temperature as an internal or external blackbody radiator. Then, from (4) or (5) we directly see that the outgoing intensity is the same as the incident intensity. Changes can only be expected, when T_E and T_G are different and/or T_G varies over the pathlength.

This already explains, why it is difficult to verify the GHE when only looking to the gas temperature. Net absorption and thus heating of the gas by incident radiation only takes place as long as the respective spectral intensity on the molecular transitions is larger than the eigen-radiation of the gas on these lines. When this has equalized, no further net exchange happens, and in this sense RT in the gas acts similar to heat conduction and convection equalizing local temperature differences.

A larger local and global warming of a GH-gas is also restricted by its own radiation. This limits the effective absorption from an IR or visible light source and impedes distinction of this contribution from the dominating waste heat released by these sources. All this is further aggravated in the presence of heat conduction and convection in a typical set-up.

A prerequisite for the observation of the GHE in the atmosphere and in the same way in a laboratory experiment is a temperature gradient in the gas, otherwise no net changes in the radiation balance can be expected.

3.2.4 Forward-Radiation

Fig. 4 shows a Line-By-Line-Radiation-Transfer (LBL-RT) calculation for 20% CO_2 in air over 111 cm. But different to Fig. 2 varies the gas temperature over the propagation length from 30°C at the earth plate to −11.4°C at the cooled plate. This corresponds to a lapse-rate of 0.373°C/cm over the gas column. The emitted radiation of the earth plate is indicated as Blue Graph on a yellow background, the transmitted spectral intensity in front of the cold plate is displayed in Plum, and the weak absorption bands as well as the semitransparent wings are plotted in Grey. The significantly lower absorption with 5.2% compared to Fig. 2 with 16.2% is obvious and is the result of the eigen-emission of the gas.

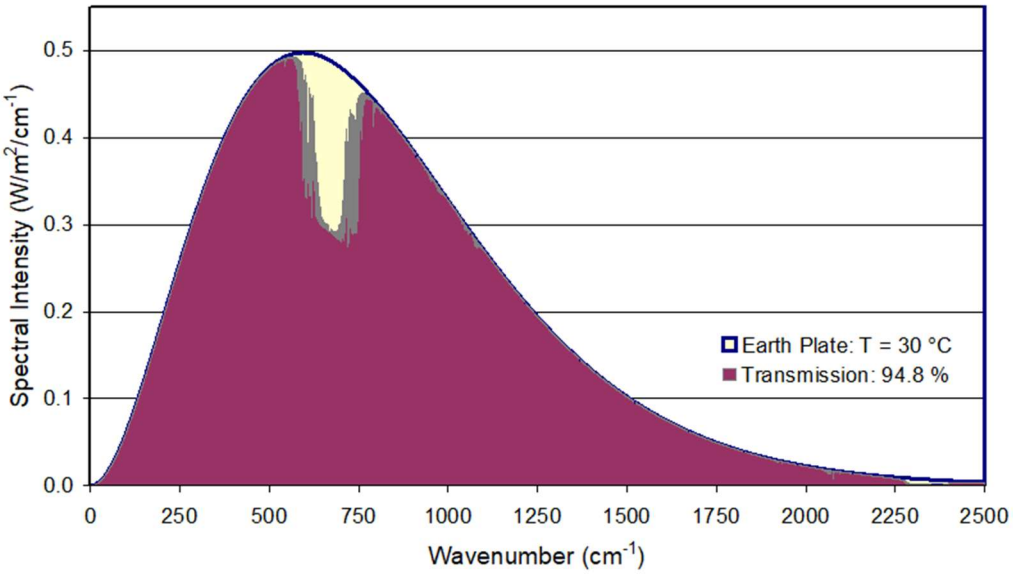

Figure 4: LBL-RT-calculation for 20% CO_2 in air over 111 cm for a lapse rate of 0.373°C/cm. Plotted is the blackbody radiation for 30°C (Blue-Yellow) and the transmitted spectral intensity (Plum-Gray).

This calculation is based on (5) and was performed with a layer thickness of Δz = 1 cm. For each layer the spectral changes of more than 12,000 lines with their pressure and temperature dependent linewidths have to be calculated to finally derive the transmitted intensity after 111 calculation steps. The pressure in the tank was assumed to be constant and the gas density considered to change according to the ideal gas equation.

Fig. 4 reproduces conditions as recorded by satellites (Tobin 1986 [24]) measuring the upwelling radiation or forward scattering, which is characterized by the typical funnel around 670 cm^{-1}. In

this spectral range is the incident radiation completely absorbed (see Fig. 2), and the observed intensity only results from thermal emission of the gas at reduced temperatures close to the lower plate. In this case the gas first absorbs 73.6 W/m^2 from the incident radiation of 479 W/m^2 (integral over the spectral intensity) and emits again 48.5 W/m^2, while a difference of 25.1 W/m^2 remains in the gas volume and can contribute to warming and/or radiation, as long as this is not lost at the walls.

To detect the forward or upwelling radiation is one way to verify the GHE, the other approach, we prefer in this contribution, is to measure the downwelling or backward radiation. In analogy to the terrestrial radiation we define the propagation from the warmer to the colder plate as positive z-direction and as upwelling radiation, although our set-up is just upside-down to EASy.

3.2.5 Back-Radiation

We have to remind that a full radiation balance has not only to consider the emission of the earth plate and the interaction with the gas but also the radiation emitted by the cold plate, which is propagating in anti z-direction through the gas towards the warmer plate. Thus, to simulate the RT for this case, we start with the spectral intensity emitted from the cold plate at $T_C = -11{,}4$°C = 261.75 K and calculate the propagation through the gas cloud for a negative lapse rate c_T = –0.373°C/cm. Fig. 5 shows the spectral intensity of the back-radiation for 20% CO_2 in air over 111 cm (Plum-Gray).

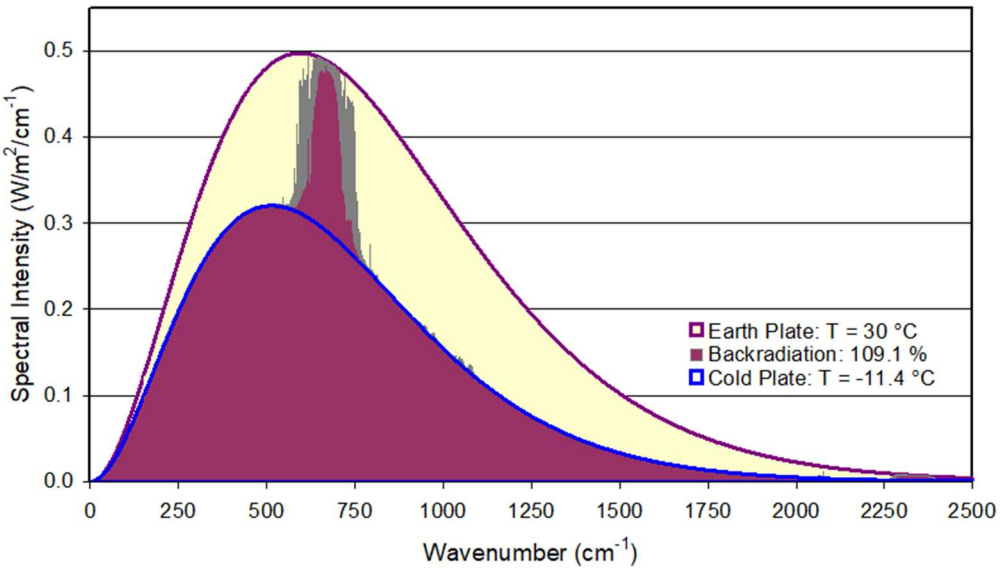

Figure 5: LBL-RT-calculation for 20% CO_2 in air over 111 cm for a lapse rate of -0.373°C/cm: Back-radiation from cold plate and gas (Plum-Gray), radiation only from cold plate (Blue) and spectral intensity of earth plate (Red-Yellow).

Also plotted is the emitted spectral intensity of the cold plate (Blue Line) and the earth plate (Red-Yellow). The eigen-radiation of the gas towards the warmer earth plate can well be identified as peak around 670 cm^{-1} (Plum area, Gray wings) on top of the broader spectrum of the lower plate. On the stronger lines at the band center the gas emission already attains saturation with spectral intensities, which are the same as those emitted by the earth plate in this spectral range.

Compared to the total radiated intensity of the cold plate with $I_C = \int I_{\tilde{\nu}}\, d\tilde{\nu} = 266\ \mathrm{W/m^2}$ the back-radiation increases by 24.2 W/m^2, which is 9.1%. This larger back-radiation is almost identical to the losses in forward direction, so that within observational accuracies the total balance of absorption and emission of the gas is zero. This is a further important aspect that speaks against measuring the gas temperature to prove the GHE. On the other hand, under the given conditions and with the apparatus presented in Section 2, it is quite possible and realistic to detect the radiation emitted

by the gas through a temperature rise of the earth plate.

4. Preliminary Studies and Calibration of the Measuring System

So far, our foregoing considerations were implicitly assuming a radiation transfer between sufficiently extended parallel plates without taking account of transversal or reflection losses in a laterally restricted radiation channel. For a direct comparison with a measurement therefore two preparatory investigations are required:

1. Assessment of radiation losses from one plate to the other.

2. Calibration of the earth plate's temperature response to the absorbed radiation.

4.1 Assessment of Radiation Losses

For the further characterization of the set-up it is advisable to distinguish between radiation losses without and with GH-gases in the radiation channel.

4.1.1 Without Infrared-Active Gases

According to our previous considerations, in the absence of GH-gases the total radiation from the lower half-plane, absorbed by the earth plate, results from the direct radiation of the cold plate. In general, however, this is additionally superimposed by radiation emitted by the side walls. Both these fractions suffer from geometrical and reflection losses on the way to the earth plate and have to be quantified in their relative and absolute contributions for a further analysis of the experiments. This is possible by measuring the electric heating power for the earth plate necessary to stabilize its temperature at 30°C while changing the temperature T_C of the cold plate over a wider range.

At thermal equilibrium the radiation and energy balance for the earth plate - or equivalently the balance of intensity fluxes - requires that all losses are just compensated by respective influxes.

Losses: As radiation losses of the earth plate only the emission to the lower half-space has to be considered, while any fluxes between the plate and dome with almost identical temperature are well balanced. The emitted intensity $I_E(T_E)$ of the earth plate at temperature T_E (in K) is the integral over Planck's distribution (1) and equivalent to the Stefan-Boltzmann-equation:

$$I_E(T_E) = \varepsilon_E \int I_\lambda(T_E) \cdot d\lambda = \varepsilon_E \int I_{\tilde{\nu}}(T_E) \cdot d\tilde{\nu} = \varepsilon_E \cdot \sigma_B \cdot T_E^4, \qquad (6)$$

with $\varepsilon_E \approx 1$ as the emissivity of the black colored plate and $\sigma_B = 5.67 \cdot 10^{-8}$ W/m^2/K as the Stefan-Boltzmann constant.

An additional loss has to be included, which is determined by heat conduction of the gas, mostly from the warmer plate to the walls. It is designated as $L(\Delta T)$ for a temperature gradient ΔT.

Savings: Radiation influxes come from the cold plate and the walls. The cold plate with an emitted intensity $I_C(T_C)$ at temperature T_C then contributes the fraction f_C to the energy balance, and the walls with a radiated intensity $I_W(T_W)$ at temperature T_W the fraction f_W. Additionally we include radiation of the earth plate itself, which is partially back-reflected from the walls with the amount $R_E(I_E)$. While the intensities can be calculated for the respective temperatures from (6), the fractions f_C and f_W and also the reflection R_E, which are representing all geometrical as well as reflection and re-emission losses on the way to the earth plate are for now unknown.

All fluxes, positive and negative ones, determine together the theoretical heating intensity H_E (electric heating power per cross section) required to stabilize the earth plate on the temperature T_E:

$$H_E^T(T_C, T_W) = I_E(T_E) - f_C \cdot I_C(T_C) - f_W \cdot I_W(T_W) - R_E(I_E) + L(\Delta T). \qquad (7)$$

This balance is used to calculate the necessary plate heating and to compare it with the measured heating, when the temperature of the cold plate and thus, the intensity I_C is changed while leaving all other parameters - as far as possible - the same (as an example see: Appendix 4, Table A4.1).

In Fig. 6 is plotted the measured heating H_E as a function of the intensity $I_C(T_C)$ (Magenta Diamonds) when changing the temperature from −12.6°C up to +10.5°C (260.6 - 283.6 K). The data show a straight line reflecting that any changes mostly can be traced back to intensity variations of the cold plate and obey Stefan-Boltzmann's equation. Heat conduction in the gas, varying linearly on a temperature scale, would cause larger deviations on the intensity scale, and thus, can widely be excluded. Also radiation changes from the walls, inclusive radiation from the earth plate, that is back-reflected from the walls, can be neglected, since primarily radiation from the upper section of the tank hits the earth plate, where the wall is only very little affected by temperature variations of the cold plate. All measurements were repeated 10 times and show excellent reproducibility.

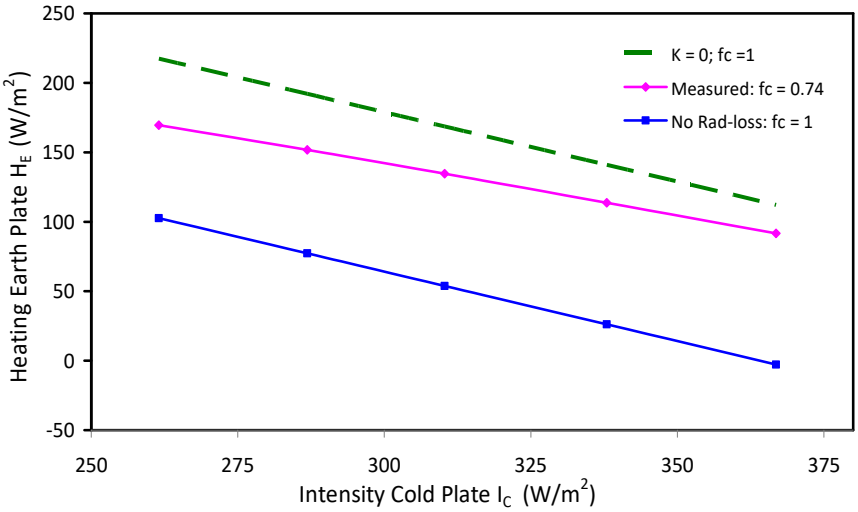

Figure 6: Measured heating of earth plate for a fixed temperature T_E of 30°C as a function of the radiated intensity I_C of the cold plate (Magenta Diamonds). Also plotted is the expected heating for f_C = 1 (Blue Squares) and $K(T_W,\Delta T)$ = 0 (Green Dashed).

Often deniers of the GHE argue that radiation from a cooler body cannot be absorbed by a warmer body, as this would be a violation of the 2nd law of thermodynamics. This relatively simple measurement is clear evidence of a wrong interpretation of this law, which explicitly includes the "*simultaneous double heat exchange by radiation*" (Clausius). In a closed system "*the colder body experiences an increase in warmth at the expense of the warmer body*", which on its own experiences a lower cooling rate. In an open system with external heating this even leads to an increasing temperature of the warmer body in the presence of additional back-radiation from a colder body.

According to (7) is the slope of the measured heating H_E the fraction of the transmitted radiation from the cold to the warm plate, for which we derive a value f_C = 0.74, i.e., 74% of the theoretically expected emission of the cold plate arrives at the earth plate. For comparison is also plotted the case of zero radiation losses, when $\Delta H_E = \Delta I_E$ (f_C = 1) (Blue Squares).

For the limiting case T_C = 0 K, thus $I_C(0)$ = 0, extrapolation of the measured data gives $H_E(0,T_W)$ = 364.1 W/m^2. Then for the radiation flux from the walls (inclusive reflections of the earth plate emission) minus the heat conduction, together represented by the quantity K, we find with (7):

$$\begin{aligned} K(T_W,\Delta T) &= f_W \cdot I_W(T_W) + R_E(I_E) - L(\Delta T) \\ &= I_E(T_E) - H_E(0,T_W) = 478.9 - 364.1 = 114.8 \text{ W/m}^2 \end{aligned}, \qquad (8)$$

which can largely be regarded as constant over the measured temperature interval of 24°C (see also Appendix 3 and Appendix 4, Table A4.2).

According to Stefan-Boltzmann's law with a wall temperature of about 28°C in the upper section of the tank, an emissivity of the polished wall surface of $\varepsilon_W \approx 0.1$ and a relatively large assumed fraction $f_W \approx 0.85$ of the emitted wall intensity, the radiation from the walls does not contribute more than 40 W/m^2. That means, a relatively large fraction of at least 75 W/m^2 or 15.6% of the earth plate radiation must be back-reflected from the walls. So, for the heat conduction $L(\Delta T_E)$ acting with opposite sign there is not too much left in the energy balance, which shows its only moderate impact on the further investigations (see also Sec. 5). Note, the highest sensitivity for detecting changes of the cold plate and also radiation of a GH-gas is given when $K(T_W,\Delta T) = 0$ and $f_C = 1$. This is represented by the Green Dashed line in Fig. 6 as a quality reference for the set-up.

4.1.2 With Infrared-Active Gases

The previous investigations with dry air in the tank, while changing the temperature of the cold plate, give a first orientation, which radiation losses from the cold to the warm plate have to be expected. But they are also an important prerequisite for a measurement with a GH-gas in the housing to answer the question, what fraction of the gas radiation can be collected by the earth plate.

With a GH-gas in the radiation channel the energy and radiation balance has to be expanded by an additional term for the emitted intensity of the gas $\Delta I_G(T_C,c_T)$, which is changing with the temperature difference between the plates and thus with the lapse-rate c_T, and which contributes the fraction f_G to the total balance:

$$H_E^T(T_C,T_W,c_T) = I_E(T_E) - f_C \cdot I_C(T_C) - f_G \cdot \Delta I_G(T_C,c_T) - K(T_W,\Delta T)\,. \qquad (9)$$

We consider here the intensity $\Delta I_G(T_C,c_T)$, which is emitted on top of the radiation from the cold plate (see Fig. 5), since otherwise the spectral interval under the Planck curve would be counted twice. For the fraction f_G we assume that it does not change with the lapse rate and gas density. K summarizes again the wall radiation, reflection and heat conduction losses according to (8).

We have performed measurements for the three IR-active gases CO_2, CH_4 and N_2O, each with 10% concentration in dry air, and as further control runs additional measurements with 10% He and 20% Ar (Appendix 4, Table A4.3). The measuring procedure is the same as described in Subsec. 4.1.1), only exchanging the gas in the tank. As example we look closer to the measurements with the CO_2-mixture as sample gas.

Table 1: Measured heating of the earth plate at varying cold plate temperature with 10% CO_2 in air.

ΔT (°C)	$H_E(CO_2)$ W/m^2	H_E (air) W/m^2	ΔH_E W/m^2	c_T °C/cm	calc. ΔI_{CO2} W/m^2	$f_{CO2} = \Delta H_E/\Delta I_{CO2}$	$f_{CO2}\cdot\Delta I_{CO2}$ W/m^2
19.6	85.03	92.1	7.09	0.177	10.65	0.67	6.93
24.7	102.75	111.3	8.56	0.223	13.08	0.65	8.52
31.4	124.70	134.8	10.10	0.283	16.10	0.63	10.48
36.5	139.90	151.4	11.51	0.329	18.28	0.63	11.90
42.9	157.00	171.2	14.17	0.387	20.86	0.68	13.58
					mean f_{CO2}:	0.65	

Table 1 displays the recorded heating in units of W/m^2 (column 2) as a function of the temperature difference ΔT between the earth plate (fixed temperature at 30°C) and the varying temperature of the cold plate (column 1). Also listed is the measurement in dry air from Subsec. 4.1.1), which works as reference for the further evaluation (column 3).

The difference between the air- and CO_2-measurements ΔH_E, displayed in column 4, then can be

compared with calculations as presented in Section 3. The RT-calculations for ΔI_{CO2} caused by 10% CO_2 and for a laterally extended plane of L = 111 cm depth (the average propagation path is $2 \cdot L = L/\cos\beta$ with $\beta = 60°$ as mean propagation angle) is a function of the lower plate temperature T_C or the lapse-rate (column 5) and listed in column 6.

ΔI_{CO2} is plotted in Fig. 7 (Magenta Diamonds) as a function of the temperature differences ΔT between the plates and can directly be compared with the measured differences ΔH_E (Blue Squares). The ratio of the measured to calculated difference defines the fraction $f_{CO2} = \Delta H_E / \Delta I_{CO2}$ of emitted CO_2 radiation, which contributes to the heating of the earth plate. As average over the different temperatures we find $f_{CO2} = 0.65$, which gives a further orientation for the expected contribution of CO_2 to the radiation balance. The trend curve as mean $f_{CO2} \cdot \Delta I_{CO2}$ is shown as Green Triangles.

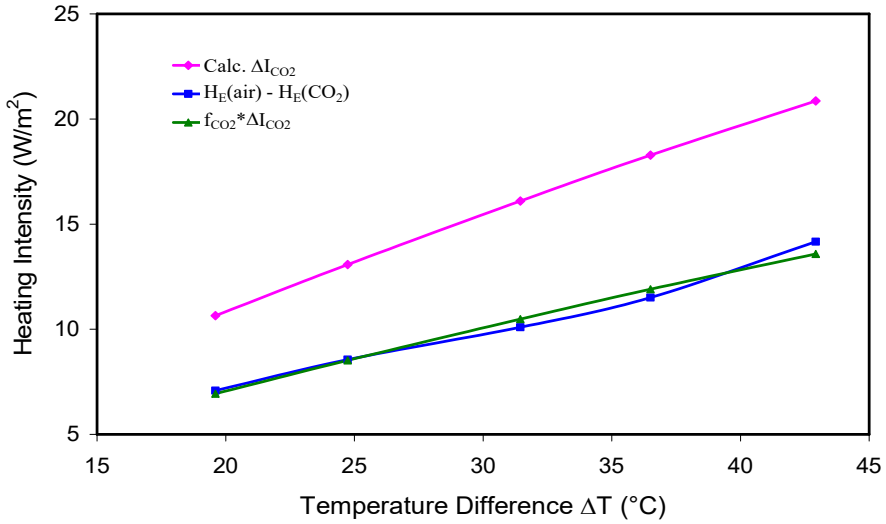

Figure 7: Calculated back-radiation ΔI_{CO2} (Magenta Diamonds), measured difference ΔH_E (Blue Squares) and theoretically expected heating $f_{CO2} \cdot \Delta I_{CO2}$ at 10% CO_2 in air (Green Triangles).

Based on the same procedure we derive the respective fraction for 10% CH_4 in dry air with f_{CH4} = 0.64 and for 10% N_2O in air with f_{N2O} = 0.62. Within our observational limits there exist no larger specific deviations between these gases, which coincide within an accuracy of less than 5%.

The relatively smaller fractions for the gas emission compared to the cold plate have to be explained by the fact that for the gases only the difference on top of the plate emission and not their full emission is considered (Fig. 5). Further differences result from a volume radiator to a surface emitter and the geometry.

A smaller change in the energy balance might also be expected due to differences in the heat conduction of the GH-gas relative to air. Therefore, control measurements with the noble gases He and Ar were performed, He with a significantly higher conductivity, Ar with a lower conductivity than air and comparable with CO_2 and N_2O. But within our measuring accuracy no differences between the noble gases and air in the energy balance can be observed (see Appendix 3). Thus, based on these experiments heat conduction as a reason for the observed changes can well be excluded.

4.2 Temperature Calibration of Earth Plate

In the previous subsection we looked to the correlation between the electric heating $H_E(T_C)$ required to stabilize the temperature of the earth plate at 30°C, when the radiated intensity $I_C(T_C)$ of the cold plate is changed. Now the temperature of the cold plate is held fixed at -11.4°C and the temperature T_E of the earth plate measured as a function of the plate heating $H_E(T_E)$. This

correlation describes the temperature sensitivity λ of the apparatus, i.e., the increase of the plate temperature ΔT_E when the heating H_E is increased by 1 W/m^2:

$$\Delta T_E = \lambda \cdot \Delta H_E(T_E)\,. \tag{10}$$

Also for the characterization of EASy, almost all known models are based on such simple relation that the ground temperature changes are scaling proportional with the changes of an external forcing ΔF. In its 6th Assessment Report (AR6) [27] the Intergovernmental Panel on Climate Change (IPCC) assumes that this forcing is almost exclusively caused by anthropogenic emissions of CO_2 with an expected likely temperature increase (including feedback effects) of 2.5 - 4°C for a doubling of the CO_2 concentration. The proportionality factor for characterizing EASy is called the Planck sensitivity λ_P or climate sensitivity parameter with $\lambda_P \approx 0.31$°C/W·m^2 (AR6-WG1-Sec.7.4).

In this context we note that different to the general understanding of radiative forcing as the net difference of radiative fluxes at the tropopause or at the top of the atmosphere, here we consider directly the measured and calculated down-welling flux ΔF at the earth plate. But RT-calculations show that their absolute contributions are almost identical (see: Subsec. 3.2.4 and 3.2.5).

In our case is λ a process parameter of the set-up that reflects the radiation exchange and heat losses. But dependent on the process-related heat losses, λ can be found to change considerably.

A measurement according to (10) starts at an initial temperature of the earth plate of T_E = 25°C and is recorded as a function of the stepwise increased heating intensity H_E. This can be performed

- with a constant dome temperature of 30°C, as applied in the previous subsection or
- with an adapted dome temperature $T_D = T_E$ to avoid a temperature difference to the earth plate.

Fig. 8 shows the difference of the two variants on λ, which gives λ = 0.082 °C/(W/m^2) for a constant dome temperature and λ = 0.184 °C/(W/m^2) with a sliding temperature.

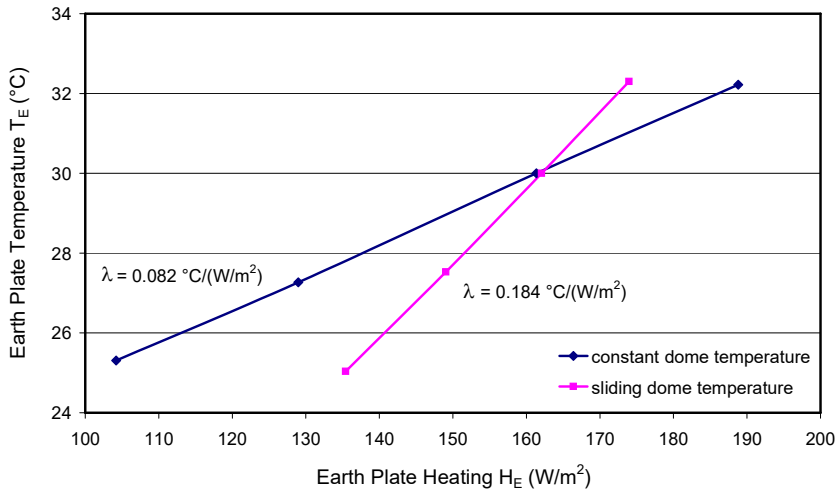

Figure 8: Temperature sensitivity for constant (Blue Diamonds) and sliding dome temperature (Magenta Squares).

The reason for this discrepancy is the different heat flow around the earth plate, which depends on the dome temperature. At constant T_D an incline of the plate temperature is strongly dampened by the increasing heat flow from the plate to the dome. At a sliding dome temperature, the loss is much lower and found as a steeper increase of the earth plate temperature with 0.184/0.082 = 2.24.

For our further investigations when directly measuring the warming of the earth plate as response to the back-radiation of GH-gases only the temperature sensitivity λ = 0.082 °C/(W/m^2) is of

relevance for comparison with theory, as all measurements are performed at a constant dome temperature.

5. Measurements and Calculation

In all experiments the temperature of the cold plate is -11.4°C and is not changed during an experiment. In a preparatory phase, the electric heating H_E of the earth plate is adjusted over the first 6 - 8 hours, till the temperature of the earth plate is exactly 30.0°C. Before adding a GH-gas to the chamber, all components of the setup must come to thermal equilibrium, as controlled by the temperature measurements taken during the first 60 minutes before the sample gas is added. The accuracy of the temperature reading is ± 0.13°C, which can only further be increased by independent measurements and averaging over several runs.

After filling the tank with a GH-gas the actual measurement is started by recording the temperature of the earth plate, and as further control, also temperatures at different positions over the gas column and at the cold plate. This happens without any external intervention till again equilibrium and a constant temperature increase ΔT_E of the earth plate is found. Then the electric heating is reduced to return to 30°C at the earth plate, allowing a direct measurement of the back radiation as difference of the required electrical heating ΔH_E of the earth plate (Fig. 9). The measurement process is explained in detail in Appendix 1.

From our investigations in Subsection 4.1b) and Appendix 3 we know that changes in the heat conductivity are negligible and the changes in H_E should directly represent the gas radiation $f_G \cdot \Delta I_G(T_C,c_T)$ collected by the plate.

5.1 CO_2-Measurement

Fig. 9 displays a typical plot, in this case for 10% CO_2 over the full recording time. The different graphs indicate the measured temperatures from the earth plate (Red), the dome (Green) and the gas at different positions over the radiation channel (T_1 - T_4, see Fig. 1).

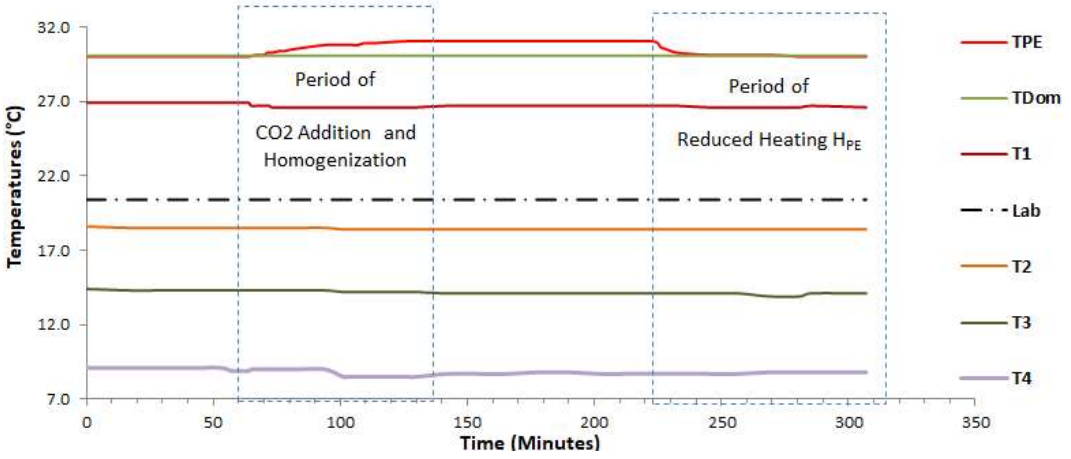

Figure 9: Typical measurement cycle, here for 10% CO_2 in dry air. Plotted are the temperatures of the earth plate (Red), the dome (Green), the gas temperature at 4 positions (T_1 - T_4) and the laboratory temperature (Black).

During the filling and recycling period of the gas smaller temperature deviations over the tank height can be observed, but when stopping this recycling, all temperatures except T_E return to their initial position. After 220 minutes the electric plate heating is reduced, till the earth plate temperature again attains 30°C.

To quantify the back-radiation of CO_2 with increasing concentration, and thus, to determine its impact on global warming, we have performed measurements over a wider range from 1.25% up

to 20% in dry air. From one measurement to the next each time the concentration is doubled up to 16x. All measurements represent the average of 5 independent runs. The results are displayed in Table 2.

Table 2: Measured earth plate temperature change ΔT_E and plate heating change ΔH_E as a function of the CO_2 concentration and comparison with RT-calculations.

CO_2	Earth Plate (°C)	Cold Plate (°C)	λ_{av} (°C/W·m²)	c_T (°C/cm)	f_{CO2}	log start ΔT_0(°C)	ΔF_{2xCO2} (W/m²)
	30.0	-11.4	0.083	-0.373	0.59	0.45	3.70
Con-cen (%)	Meas. ΔT_E (°C)	Meas. ΔH_E (W/m²)	$\lambda=\Delta T_E/\Delta H_E$ (°C/W·m²)	Calc. ΔI_{CO2} (W/m²)	f_{CO2} = $\Delta H_E/\Delta I_{CO2}$	$\lambda_{av} \cdot f_{CO2} \cdot \Delta I_{CO2}$ (°C)	log fit ΔT_E (°C)
1.25	0.45	5.05	0.089	9.92	0.51	0.49	0.45
2.5	0.63	7.44	0.085	13.05	0.57	0.64	0.63
5.0	0.79	9.76	0.081	16.48	0.59	0.81	0.81
10.0	1.00	11.80	0.085	20.15	0.59	0.99	0.99
20.0	1.18	14.09	0.084	24.13	0.58	1.18	1.17

Column 2 shows the measured temperature increase ΔT_E and column 3 the reduced plate heating ΔH_E. Their ratio (column 4) allows to determine independently the temperature sensitivity λ, which as average of these measurements is found to be a few % larger than in Subsec. 4.2. Therefore, as a basis for the further evaluation of the data we use a mean sensitivity $\lambda_{av} = 0.083$ °C/(W/m²). Column 5 specifies the calculated back-radiation ΔI_{CO2}, and column 6 the ratio of $\Delta H_E/\Delta I_{CO2}$. This ratio directly gives the fraction f_{CO2}, which contributes to the heating of the earth plate. The average deviates by 12% from the previously derived value of 0.65 in Subsec. 4.1.2, which was found by varying the cold plate temperature T_C up to 24°C. Since these measurements allow direct deduction of f_{CO2} with only little or no temperature changes in the system and including smaller absorption losses from the wall radiation, we use for the further evaluation a mean value of $f_{CO2} = 0.59$. The calculated temperature change $\Delta T_E = \lambda_{av} \cdot f_{CO2} \cdot \Delta I_{CO2}$ as a function of the CO_2-concentration is listed in column 7. The last column displays a logarithmic fit (log-fit) to the measurements.

Plotted in Fig.10a) is the measured temperature increase ΔT_E as a function of the CO_2-concentration (Blue Diamonds, col. 2) and as direct comparison the calculation $\lambda_{av} \cdot f_{CO2} \cdot \Delta I_{CO2}$ (Magenta Squares, column 7). Additionally displayed is the calculated CO_2 radiation ΔI_{CO2} (Green Diamonds, column 5).

Despite the short propagation path all graphs show clear saturation with increasing CO_2 concentration, and in the same way also the emission saturates at these concentrations. The temperature variation ΔT_E can well be represented by a logarithmic curve of the form:

$$\Delta T_E(C_{CO2}) = \Delta T_0 + \lambda_{av} \cdot f_{CO2} \cdot \Delta F_{2xCO2} \cdot \ln(C_{CO2} / C_0) / \ln 2\,, \qquad (11)$$

with ΔT_0 as the temperature increase at the concentration C_0, here 1.25%, and ΔF_{2xCO2} as radiative forcing when doubling the CO_2 concentration. Superimposed in Fig. 10a) is a fit based on (11) with $\Delta T_0 = 0.45$°C and $\Delta F_{2xCO2} = 3.70 \pm 0.05$ W/m² (Brown Crosses, column 8), which on first glance shows excellent agreement with Myhre et al. [28], but is derived under different conditions (see Sec. 6).

The measured plate heating variation ΔH_E as an independent means for detecting the back-radiation is plotted in Fig. 10b) (Blue Diamonds, column 3). It can directly be compared with the calculated back-radiation $f_{CO2} \cdot \Delta I_{CO2}$ (Green Triangles) with f_{CO2} as the free parameter for a fit to the measurements. From this fit we derive the fraction $f_{CO2} = 0.59$ of the emitted gas, which within our limits of observation is in good agreement with Table 2, column 6.

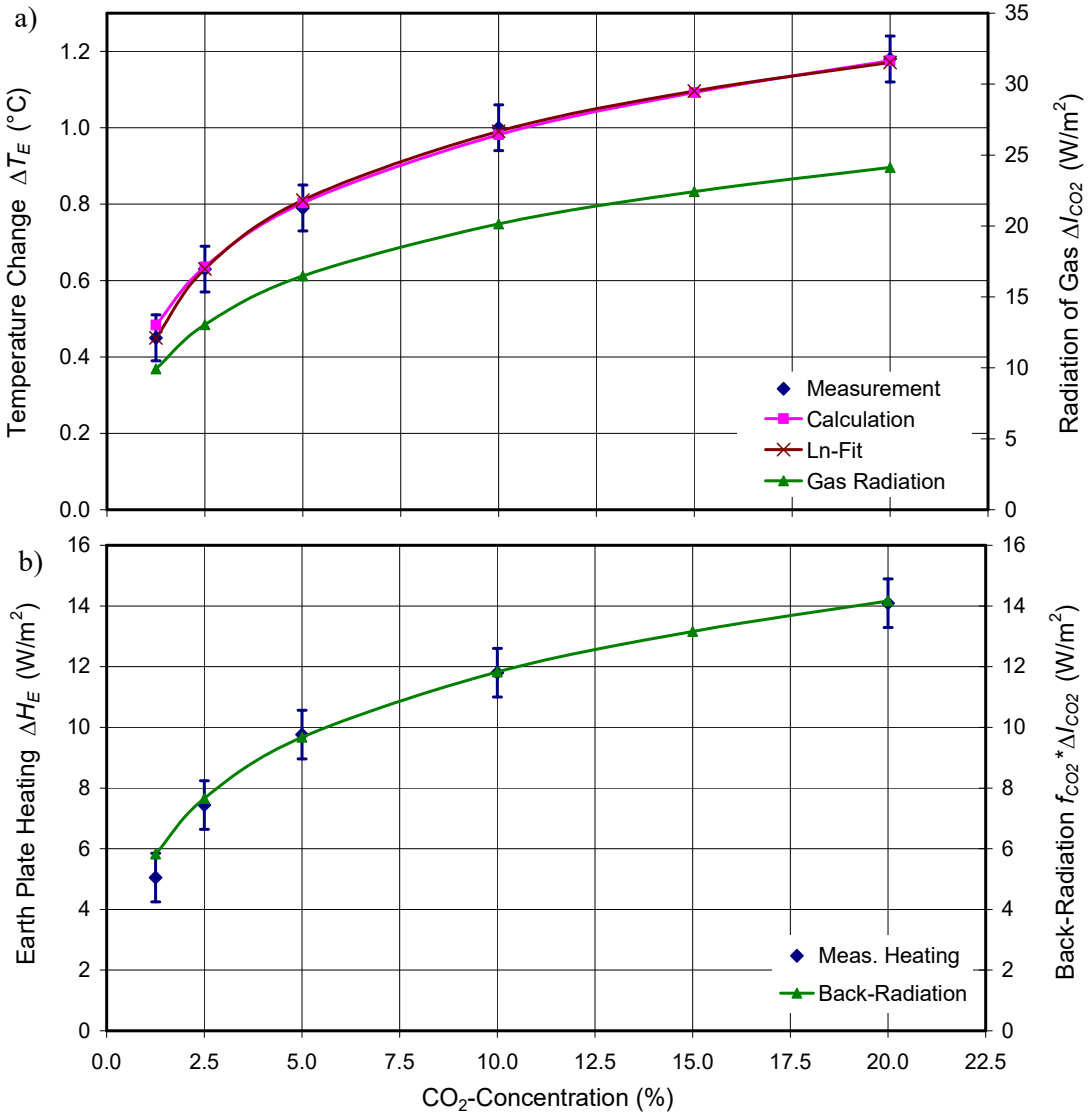

Figure 10: a) Measured temperature change of the earth plate as a function of the CO_2-concentration in dry air (Blue Diamonds) and calculation (Magenta Squares). Superimposed is a logarithmic fit (Brown Crosses) and the LBL-RT-calculation of the back-radiation ΔI_{CO2}. b) Comparison of measured plate heating ΔH_E (Blue Diamonds) and calculated back-radiation collected by the earth plate $f_{CO2}\cdot\Delta I_{CO2}$ for $f_{CO2} = 0.59$ (Green).

5.2 CH_4-Measurements

Measurements with CH_4 as sample gas were performed under identical experimental conditions as in Subsec. 5.1. The concentration was varied from 1.25% to 10%. Plotted in Fig. 11a) is the measured temperature variation ΔT_E of the earth plate with increasing CH_4-concentration (Blue Diamonds), which can directly be compared with the calculated temperature change $\lambda_{av}\cdot f_{CH4}\cdot\Delta I_{CH4}$ (Magenta Squares). The respective calculated CH_4 radiation ΔI_{CH4} is shown as Green Triangles.

The temperature sensitivity is the same as found previously (Subsec. 5.1) with $\lambda_{av} = 0.083$ °C/(W/m²), and the fraction of CH_4 radiation, which contributes to the plate heating, is, independent from Subsec. 4.1, now confirmed by Fig. 11b) with $f_{CH4} = 0.64$ when comparing the measured plate heating ΔH_E (Blue Diamonds) with the calculated back-radiation $f_{CH4}\cdot\Delta I_{CH4}$ (Green Triangles).

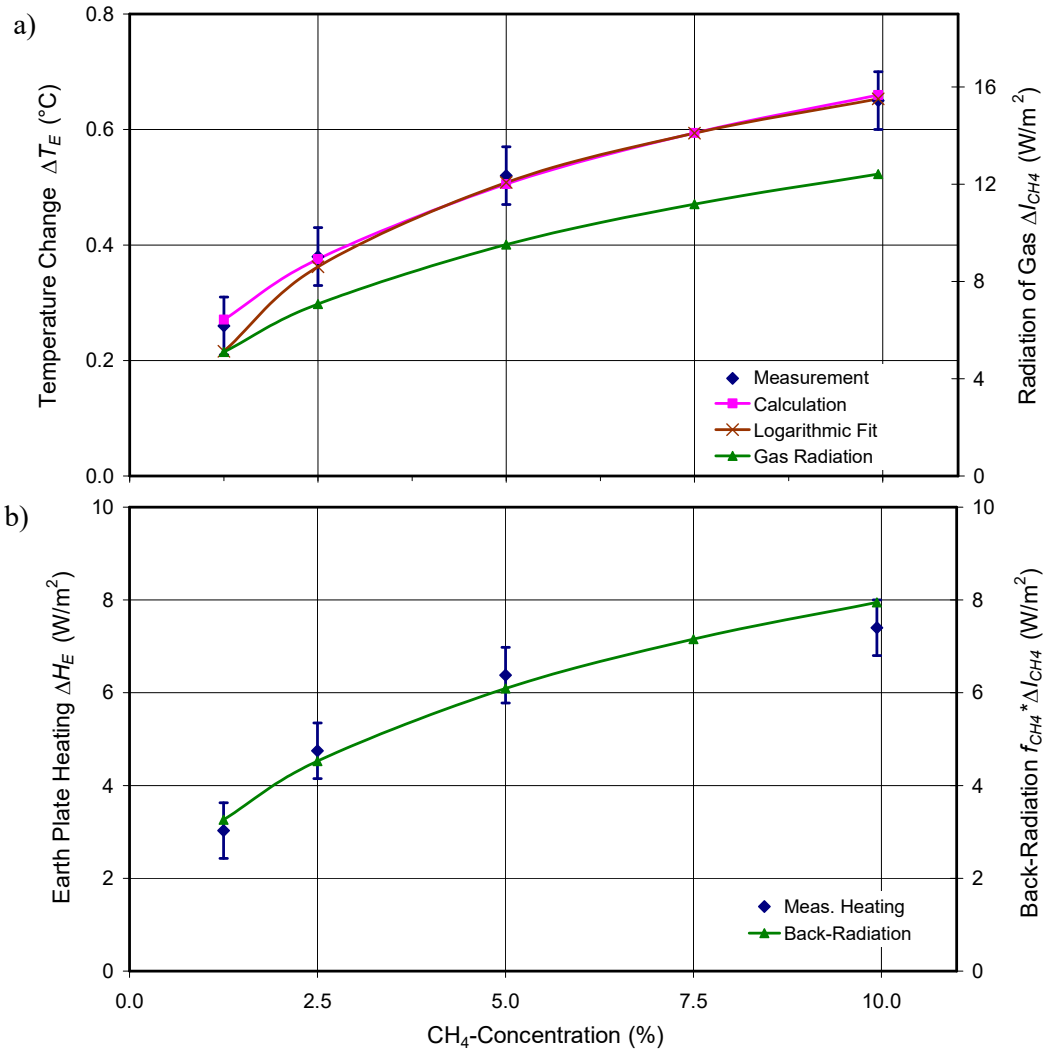

Figure 11: a) Measured temperature change of the earth plate as a function of the CH_4-concentration in dry air (Blue Diamonds) and calculation (Magenta Squares). Superimposed is a fit assuming a logarithmic function (Brown Crosses) and the LBL-RT-calculation of the back-radiation ΔI_{CH4}. b) Comparison of measured plate heating ΔH_E (Blue Diamonds) and calculated back-radiation collected by the earth plate $f_{CH4}\cdot\Delta I_{CH4}$ for f_{CH4} = 0.64 (Green Triangles).

As good approximation, except at the lower concentrations before the CH_4 lines come to saturation, can the measurement and the calculation again be represented by a logarithmic function:

$$\Delta T_E(C_{CH4}) = \Delta T_0 + \lambda_{av} \cdot f_{CH4} \cdot \Delta F_{2xCH4} \cdot \ln(C_{CH4}/C_0)/\ln 2\,, \qquad (12)$$

with ΔT_0 = 0.22°C at C_0 = 1.25% and ΔF_{2xCH4} = 2.75 W/m^2. A third-root approximation even shows still better agreement with the measurements and calculation, but to compare the forcing with the other gases and for the same concentration range, particularly at doubled concentration, we prefer a logarithmic representation.

5.3 N_2O-Measurements

The experimental conditions for the measurements with N_2O are the same as in Subsec. 5.1 and 5.2. The concentration was varied from 1.25% to 15%. Fig. 12a) displays the measured temperature variation ΔT_E of the earth plate with increasing N_2O-concentration (Blue Diamonds) and can again be compared with the calculated temperature change $\lambda_{av}\cdot f_{N2O}\cdot\Delta I_{N2O}$ (Magenta Squares). The respective theoretical N_2O radiation ΔI_{N2O} is shown as Green Triangles.

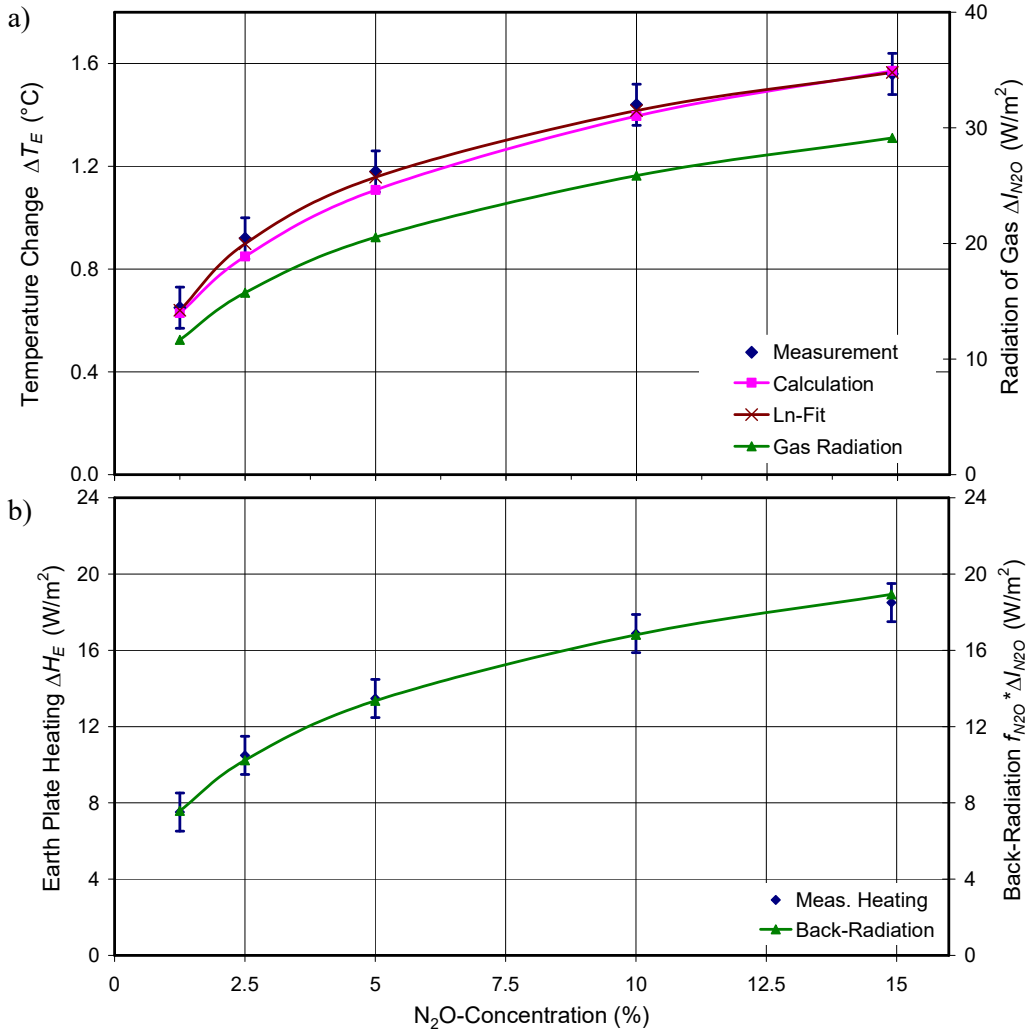

Figure 12: a) Measured temperature change of the earth plate as a function of the N_2O-concentration in dry air (Blue Diamonds) and calculation (Magenta Squares). Superimposed is a fit with a logarithmic function (Brown Crosses) and the LBL-RT-calculation of the back-radiation ΔI_{N2O}.
b) Comparison of measured plate heating ΔH_E (Blue Diamonds) and calculated back-radiation collected by the earth plate $f_{N2O} \cdot \Delta I_{N2O}$ for $f_{N2O} = 0.65$ (Green Triangles).

In Fig. 12b) is plotted the measured plate heating ΔH_E (Blue Diamonds) and the calculated back-radiation $f_{N2O} \cdot \Delta I_{N2O}$ (Green Triangles). From a fit of the theoretical back-radiation to the measurement we derive for the N_2O radiation contributing to the plate heating, the fraction $f_{N2O} = 0.65$, which agrees with the value deduced in Subsec. 4.1 within 5%. The temperature sensitivity is further assumed with $\lambda_{av} = 0.083$ °C/(W/m²).

The measured temperature (see Fig. 12a), Blue Diamonds) can well be represented by a logarithmic curve (Brown Crosses) of the same type as (11) and (12) with:

$$\Delta T_E(C_{N2O}) = \Delta T_0 + \lambda_{av} \cdot f_{N2O} \cdot \Delta F_{2xN2O} \cdot \ln(C_{N2O} / C_0) / \ln 2\,, \qquad (13)$$

now with $\Delta T_0 = 0.62$°C at $C_0 = 1.5\%$ and $\Delta F_{2xN2O} = 5.0$ W/m². The agreement with the theoretical curve (Magenta) is not perfect but is still within our limits of observation. A better agreement with the calculated data but a slightly worse fit to the measurements can be obtained with:

$$\Delta T_E(C_{N2O}) = \Delta T_0 + \lambda_{av} \cdot f_{N2O} \cdot \Delta F_{2xCo} \cdot \sqrt[2]{(C_{N2O} - C_0) / C_0}\,, \qquad (14)$$

with $\Delta T_0 = 0.6$°C, $C_0 = 1.5\%$ and $\Delta F_{2xCo} = 5.5$ W/m², where ΔF_{2xCo} now only represents the forcing

at doubled concentration C_0. We note that such approximations different to a logarithmic function are well known in the literature (see, Myhre et al. [28]).

6. Discussion of Results

Differences to Atmospheric Conditions: The experimental set-up as presented in Section 2 has proven to be appropriate for demonstrating the atmospheric GHE in the laboratory. Although the pathlength through the atmosphere is about a factor of 80,000 larger than in the tank, this is partially compensated by a 500x higher concentration for CO_2, a 50,000x larger CH_4-concentration, and it is even significantly overcompensated for N_2O with an almost 500,000x higher concentration relative to the sea-level values. Not so much the absolute values are relevant, more important is the optical depth, which scales with the absorption coefficient × pathlength.

On the other hand is the lapse rate over the troposphere with 6.5°C/km 5.700x smaller than in our experiment, while the absolute temperature difference is almost comparable.

But most important for the verification of the GHE and the back-radiation from IR-active gases is their emission in the presence of collisions, and this under conditions as found in the lower troposphere. The experiments definitely confirm that GH-gases are radiating on their transitions, and within an optically thick layer even comparable to a black-body radiator at the same temperature as the gas.

Impact of Background Radiation: Under real atmospheric conditions is the back-radiation of the GH-gases superimposed by the much broader radiation from clouds, which in first approximation can be assumed as grey emitters at temperature T_{cl} and with a spectral distribution according to (1), only with an emissivity $\varepsilon < 1$. This can further be covered by Mie-scattering from aerosols or mist, and together they significantly enhance the observed GHE.

In our experiment clouds and any backscattering are represented by the cold plate and walls with their transmitted intensities, which additionally to the GH-gas emission are absorbed by the earth plate. This total back-radiation is strongly changing with the temperature of the cold plate T_C (see Subsec. 4.1a) and in this way simulates the impact of clouds of different heights, and thus temperatures. But it also affects the size of the GH-gas contribution, which depends on the temperature difference between the plates and by this on the lapse-rate. This contribution develops just opposite to the plate's fraction as demonstrated by the measurements in Subsec. 4.1b). Fig. 7 show the increasing absorption ΔH_E of the earth plate with rising temperature difference ΔT and vice versa. Transferred to the atmosphere this means that with clouds the back-radiation is larger than for clear sky, but the relative contribution caused by GH-gases is declining (Harde 2017 [29], Sec. 3 and 4.2).

Reproducibility and Accuracy: The reproducibility of the measurements is strongly dependent on the equilibrium conditions of the whole equipment before filling the compartment with the GH-gas, and this applies also for the further recording of data. The temperature reading is limited to ±0.13°C, and thus, essentially determines the accuracy of the measurements. Also, the electric plate heating is affected by the temperature reading, as any initial and final tracing to derive the difference ΔH_E, requires two temperature measurements. Apparently, this is the main reason for some deviations from one run to the next. Additional perturbations go back to slight variations of the room temperature, which can only be controlled within ±0.2°C.

The error for an individual measurement of the temperature increase ΔT_E and the reduced plate heating ΔH_E we estimate at the lower concentrations as ±20% and at the higher concentrations as about ±10%. However, the overall accuracy can further be improved by repeating the measurements several times. This allows to determine the general trend of a series well within ±5%.

Comparison with Theory: For a direct comparison of the measurements with a calculation the key parameters are the temperature sensitivity λ and the fraction f_G of the gas emission absorbed

by the earth plate. While in the absence of a GH-gas λ can directly be deduced from the slope of the measured temperature increase as a function of the electric heating (see Fig. 8), f_G as the ratio of $\Delta H_E/\Delta I_G$ requires a measurement with the individual GH-gases. Unfortunately, can the emitted fraction of a gas not independently be derived only from our measurements, this would require a known volume radiator as reference; the absorbed fraction f_C from the cold plate can only work as a first orientation. Instead, we are using a theoretical reference, the calculated emission of the gas. This allows a direct comparison of ΔH_E with $f_G \cdot \Delta I_G$, as plotted in Figs 10b) - 12b), and from a fit of the theoretical curve to the measured data we finally get f_G.

The good agreement for all three gases with the calculations can be seen for the temperature data as well as for the plate heating (Figs 10 - 12). Particularly the increasing saturation and the characteristic gradation with inclining gas concentration is well confirmed by the calculations and excludes any larger impact by heat conduction. At the same time these graphs demonstrate the only small further impact on global warming with increasing GH-gas concentrations (see, Harde 2017 [29]).

While the coincidence in the absolute values of measured and calculated data is a consequence of using the theoretical reference for deriving f_G as scaling factor for the absorbed back-radiation and also for the temperature plots, is the almost exact agreement of the derived radiative forcing for CO_2 with $\Delta F_{2xCO2} = 3.70$ W/m^2 more an unexpected coincidence with the literature. So, Myhre et al. [28] present a simplified expression for the CO_2 forcing as $\Delta F = \alpha \cdot \ln(C/C_0)$ with $\alpha = 5.35$ W/m^2, which gives a forcing at doubled CO_2-concentration of $\Delta F_{2xCO2} = \alpha \cdot \ln 2 = 3.71$ W/m^2. But this applies for a lot of different conditions in the atmosphere with a significant impact on ΔF_{2xCO2}.

So, a comparable Earth-atmosphere scenario to our measurement would be a surface temperature of $T_E = 30$°C, a dense cloud cover at about 5,200 m altitude, a CO_2 concentration of 42.7 ppm and no other GH-gases. The cloud cover at this altitude then has a temperature of −11.4°C (slightly increased lapse rate at the higher ground temperature) and radiates with 266 W/m^2 (assuming 100% emissivity), while the reduced CO_2 concentration over a pathlength of 5.2 km ensures a comparable optical path to the experiment (20% ×1.11 m). A simulation under these conditions almost reproduces the measurement with a CO_2 induced back-radiation of 23.5 W/m^2 and a radiative forcing for doubling the concentration from 21.35 ppm to 42.7 ppm of $\Delta F_{2xCO2} = 3.74$ W/m^2. This already includes a first smaller correction due to the declining pressure with altitude, and thus a lower collisional broadening, which reduces the forcing by about 0.2 W/m^2, while the pressure in our measurement and calculation was considered to be constant.

A much larger impact on the back-radiation and the radiative forcing, however, emanates from other GH-gases in the atmosphere, particularly from water vapor. So, under conditions as above and assuming only about one tenth of the regular concentration of H_2O, CH_4 and N_2O, the back-radiation increases by 80 W/m^2, while the CO_2 induced forcing decreases by 1 W/m^2 to 2.71 W/m^2.

When repeating the above calculation with the actual concentrations of the GH-gases (CO_2: 400 ppm; H_2O: 1.46%; CH_4: 1.8 ppm; N_2O: 0.3 ppm), the back-radiation further increases to 418 W/m^2, which is already 87.5% of the up-welling surface emission (478 W/m^2), but due to the strongly overlapping and saturated absorption bands the forcing even reduces to $\Delta F_{2xCO2} = 2.06$ W/m^2. For a ground temperature of 16 °C it further goes down to 1.47 W/m^2 (see Appendix 5, Fig. A5).

A more realistic scenario with a global mean Earth temperature of 16°C, a mean cloud cover of 66%, a cloud emissivity of 63% and calculating the radiative forcing at the top of the atmosphere (TOA) finally gives a value of $\Delta F_{2xCO2} = 3.4$ W/m^2 (see also Appendix 5). So, this must be seen more as a coincidence, when our measurement almost reproduces this measure with its different impacts, which even partly compensate each other. Nevertheless, is this an important orientation, and both the back-radiation by CO_2 and the almost logarithmic variation of the radiative forcing with concentration changes, as expected from the calculations, can well be confirmed by our

measurements. With a Planck response of λ_P = 0.31 °C/(W/m^2), as specified by the IPCC [27] and without feedbacks this gives a basic Equilibrium Climate Sensitivity of $ECS_B = \lambda_P \cdot \Delta F_{2xCO2} \approx$ 1.05°C.

Respective values for CH_4 and N_2O can only indirectly be compared with the literature, as they are only specified for a concentration range (parts per billion) before saturation is observed.

Lineshape Considerations: While standard calculations are using a Lorentzian lineshape for the individual collision broadened transitions, some deviation is expected when assuming a different profile. Measurements by Edwards and Strow [30] on bands of CO_2, e.g., suggest that the far wings decrease approximately exponentially with detuning from the line center, while Lorentz profiles give too much absorption for larger detunings. The reason is that Lorentzian lineshapes result from assuming an infinitely short collision duration between molecules, but in reality collisions typically take a few ps (see also Wijngaarden & Happer, 2020 [31]).

Such a modified shape can be expressed by a core profile, which is multiplied by a wing-suppression factor. To assess the influence of a reduced wing absorption and thus also a reduced back-radiation we have performed LBL-RT calculations with a Lorentzian core profile and a sech^2-wing-suppression function:

$$g_{L,\mathrm{mod}}(\tilde{\nu}) = \frac{\Delta\tilde{\nu}_{mn}/2\pi}{(\tilde{\nu}-\tilde{\nu}_{mn})^2 + (\Delta\tilde{\nu}_{mn}/2)^2} \cdot \left\{ \frac{2}{e^{(\tilde{\nu}-\tilde{\nu}_{mn})/\Delta\tilde{\nu}_S} + e^{-(\tilde{\nu}-\tilde{\nu}_{mn})/\Delta\tilde{\nu}_S}} \right\}^2, \qquad (15)$$

with $\tilde{\nu}_{mn}$ as the transition wavenumber, $\Delta\tilde{\nu}_{mn}$ as the full linewidth caused by collisions (FWHM) and $\Delta\tilde{\nu}_S$ as detuning, at which the wings are declining to 0.42 of their original value.

We use a detuning parameter of $\Delta\tilde{\nu}_S = 10 \cdot \Delta\tilde{\nu}_{mn}$, which for $\Delta\tilde{\nu}_{mn} \approx 0.18\,\mathrm{cm}^{-1}$ corresponds to a detuning of $\Delta\tilde{\nu}_S \approx 1.8\,\mathrm{cm}^{-1}$ and a collision time of a few ps. With the reduced wings also the calculated gas emission ΔI_G is declining, and thus gives a larger f_G to fit the measurements. But a larger f_G finally results in a smaller radiative forcing compared to a pure Lorentzian shape. Table 3 displays a comparison without and with wing-suppression. The radiative forcing for CO_2 and N_2O reduces by about 10%, for CH_4 even by 20%.

Table 3: Comparison of radiative forcings without and with wing-suppression for CO_2, CH_4 and N_2O.

RF (W/m^2)	no wing suppression	with wing suppression
ΔF_{2xCO2}	3.70	3.4
ΔF_{2xCH4}	2.75	2.2
ΔF_{2xN2O}	5.00	4.5

We note that the values in Table 3 were derived from a logarithmic fit to the temperature data to directly compare the radiative forcings of these gases at doubled concentration. Despite the significantly different concentrations of these gases in the atmosphere with differences of more than a factor of 1,000 and thus with a different inset of saturation effects, the radiative forcings are an appropriate means to characterize the gases in terms of their radiative properties. So, we see that individual CH_4 molecules only contribute 65% relative to CO_2 molecules and less than 50% relative to N_2O molecules to the GHE under otherwise same conditions. This also holds in good approximation when considering the gases at considerably lower concentrations before saturation is dominant (see, Harde 2021 [32]).

In this context we have to point to an often-found misinterpretation concerning the global warming potential of methane. So, the radiative efficiency of CH_4 with 3.7x10^{-4} W/m^2/ppb is classified to be 25x larger than that of CO_2 with 1.4x10^{-5} W/m^2/ppb. Such values are derived from the changing absorptivity or emissivity of the gases, when their concentration is changing by 1ppb (parts per billion). But what is done in this case is to compare two gases under completely different conditions: CH_4 at a concentration of 1.8 ppm and CO_2 at a 200x larger concentration, when

it is already strongly saturated. Also, the interference with other green-house gases, particularly with water vapor, is for both gases completely different. Only these diverse conditions pretend a much higher radiative efficiency of methane, respectively a considerably lower value for CO_2. So, at a concentration of 400 ppm in the atmosphere or at 10% in the laboratory experiment the radiative efficiency of CH_4 drops to about 60% of CO_2 (see Table 3), and at a concentration of 1.8 ppm the efficiency of CO_2 is about 1.5 times larger than for CH_4 (see also Wijngaarden & Happer 2019 [33]). Only due to the different saturation strengths on quite different scales is CH_4 assumed to have a 25x larger global warming potential, while a more realistic consideration supposing a doubling each of the actual CH_4, N_2O and CO_2 concentrations shows that CH_4 does not contribute more than about 2% to global warming (Harde 2021 [32]) and N_2O only about 1% relative to CO_2.

7. Conclusion

To our knowledge we present the first demonstration of the atmospheric greenhouse effect in a laboratory experiment, which also allows quantitative measurements under conditions as in the lower troposphere. We use an experimental set-up consisting of two plates in a closed housing, one plate in the upper position heated to 30°C, the other at the bottom and cooled to -11.4°C. The plates have a distance of 1.11 m to each other, and the tank can be filled with the gases of interest to study the radiation transfer between the plates. This set-up largely eliminates convection or heat conduction and allows to reproducibly study the emission of the GH-gases as additional warming of the heated plate due to back-radiation of the gases. We have investigated the GH-gases carbon dioxide, methane and nitrous oxide as a function of the gas concentration. In addition, and independent of the temperature measurements is the back radiations of the GH gases directly recorded as reduced electrical heating of the upper plate.

These measurements clearly demonstrate that contrary to the often misinterpreted 2nd law of thermodynamics a warmer body can further be heated by absorbing the radiation from a colder body, here the radiation from the cooled plate and a GH-gas. The measurements are well confirmed by extensive LBL-RT calculations, which are in full agreement with the recorded temperature and electric heating data, this in absolute numbers and over the whole progression as a function of the gas concentrations. Any noticeable impact in the energy balance due to heat conduction can be excluded by control experiments with noble gases.

At the same time reveal our theoretical studies the principal difficulties to measure the GH-effect as increasing temperature of the gas. More careful examination shows that such trials simply demonstrate heating via absorption of IR or NIR light by the compartment walls, only to some smaller degree by absorption of a gas. But these experiments miss that the greenhouse effect is mainly the result of a temperature difference over the propagation path of the radiation and thus the lapse rate in the atmosphere. A declining GHE with reduced temperature difference between the plates is clearly demonstrated. And *it is an interesting curiosity that, had convection produced a uniform temperature, there wouldn't be a greenhouse effect* (Lindzen 2018 [34]).

Simply expressed: the greenhouse effect contributes to some warming of the Earth's surface and by this also to some additional convection, but not to any remarkable direct warming of the air temperature. At least that is the lesson learned from the experiments with CO_2, methane and nitrous oxide. This finding is of particular importance since air warming is a necessary prerequisite for the alleged CO_2-water vapor feedback, without which there would be no threatening Earth warming.

From our measurements and their comparison with the calculations we derive the radiative forcing of the gases when doubling their concentrations. This is an important measure to characterise the emissivity of the gases under higher concentration levels, when already stronger saturation on the absorption bands is observed, but it also serves as a relative measure at lower concentrations. The found forcings are in good agreement with literature values, which to some degree is also the

result of calibrating the set-up to the spectral calculations based on the HITRAN database, but which independently determine the impact of the gases as a function of their concentration.

While standard calculations for such comparison are using a Lorentzian lineshape for the individual collision broadened transitions, measurements on absorption bands of CO_2 suggest that the far wings decrease approximately exponentially with detuning from the line center, and thus are contributing less absorption for larger detunings than Lorentz profiles. Therefore, we have performed additional calculations with a $sech^2$-wing-suppression profile, and under our experimental conditions we find for the radiative forcing of CO_2 at doubled concentration: $\Delta F_{2xCO2} = 3.4$ W/m^2, for CH_4: $\Delta F_{2xCH4} = 2.2$ W/m^2 and for N_2O: $\Delta F_{2xN2O} = 4.5$ W/m^2. These values are for CO_2 and N_2O about 10% and for CH_4 20% lower than the standard values.

Water vapor as the by far strongest GH-gas in the atmosphere could not be investigated in our set-up. This would require some systematic modifications to realize a similar vapor density profile over the lapse rate as in the atmosphere, and in particular, to avoid condensation at the cold plate. But it would be highly desirable to realize also for this GH-gas quantitative measurements, together with CO_2 as a mixture, to study the interdependence of these gases in their overlapping absorption spectra and by this to collect more reliable data about their impact on our climate. Based on a set-up as presented here but with a further developed equipment, particularly with well stabilized components and an improved temperature recording such investigations would be very helpful for objectification of the further climate debate.

Already the presented measurements and calculations demonstrate the only small impact on global warming with increasing GH-gas concentrations due to the strong saturation. Therefore, we strongly recommend not to further provoke crying and jumping kids by fake experiments and videos only to generate panic, but to teach them in serious science with realistic demonstrations and information about the impact and also benefits of GH-gases. Then scholars and also adults can decide, if it is worthwhile to further demonstrate on streets for a stable climate, which apparently is mainly controlled by natural impacts (see Harde & Salby 2021 [35]; Salby & Harde 2021 [36, 37]), and if we are really living on a planet, which can only be rescued by stopping all fossil fuel emissions without a realistic perspective for a secure and healthy future of our lives. In the long term, an economic shift to new forms of energy generation, of whatever kind, is inevitable, since the supply of fossil fuels is finite. However, there is no need to drive this process blindly and hastily; otherwise, there is a risk of deindustrialization, which would then really trigger a dire future for the next generations.

Funding

This research did not receive any specific grant from funding agencies in the public, commercial, or not-for-profit sectors. The experimental set-up was developed and paid privately by MS.

Guest-Editor: Prof. Jan-Erik Solheim; Reviewers were anonymous.

Acknowledgements

We thank Eike Roth and Christoph Marvan for stimulating discussions and valuable advices. Also, we thank Ulrich Tengler for his support with a cryostat. Further we would like to express our special thanks to the editors and reviewers for their comments and support of this publication.

Appendix 1 - Experimental Set-Up

The main components of the experimental setup consist of the tank, the earth plate, the cold plate, and the upper dome (Fig. 1). The earth plate is a composite of a 0.8 mm thick blackened aluminum disk (Ø = 16.7 cm) with an equally sized self-adhesive heating foil (12 V/DC, AC 14 W) on its back side. As insulation between the heating foil and upper dome works a 2 cm thick Styrofoam

disc (Ø = 17 cm) which is glued to the dome (Fig. A1.1a).

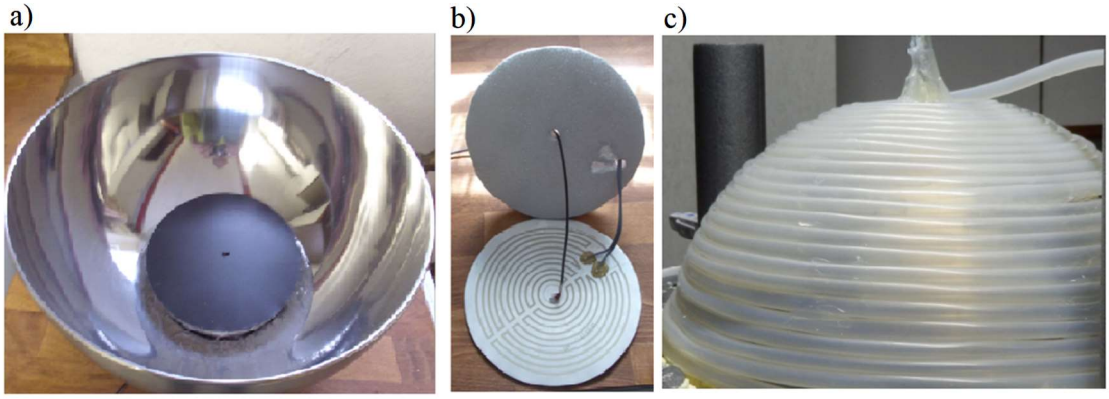

Figure A1.1: a) Earth plate with temperature sensor in the upper dome, b) Back side of the earth plate with heating foil and polystyrene disc, c) Outside of the dome with vinyl tubing for the thermostated water. In the background one of the 23 pipe insulations, made of flexible polyethylene foam for the tank and dome insulation.

The temperatures of the earth plate, the upper dome and the cold plate are measured by temperature sensitive diodes (Infineon KTY 11-5: TO-92) and are recorded every 3 minutes by a computer. The calibration is described in Appendix 2.

The earth plate heating is supplied by a digital laboratory power device (KA3005D, 0 – 15 V, resolution 0.01 V) in constant voltage mode. The heating power is the voltage times current for the earth plate of 219.04 cm^2. This value is multiplied by 45,654 to convert to an area of 1 m^2 (H_{PE}).

For a temperature increase δT_E of 0.13°C the voltage must be changed by 0.03 V. The accuracy of the temperature reading of the earth plate is ± 0.13°C, which is our limit of detection. Due to this digital display two heating values, an upper and a lower value, are recorded at intervals of 0.01 V and their average determines the temperature T_E (Appendix 4, Table A4.1).

The upper dome is wrapped with a vinyl tube (Ø = 10 mm) through which thermostated water flows (ESCO ES 10) with a temperature of 30.0 ± 0.1°C (Fig. A1.1c). The free space above the dome is filled with Styrofoam flakes and sealed with a 5 cm thick Styrofoam disc.

The tank consists of two 0.8 mm thick, 1 x 1 m aluminum sheets bonded with silicone (Fig. A1.2a). The inside is polished and the two seams are covered with aluminum foils (Fig. A1.2b). From the outside, the tank is wrapped in three sections, each with 25 m (Ø =12 mm) PVC tubing, through which thermostated water flows, only for calibration of the temperature sensors (Fig. A1.2c). For all other measurements, the water is removed from the PVC hoses.

In distances of 25 cm the tank has 3 small holes and one hole in the upper dome to place thermometers (TFA 30.1040) 2 cm deep, which measure the wall temperatures T_1 to T_4 at these positions. Since all measurements are made at thermal equilibrium, it is assumed that the air in the tank has approximately the same temperature as the wall at that position.

The cold plate in the lower dome consists of a 0.6 mm thick copper disk (Ø = 35.5 cm) with a diode (Infineon KTY 11-5: TO-92) and 5 thermocouples (TEC1-12706, 40 x 40 x 3.8 mm) mounted in the center (Fig. A1.3a). The voltage of the thermocouples is measured with a digital multimeter (HP-760D) and indicates the injection of heavy sample gases in the lower dome by a voltage drop.

A 6 m long (Ø = 8 mm) copper tube is soft soldered to the back of the cold plate, through which an ethanol-water mixture flows, which can be cooled down to -16 °C by a cryostat (Isotemp

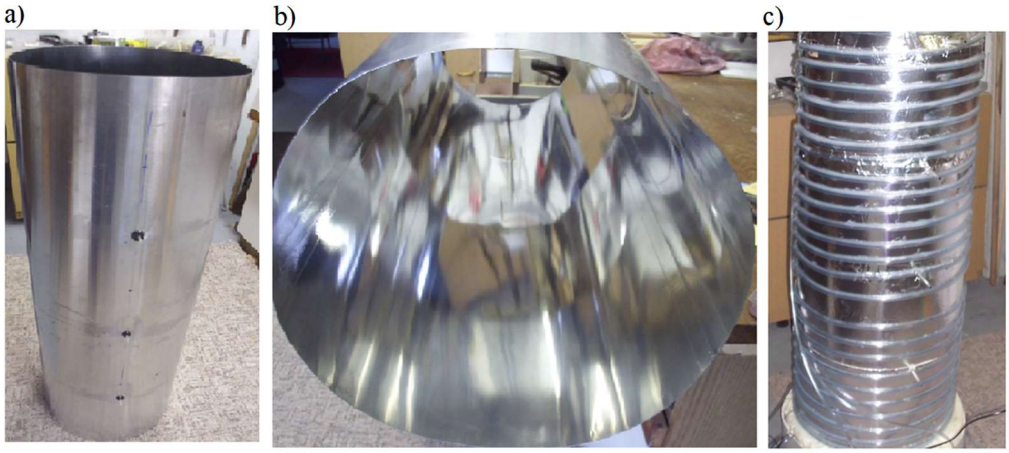

Figure A1.2: a) Exterior view of the tank with the rubber discs for placing thermometers, b) Interior view of the polished Al-tank, c) PVC hoses for temperature control of the tank.

1016S). The copper tubes are thermally insulated with urethane construction foam and the insulation layer sealed with bottom paint.

To insulate the tank and the two domes, 23 polyethylene soft foam pipe insulations (5 x 140 cm) are glued to the pipe wall, the interiors are filled with 1 mm polystyrene balls and wrapped with 7 layers of aluminum-laminated polystyrene wallpaper, creating a 7 cm thick insulation layer. The room temperature is thermostated (ESCO ES 10) to 20.5 ± 0.2°C by a fan heater and two additional fans.

Figure A1.3: a) Cold plate with 5 thermocouples and temperature sensor in the lower dome, b) Back side of the cooling plate with copper spiral connected to the cryostat, c) Polyurethane insulation of the copper spiral.

Prior to each measurement, the air in the tank is pumped around for 12 hours with a flow rate of 1.5 l/min over solid sodium hydroxide, minimizing water vapor and CO_2 concentrations in the air (Fig. 1). The sodium hydroxide container is then removed directly before starting a run. 6 - 8 hours earlier the room thermostat, the heater for the earth plate and the cryostat for the cold plate are switched on to stabilize the set-up at the desired temperatures.

The IR-active gases CO_2, CH_4 and N_2O are stored in small gas bottles or cans and the respective quantities are determined by weighing. The volumes of helium and argon are metered via a rotameter (Brooks instrument 0 - 3.5 l/min). The gases are injected through 10 cm long copper tubes (Ø = 6 mm) either into the lower dome below the cold plate or into the upper dome below the earth plate, depending on their specific density compared to air (Fig. 1). An air pump then sucks the air out of the upper dome and fills it back into the lower inlet to mix the air and gas evenly. The measurement of the oxygen concentration (Sumatec technical diving) ensures that air and sample gases have been completely homogenized (Fig. 1). For the purity of the sample gases see Table A1.

Table A1: Origin and purity of the sample gases

Gas	Distribution	Purity (%)
CO_2	Cosmeda	99.9
CH_4	WINDAUS-Labortechnik	99.9
N_2O	LG Engros ApS	99.7
Ar	Hornbach	99.9
He	Amazon	99.9

Appendix 2 - Calibration of the Temperature Sensors

The calibration of the temperature sensor (diode) for the earth plate (T_E) and the thermometers (T_1 - T_2) is carried out by gradually heating the entire apparatus from 20 to 34°C (Fig. A2a) . For this purpose, water at a defined temperature (from a water thermostat (ESCO ES 10) with a calibrated thermometer GDR, TGL 11996 N, 0.2 K) is pumped simultaneously through the pipes of the cooling plate (Fig. A1.3a), the tank (Fig. A1.2c) and the dome (Fig. A1.1c). The recorded signals are correlated with the water temperatures. The absolute temperature of the earth plate can deviate from the specified values by up to 0.2 °C due to the limited accuracy of the calibration thermometer.

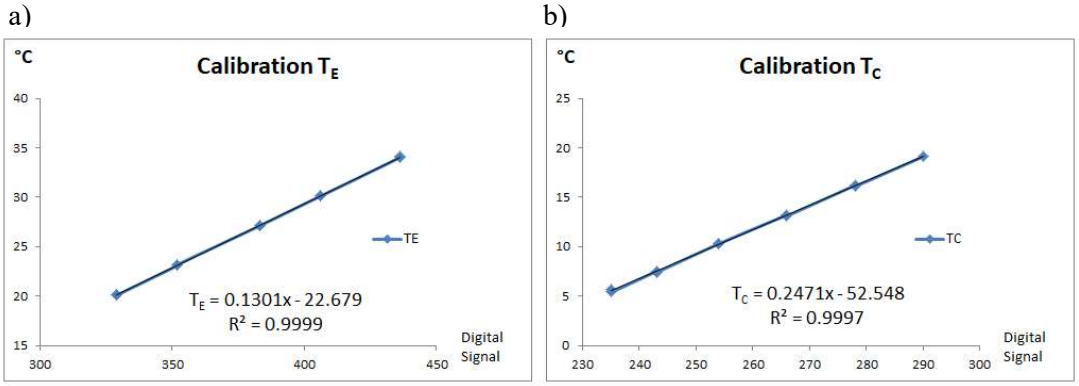

Figure A2: Calibration of the temperature sensors, a) Temperature of the earth plate T_E, b) Temperature of the cold plate T_C.

The calibration of the cold plate diode (T_C) and the thermometers (T_3 - T_4) is performed in the same way except that instead of a thermostat, the Isotemp 1016S cryostat is connected and the water temperature is gradually cooled from 20 to 5°C (Fig. A2b). When the water temperature is further reduced, larger heat losses occur and the linear trend is no longer given. Therefore, a temperature measurement T_C < 5°C is done by extrapolation with a linear trend according to Fig. A2b). The absolute temperature of the cold plate can deviate from the specified values by up to 0.2 °C due to the limited accuracy of the calibration thermometer.

Appendix 3 - Influence of Heat Conduction

When the tank is filled with a sample gas, as described in Subsec. 5.1 to 5.3, the heat conductivity $L(\Delta T)$ of the gas mixture changes as a function of temperature and gas concentration, since air and sample gas have different thermal conductivities (Table A3). This could change the heat transport and according to eq. (8), $K(T_W, \Delta T)$ as well as the temperature of the earth plate T_E could change.

Table A3: Heat conductivity of air and sample gases

Gas	Heat Conductivity 25 °C κ (W/m·K)
CO_2	0.016
N_2O	0.017
Ar	0.018
Air	0.026
CH_4	0.034
He	0.150

Such objection can be checked by control experiments with the noble gases Ar and He (Fig. A3), which are IR-inactive but have different thermal conductivities compared to air (Table A3). The measurements with these gases were performed under identical experimental conditions as described in Subsec. 5.1 and with concentrations of 10% and 20%, respectively.

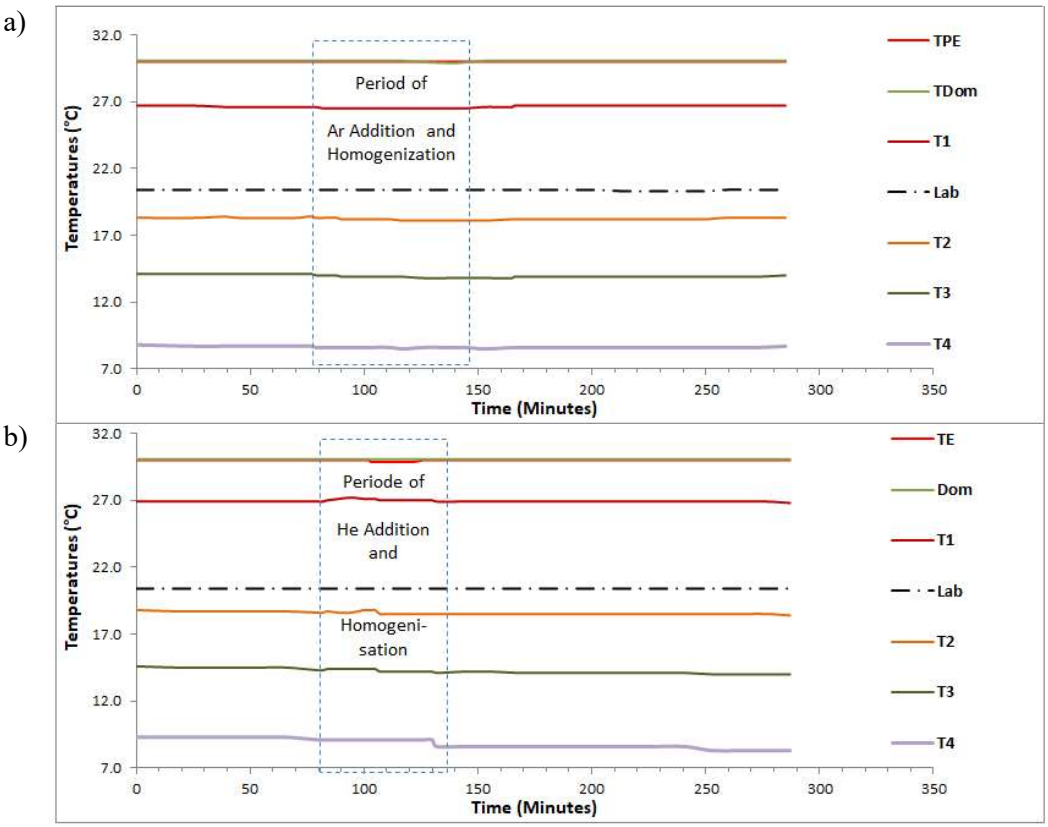

Figure A3: a) Control test with 10% Ar and b) with 20% He. Plotted are the temperatures of the earth plate (Red), the dome (Green), the gas temperature at 4 positions (T_1 - T_4) and the laboratory temperature (Black).

None of these trials showed any change of the earth plate temperature T_E. This is not really surprising, because already the cooling experiments with the noble gases in Sec. 4 (see also Appendix 4, Table A4.3) had no influence, although the temperatures were changing over a much wider range.

Appendix 4 - Details for the Validation of the Measuring System (Section 4)

In this appendix we have compiled typical data for the cooling experiment of Subsec. 4.1 when changing the temperature T_C of the cold plate between -12.9°C and +10.9°C (Table A4.1, column

2) while measuring the electric heating intensity H_E for the earth plate (column 3) to stabilize the temperature T_E of the earth plate at 30°C (column 1). Due to the thermal inertia of the measuring system, two values for H_E are always recorded for one temperature step.

Table A4.1: Example of a cooling experiment; T_C from -12.9°C up to +10.9°C

T_E °C	T_C °C	H_E W/m²	I_E W/m²	I_C W/m²	ΔT °C	I_E-I_C W/m²	Room T_p °C
30.0	-12.9	169.6	478.9	260.3	42.9	218.6	20.3
30.0	-12.9	169.9	478.9	260.3	42.9	218.6	20.3
30.0	-7.2	153.9	478.9	283.6	37.2	195.3	20.4
30.0	-7.2	152.8	478.9	283.6	37.2	195.3	20.4
30.0	-1.1	133.9	478.9	310.6	31.1	168.3	20.4
30.0	-1.1	133.7	478.9	310.6	31.1	168.3	20.4
30.0	5.3	111.9	478.9	340.7	24.7	138.2	20.4
30.0	5.3	111.3	478.9	340.7	24.7	138.2	20.4
30.0	10.9	90.5	478.9	369.0	19.1	109.9	20.3
30.0	10.9	89.7	478.9	369.1	19.1	109.8	20.3

Table A4.2: $f_C = \Delta H_E/\Delta I_C$ and $H_E(0,T_W)$ in air; T_C from -13°C to +11°C, T_E = 30°C

No.	$\Delta H_E/\Delta I_C$	$H_E(I_C=0)$
1	0.73	361.4
2	0.75	366.1
3	0.74	363.7
4	0.74	362.5
5	0.75	365.6
6	0.74	361.8
7	0.74	363.9
8	0.75	366.1
9	0.75	366.8
10	0.74	363.5
Ø	0.74	364.1
Std Dev.	0.005	1.8

The repeatability and accuracy of such measurements is demonstrated by a series of 10 independent runs (see Table A4.2). These data are compared with the difference of the calculated intensity I_E of the earth plate as loss and the emitted intensity I_C of the cold plate as maximum possible radiation, which can be absorbed by the earth plate to partially compensate for the losses. According to eq.(7) from these data we derive the fraction f_C of the cold plate radiation, which is absorbed by the earth plate (see Fig. 6).

Table A4.3 displays identical measurements only with different sample gases.

Table A4.3: Slope $\Delta H_E/\Delta I_C$ and $H_E(0,T_W)$ with sample gases; T_C from -13°C to +11°C, T_E = 30°C

Gas	C Vol.-%	$\Delta H_E/\Delta I_C$	$H_E(I_C=0)$ (W/m²)
Ar	10	0.73	362
Ar	20	0.75	367
He	10	0.74	365
He	20	0.74	362
CH_4	10	0.70	345
CO_2	10	0.68	335
N_2O	10	0.66	324

Appendix 5 - Different Impacts on Radiative Forcing

To assess the different contributions, which mainly modify the radiative forcing under atmospheric conditions and also determine the difference to our measurement, we start with conditions comparable to the experiment and then adapt them step by step to the atmospheric situation to evaluate their individual impacts on ΔF_{2xCO2}.

For a ground temperature T_E = 30°C and a cloud cover at 5.2 km altitude the optical path through a dry atmosphere with a CO_2 concentration of 42.69 ppm would be the same as for a 20% CO_2 concentration in air over a distance of 111 cm. At this altitude the clouds have a temperature of −11.4°C and are supposed to emit like a black body. A simulation under these conditions gives a forcing of ΔF_{2xCO2} = 3.74 W/m^2 and almost exactly reproduces the laboratory experiment, but already includes a first correction due to the declining pressure with altitude. This contributes to a lower collisional broadening and reduces the forcing by 0.22 W/m^2, while with a constant pressure in the tank this gives a theoretical forcing of 3.96 W/m^2 (see below). Fig. A5 reveals the individual changes of the forcing as up or down directed arrows in W/m^2.

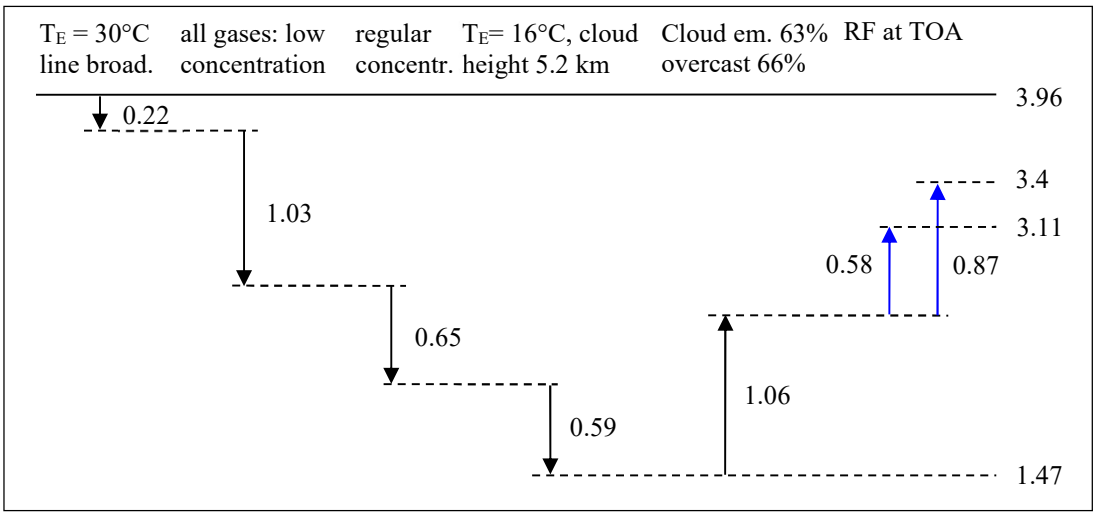

Figure A5: Changes of radiative forcing ΔF_{2xCO2} in W/m$_2$ caused by different impacts. Black arrows indicate changes in the back-radiation, blue arrows in forward radiation (to TOA).

A significantly stronger impact emanates from other GH-gases in the atmosphere, particularly from water vapor. Assuming only about one tenth of the regular concentration of H_2O, CH_4 and N_2O, the back-radiation already increases by 80 W/m^2 (from 289.5 to 369.0 W/m^2), while the CO_2 induced forcing decreases by 1.03 W/m^2 to 2.71 W/m^2.

When supposing regular concentrations in the atmosphere with 400 ppm CO_2, without other GH-gases the forcing would jump up to 5.7 W/m^2 (not shown), but in the presence of the other gases at normal concentrations (H_2O: 1.46%; CH_4: 1.8 ppm; N_2O: 0.3 ppm) the forcing further declines. While the back-radiation increases to 418 W/m^2, which is already 87.5% of the up-welling surface emission (478 W/m^2), owing to the strongly overlapping and saturated absorption bands the forcing even declines by additional 0.65 W/m^2 to ΔF_{2xCO2} = 2.06 W/m^2.

A further decrease by 0.59 W/m^2 to 1.47 W/m^2 is expected when lowering the ground temperature to 16°C at otherwise same conditions. On the other hand, semitransparent clouds with an emissivity of 0.63 and an overcast of 66% increase the forcing by 1.06 W/m^2 to 2.53 W/m^2, which is just 64% of the initial value.

However, direct comparison with literature often requires to consider the forcing in upward direction from the surface to TOA, which due the longer interaction over the whole atmosphere and with varying O_3 concentration over the stratosphere further raises the forcing by 0.58 W/m^2 to ΔF_{2xCO2} = 3.11 W/m^2 (left Blue Arrow in Fig. A5). Different to this more straight forward

calculation other approaches consider the forcing as difference of the upwelling and downwelling sw and lw radiation in the tropopause, while simultaneously assuming stratospheric thermalization (Myhre et al. [28]). These different attempts rely on the applied models used to calculate the global warming caused by the GH-gases, and therefore they also differ in their size.

We note that the calculated forcings at doubled CO_2 concentration not strictly obey a logarithmic dependency but show relatively higher values for higher concentrations. E.g., a calculation for 200 ppm doubled gives a forcing 0.4 W/m^2 larger than the respective calculation for 100 ppm. While our experimentally derived value with ΔF_{2xCO2} = 3.7 W/m^2 was determined by a fit to the measured data over a wide range from 1.25% up to 20% (16x), only doubling from 10% to 20% gives a value of 3.96 W/m^2. This also explains the higher start value in Fig. A5, and all other forcings or changes in this subsection, which relate to this figure were found by doubling 21.35 ppm resp. 200 ppm.

All black arrows in Fig. A5 designate changes in the back-radiation, whereas blue arrows indicate the difference to a calculated upward forcing at the TOA. In this case is the upward forcing 0.58 W/m^2 larger than the downward forcing. And when calculating the doubling with an initial concentration as assumed in pre-industrial times with 280 ppm, this gives a final radiative forcing at TOA of ΔF_{2xCO2} = 3.4 W/m^2.

References

1. J. B. Fourier, 1824: *Remarques Générales Sur Les Températures Du Globe Terrestre Et Des Espaces Planétaires.* In: *Annales de Chimie et de Physique*, Vol. 27, 1824, S. 136–167. https://books.google.co.uk/books?id=1Jg5AAAAcAAJ&pg=PA136&hl=pt-BR&source=gbs_selected_pages#v=onepage&q&f=false, Oct.21
2. J. Tyndall, 1861: *On the Absorption and Radiation of Heat by Gases and Vapours, and on the Physical Connexion of Radiation, Absorption, Conduction*, The Bakerian Lecture, The London, Edinburgh, and Dublin Philosophical Magazine and Journal of Science, Series 4, Vol. 22, https://www.jstor.org/stable/108724, Oct.21
3. G. Kirchhoff, 1859: *Monatsberichte der Akademie der Wissenschaften zu Berlin*, Sessions of Dec. 1859, 1860, Berlin, pp. 783-787).
4. J. Stefan, 1879: *Über die Beziehung zwischen der Wärmestrahlung und der Temperatur*, in: Sitzungsberichte der mathematisch-naturwissenschaftlichen Classe der kaiserlichen Akademie der Wissenschaften, Bd. 79 (Wien 1879), pp. 391-428.
5. L. Boltzmann, 1884: *Ableitung des Stefan'schen Gesetzes, betreffend die Abhängigkeit der Wärmestrahlung von der Temperatur aus der electromagnetischen Lichttheorie*, Annalen der Physik und Chemie. Bd. 22, pp. 291–294, https://doi.org/10.1002/andp.18842580616.
6. M. Planck, 1900: *Zur Theorie des Gesetzes der Energieverteilung im Normalspectrum*, Verh. Deutsche Phy. Gesell. 2, No. 17, p. 220 and pp. 237-245.
7. S. Arrhenius, 1896: *On the influence of carbonic acid in the air upon the temperature of the ground*. In: Philosophical Magazine and Journal of Science. Vol. 41, No. 251, April 1896, S. 237-276, https://doi.org/10.1080/14786449608620846, Oct.21
8. R. W. Wood, 1909: *Note on the Theory of the Greenhouse*, London, Edinborough and Dublin Philosophical Magazine, Vol. 17, pp. 319-320.
9. N. S. Nahle, 2011: *Repeatability of Professor Robert W. Wood's 1909 experiment on the Theory of the Greenhouse,* Biology Cabinet Online-Academic Resources and Principia Scientific International, Monterrey, N. L.
10. V. R. Pratt, 2020: *Wood's 1909 greenhouse experiment, performed more carefully*, http://clim.stanford.edu/WoodExpt/, Dec. 2021.

11. E. Loock, 2008: *Der Treibhauseffekt - Messungen an einem Wood'schen Treibhaus*, https://docplayer.org/30841290-Der-treibhauseffekt-messungen-an-einem-wood-schen-treibhaus-von-ehrenfried-loock-version.html, Oct.21.

12. T. O. Seim, B. T. Olsen, 2020: *The Influence of IR Absorption and Backscatter Radiation from CO_2 on Air Temperature during Heating in a Simulated Earth/Atmosphere Experiment*, Atmospheric and Climate Sciences, 10, pp. 168-185, https://doi.org/10.4236/acs.2020.102009, Oct.21.

13. H. v. Ditfurth, 1978: *Treibhauseffekt*, https://www.youtube.com/watch?v=lORAR1nvfjs, Oct.21.

14. M. Schnell, 2020: *Die falschen Klimaexperimente*, https://www.eike-klima-energie.eu/2020/11/06/die-falschen-klima-experimente/, Oct.21

15. A. Gore, D. Guggenheim, 2006: *An Inconvenient Truth*, Movie, https://www.imdb.com/title/tt0497116/, Oct.21

16. A. Watts, 2011: *Replicating Al Gore's Climate 101 video experiment shows that his "high school physics" could never work as advertised*, https://wattsupwiththat.com/2011/10/18/replicating-al-gores-climate-101-video-experiment-shows-that-his-high-school-physics-could-never-work-as-advertised/?cn-reloaded=1, Oct.21

17. J.-E. Solheim, 2016: *Start des zweitägigen „Al Gore-Experiments"*, 10. Internationale Klima- und Energie-Konferenz (10. IKEK), EIKE, Berlin, https://www.eike-klima-energie.eu/2017/02/04/10-ikek-prof-em-jan-erik-solheim-start-des-zweitaegigen-al-gore-experiments/, October 2021

18. L. S. Rothman, I. E. Gordon, A. Barbe et al., 2009: *The HITRAN 2008 molecular spectroscopic database*, J. Quantitative Spectroscopy and Radiative Transfer, vol. 110, no. 9-10, pp. 533–572.

19. H. Harde, 2013: *Radiation and Heat Transfer in the Atmosphere: A Comprehensive Approach on a Molecular Basis*, Intern. Journal of Atmospheric Sciences, vol. 2013, Article ID 503727, 26 pages, http://dx.doi.org/10.1155/2013/503727, Oct.21.

20. H. Harde, J. Pfuhl, 2016: *MolExplorer - A Program-Platform for the Calculation of Molecular Spectra and Radiation Transfer in the Atmosphere*, Helmut-Schmidt-University Hamburg, http://hharde.de/#xl_xr_page_research%20j, Oct.21.

21. K. Schwarzschild, 1906: *Über das Gleichgewicht der Sonnenatmosphäre*. In: Nachrichten von der Königlichen Gesellschaft der Wissenschaften zu Göttingen, Mathematisch-Physikalische Klasse, 1906, Heft 1, pp. 41–53 (13. Januar 1906).

22. M. Wolff, H. Harde, 2003: *Photoacoustic Spectrometer Based on a Planckian Radiator with Fast Time Response*, Infrared Physics and Technology 44, pp. 51-55.

23. H. Harde, G. Helmrich, M. Wolff, 2010: *Opto-Acoustic ^{13}C-Breath Test Analyzer,* BIOS, Proc. SPIE 7564, Photons Plus Ultrasound: Imaging and Sensing 2010, 75641E (24 Feb. 2010), San Francisco, https://doi.org/10.1117/12.841660, Oct21.

24. D. Tobin, 1986: *Data Courtesy of D. Tobin*, Space Science and Engineering Center, University of Wisconsin-Madison, Madison, USA.

25. P. Arnott, 2008: *Graphic from Pat Arnott*, University of Nevada, Reno, USA, ATMS 749

26. D. R. Feldman, W. D. Collins, P. J. Gero, M. S. Torn, E. J. Mlawer, T. R. Shipert, 2015: *Observational determination of surface radiative forcing by CO_2 from 2000 to 2010,* Nature 519, No. 7543, p. 339. https://doi.org/10.1038/nature14240, Oct21.

27. Sixth Assessment Report (AR6) of the IPCC, 2021: *Summary for Policymakers*. In: Climate Change 2021: The Physical Science Basis. Contribution of Working Group I to the Sixth

Assessment Report of the Intergovernmental Panel on Climate Change [Masson-Delmotte, V. et al. (eds.)]. Cambridge University Press.

28. G. Myhre, E. J. Highwood, K. P. Shine, and F. Stordal, 1998: *New estimates of radiative forcing due to well mixed greenhouse gases*," Geophysical Research Letters, vol. 25, no. 14, pp. 2715–2718.
29. H. Harde, 2017: *Radiation Transfer Calculations and Assessment of Global Warming by CO_2* , International Journal of Atmospheric Sciences, Volume 2017, Article ID 9251034, pp. 1-30, https://doi.org/10.1155/2017/9251034, https://www.hindawi.com/journals/ijas/2017/9251034/, Oct21.
30. D. P. Edwards, L. L. Strow, 1991: *Spectral Lineshape Considerations for limb Temperature Sounders*, J. Geophys. Res. 96, p. 20859.
31. W. A. van Wijngaarden, W. Happer, 2020: *Dependence of Earth's Thermal Radiation on Five Most Abundant Greenhouse Gases,* arXiv.org > physics > arXiv:2006.03098 https://arxiv.org/pdf/2006.03098.pdf, Oct21.
32. H. Harde, 2021: *Methane Sensitivity*, http://hharde.de/#xl_xr_page_climate%20b, Oct21.
33. W. A. van Wijngaarden, W. Happer, 2019: *Methane and Climate*, https://co2coalition.org/wp-content/uploads/2021/08/Methane-and-Climate.pdf, Oct21.
34. R. Lindzen, 2018: *The 2018 Annual GWPF Lecture: Global Warming for the Two Cultures,* The GlobalWarming Policy Foundation, 2018 Annual GWPF Lecture, Institution of Mechanical Engineers, London, 8 October 2018, https://www.thegwpf.org, Oct21.
35. H. Harde and M. L. Salby, 2021: *What Controls the Atmospheric CO_2 Level*?, Science of Climate Change, Vol. 1, No. 1, pp. 54-69, https://doi.org/10.53234/scc202106/22, Oct21.
36. M. L. Salby, H. Harde, 2021: *Control of Atmospheric CO_2 - Part I: Relation of Carbon 14 to Removal of CO_2*, Science of Climate Change, Vol. 1, No.2, pp. 177-195, https://doi.org/10.53234/scc202112/30.
37. M. L. Salby, H. Harde, 2021: *Control of Atmospheric CO_2 - Part II: Influence of Tropical Warming*, Science of Climate Change, Vol. 1, No.2, pp. 196-212, https://doi.org/10.53234/scc202112/12.

Some Climate Simplicities

Correspondence to corkhay-den@comcast.net

Vol. 2.1 (2022)

pp. 34-37

Howard "Cork" Hayden

Prof. Emeritus of Physics, University of Connecticut, USA

Submitted 02-01-2022, Accepted 14-02-2022. https://doi.org/10.53234/scc202203/11

Question: If I add heat to something, how much does the temperature rise? Answer: It depends.

If you add heat to ice water, you melt ice, but the temperature remains constant until all the ice is gone. The same amount of heat that would raise the temperature of a kilogram of water by 1ºC would, if delivered rapidly, easily be enough to set a tree leaf on fire. If heat were added to a rocky surface, the surface temperature would depend on how much heat would be re-radiated and how much heat would be conducted through the rock to the cooler ground beneath it. Heat added to a square meter of a puddle would have an entirely different effect than the same amount of heat added to a square meter of ocean water.

Therein lies the problem with climate models that attempt to estimate temperature rise due to increases in CO_2 and H_2O, or more specifically to increases in heat retention due to those greenhouse gases. You can get anything you want.

There are, however, some unambiguous simplifications that arise from simply asking answerable questions.

Question 1: How much IR does the earth radiate to outer space?

There is an equation known as the Planetary Heat Balance equation which asserts that the heat absorbed from the sun equals the heat radiated to outer space: $I_{in} = I_{out}$, both variables representing average fluxes over the surface of the planet. There can be imbalances, due to orbital eccentricity or changing conditions, of course. For the earth at present, there is a net imbalance: $I_{in} - I_{out}$ = 0.6-0.7 W/m^2 (Figure 2.11 from IPCC's *Fifth Assessment Report*) amounting to less than 0.3 % of I_{in}. At equilibrium—defined as equality of the two quantities—$I_{in} = I_{out}$. This simplicity becomes, with α representing the albedo,

$$I_{out} = \frac{I_{sun}}{4}(1-\alpha) \tag{1}$$

This simple equation tells us that at equilibrium I_{out} is calculable from exactly two variables: the solar intensity at orbit and the planetary albedo. To calculate I_{out} specifically does not require knowledge of the amounts of greenhouse gases, polar vortices, winds,

the lapse rate, or any other phenomena normally associated with weather and/or climate. For the earth I_{out} = 239 W/m^2.

Another conclusion that can be drawn from Equation (1) is that if infrared radiation to outer space (I_{out}) changes, it can happen only if the solar flux I_{sun} changes, the albedo changes, or both. If, for example, a climate model says that I_{out} increases, but does not acknowledge (and explain) how the solar flux and/or the albedo changes, the model is faulty.

Question 2: How much IR is emitted from the surface?

The Stefan-Boltzmann law tells us how much IR the surface emits. Assuming an emissivity of 1.0, climate scientists are in agreement that approximately 398 W/m^2 (averaged over the surface[1]) is emitted from the surface, whose average temperature is ca. 289 K. The numbers vary slightly, depending on the source of the data, but those minor differences are not of importance in this discussion; nor would a few percent decrease in assumed emissivity have an appreciable effect on the results.

The 159 W/m^2 difference between the surface emission (398 W/m^2) and the emission to space (239 W/m^2) is—*finally*, in IPCC's *Sixth Assessment Report*—assigned a name and a variable: the greenhouse effect *G*. Thus

$$I_{out} = \sigma T_{surf}^4 - G \tag{2}$$

The processes by which the atmosphere causes the reduction in IR are many and complicated. If IR is absorbed by a GHG, the molecule can radiate IR or it can shed the excess energy by collisions with atmospheric molecules. Molecular collisions can cause excitation in GHGs that can radiate IR in random directions. The absorption cross-sections and emission rates are dependent on both temperature and pressure. Reflection of IR from the bottoms of clouds can send IR back to the surface. Refraction of IR through water droplets can change the direction, and multiple events can send IR back to the surface. Winds can move the absorbed energy around. It takes real expertise to keep track of all the complications.

Despite all the complications, there remains the fact that the *net* effect of the atmosphere is the greenhouse effect *G*. Presently the net effect of the atmosphere is to reduce the surface radiation by 159 W/m^2.

A = B and A = C $\Rightarrow$ B = C

Equations (1) and (2) can be combined simply, with the result

$$\sigma T_{surf}^4 - G = \frac{I_{sun}}{4}(1-\alpha) \tag{3}$$

Equation (3) is the summary of the two simplicities. It is not a predictor of future climate, but rather a general constraint that applies to all planets and moons that have a surface. Without atmosphere, G is zero. Alternatively, it may be regarded as an acid test

[1] 395,6 W/m^2

for climate models. Whatever future temperature the model predicts, Equation (3) must be balanced.

Question 3: If the surface warms up, how much more IR does it radiate?

We began this discussion by asking how much the temperature would change if we added some fixed amount of heat, and immediately ran into complications. However, if we turn the question around and ask how much more would the surface of the earth radiate if the temperature changed by (say) 1 ºC, the answer is simple and unambiguous.

Let us find the first differential of Equation (3):

$$4\sigma T_{\text{surf}}^3 dT - \left(dG_{\text{CO2}} + dG_{\text{other}}\right) = \frac{dI_{\text{sun}}}{4} - \frac{I_{\text{sun}}}{4} d\alpha \tag{4}$$

This equation relates changes in temperature to changes in the greenhouse effect (due to changing amounts of CO_2 or of other gases), changes in the solar flux and changes in the albedo.

Application to models

From the beginning, the IPCC has used the term *radiative forcing*, expressed as ΔF, to represent any changes in the greenhouse effect from any cause. The Δ indicates that there is a difference in net radiative blocking; however, the historical use of F is at odds with the use of G to represent the same thing. The radiative forcing should be expressed in the modern symbology as dG or ΔG. In any case, the amount of greenhouse effect attributable to 400 ppmv (G_{CO2}) of CO_2 is about 30 W/m^2 (van Wijngaarden and Happer, "Dependence of Earth's Thermal Radiation on Five Most Abundant Greenhouse Gases," arXiv:2006.03098v1 4 June 2020) and the increase due to doubling to 800 ppmv would be 3.7 W/m^2.

The IPCC's 2021 *Sixth Assessment Report* asserts that the most probable temperature rises due to doubling CO_2 concentration is 3 ºC, with any rise outside the range of 2 ºC to 5 ºC to be very improbable. We will only consider their most probable value, and we will assume their radiative forcing (dG_{CO2}) due to CO_2 doubling to be 3.7 W/m^2.

Using the Stefan-Bolzmann constant

$$5.6704 \cdot 10^{-8}\, Js^{-1}\, m^{-2}\, K^{-4}$$

the left hand side of Equation (4) becomes

$$4 \cdot 5.6704 \cdot 10^{-8} \cdot 289^3 \cdot 3 - (3.7 + dG_{other})$$

With these numbers, and IPCC's assumption of no change in solar intensity, Equation (4) becomes

$$16.5 - 3.7 - dG_{\text{other}} = -\frac{I_{\text{sun}}}{4} d\alpha \qquad \left(\frac{\text{W}}{\text{m}^2}\right) \tag{5}$$

If the IPCC's model is to be believed, then IPCC must account for 12.8 W/m^2 by an increase in dG_{other} or a decrease in albedo or both. They present no evidence whatsoever that they have done it.

It is also very interesting to observe the large negative Stefan-Bolzmann feedback effect, an increase of 3 degrees in surface temperature results in a 16.5 W/m^2 increase in emitted radiation, a value more than 4 times the effect of doubling CO_2. This means the Stefan-Bolzmann radiation is an important surface temperature regulator.

Reference

van Wijngaarden A and Happer W, Dependence of Earth's Thermal Radiation on Five Most Abundant Greenhouse Gases. ***https://arxiv.org/abs/2006.03098***, 4 June 2020

Norwegian, Nordic and International Climate Realist Conferences 2014-2018

Correspondence to janesol@online.no

Vol. 2.1 (2022)

pp. 38-40

Jan-Erik Solheim

Independent scientist, Bærum, Norway

Submitted 15-09-2021, Accepted 21-12-2021. https://doi.org/10.53234/scc202203/12

1.Introduction

The organization Climate Realists of Norway was started in 2009 and part of our activity is to present facts about climate and climate change in public meetings. It soon became evident that many of our members wanted to learn more about climate to be stronger in the public debate. We therefore started internal seminars and a newsletter in addition to information in social media.

The seminars evolved into conferences, first for own members (2014 and 2015), then together with Nordic sister organizations (2017-2019). In the following I will present a summary of the four previous conferences as an introduction to the 2019 Oslo Conference, which also marked the 10th anniversary of the Climate Realists of Norway.

2. 2014 September 28-30: Conference cruise Oslo-Copenhagen-Oslo

38 participants boarded the ship *Pearl Seaways* in Oslo a few hours before it departed. We had tree lecturers and showed part of the film *The Global Warming War* before the ship left Oslo at 16:30. Sailing out the Oslo Fjord professor Ole Humlum told how the landscape was formed during the previous ice age.

Figure 1. Visit to Center for Sun-Climate Research at Denmark's Technical University. The host Professor Henrik Svensmark is no 5 from the right in the first row. (Photo: Yngvar Engebretsen).

The ship arrived in Copenhagen the next morning at 9:45 and we went by bus to Denmark Technical University (DTU) Center for Sun-Climate Research headed by Prof. Henrik Svensmark. Here we had lectures about the research of the Svensmark Group and a tour of their laboratory in addition to two lectures on DTU's Greenland research.

On the ship back to Oslo we had lectures by Trygve Eklund, Helge Gerhard Gran, Ole Humlum, Jan-Erik Solheim, Per Strandberg, Odd Vaage and Harald Yndestad in addition to internal discussions.

3. 2015 June 7-9: Conference cruise Oslo-Kiel-Oslo

23 participants from Norway and Sweden had a conference on the ship *Color Magic*, which left Oslo at 14:00 and arrived in Kiel the next morning at 10:00. In Kiel the ship was in port for four hours and Professor Fritz Vahrenholt from Hamburg, came on board and gave a special lecture on *The German situation with respect to climate science and energy policy*. During the crossing from Oslo to Kiel and back we had talks by Fred Goldberg, Göran Henriksson, Niklas Mörner, Ole Humlum, Jan-Erik Solheim and Geir Aaslid. At the end of the cruise Dr. Fred Goldberg invited us for a next conference together with Swedish climate realists in Stockholm the following year.

Figure 2. Climate Cruise to Kiel 7-9 June 2015. Professor Vahrenholt is no 5 from the right in the second row. (Photo: Yngvar Engebretsen)

4. 2016 October 7-9: Stockholm and Uppsala

The first part of the conference was held on Högberga Gård, Lidingø, Stockholm and was a cooperation between Swedish Polar Institute AB, Norwegian Climate Realists, and the Swedish network Climate Sense. In total 74 participants attended the meeting. Speakers were Stein Bergsmark, Trygve Eklund, Martin Hovland, Ole Humlum, Hans Jelbring, Anders Lindroth, Nils-Axel Mörner, Torstein Seim, and Jan-Erik Solheim. The local organizing committee consisted of Fred Goldberg, Tege Tornvall and Sture Åström.

On the last day the Norwegian participants were invited by ICOS (Integrated Carbon Observatory System) Director Anders Lindroth to visit their measuring station Norunda north of Uppsala. The station has a 100 m high mast, where air can be sampled and analyzed. On the tour we had a talk by Göran Henriksson and in Odin Restaurant in Gamla Uppsala, we had a lecture by Wibjörn Karlén, member of Royal Academy of Sweden and expert on CO_2 and temperature measurements. Figure 3 shows measurements of CO_2 at elevation 100 m at Norunda since 2015

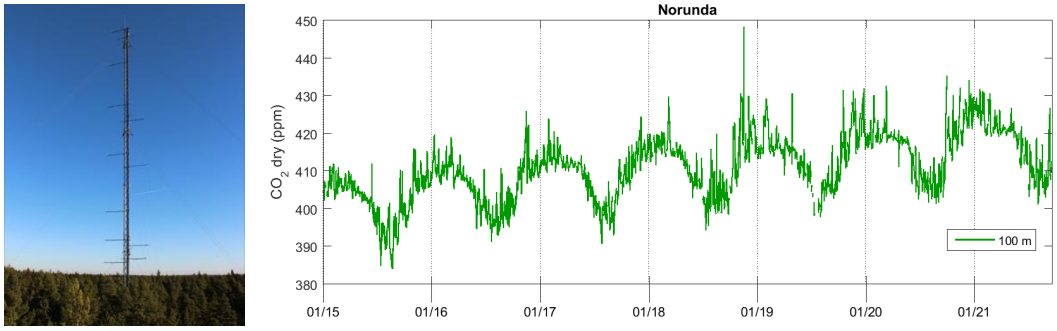

Figure 3. The ICOS measuring tower and CO_2 measurements 2015-2021

5. 2018 February 16-17: Climate Sense, Mölndal, Göteborg

The conference was organized by the Swedish Climate Sense and Norwegian Climate Realists with support by CLEXIT and the Stockholm Initiative. The conference took place in the Scandic conference hotel in Mölndal in the outskirts of Göteborg. Local organizers were Tege Tornvall and Sture Åström and the Norwegian organizer Elen Roaldset. Specially invited was Dr. Wille Soon from U.S.A. The first part of the conference was held in English, the second part in Nordic languages. In total we had 123 participants from Sweden, Norway, and Denmark.

Talks were given by Stein Bergsmark, Rögnvaldur Hanneson, Jens Morten Hansen, Ole Humlum, Claes Johnson, Søren Holst Kjærsgård, Nils-Axel Mörner, Jacob Nordangård, Jan-Erik Solheim, Wille Soon, Henrik Svensmark, Tege Tornvall, Gösta Walin, Per Wellander, Staffan Wennberg and Sture Åström. In addition, we had some posters.

On the return trip to Oslo next day, the 40 Norwegian participants visited Båhus Castle, the Shell Bank Museum in Uddevalla, a Wind-power company in Rabbaldshede, the World Heritage Rock Carvings in Tanum and the Solberg tower in Skjeberg where the land rising after the last Ice age is well documented.

Figure 4. The Mölndal conference participants. (Photo: Yngvar Engebretsen)References

6. Conclusion

As a response to the growing interest for Nordic Climate Conferences, with international speakers, it was time to invite to the next one in Norway. The next one took place in Oslo October 18-19, 2019 and had the theme *Natural Variability and Tolerance*, and abstracts of the talks are presented in the following papers.

World Climate Declaration[1]

Guus Berkhout

Climate Intelligence Foundation, The Netherlands

Correspondence to office@clintel.org

Vol. 2.1 (2022)

pp. 41-47

Submitted 21-12-2021. Accepted 29-12-2021. 30, https://doi.org/10.53234/scc202203/13

The past 150 years show that affordable and reliable energy is key to financing basic needs, such as food, health, sanitation, housing, electricity, and education. The past 150 years also show that more CO_2 is beneficial for nature, greening the Earth and increasing the yield of crops. Why do world leaders ignore these hard facts? Why do world leaders do the opposite with their 'Green New Deal' and lower the quality of life by forcing high-cost, dubious low-carbon energy technologies upon their citizens? To get it their way, fear is used but fear has never led to sensible policies.

A global network of critical scientists and engineers (CLINTEL) has prepared a simple message: *"There is no climate emergency." Yes*, climate change exists and must be addressed, but the network emphasizes that there is NO cause for panic and alarm. The CLINTEL scientists strongly

[1] The talk at the conference can be seen here: https://www.youtube.com/watch?v=smunmRB2yqYh (Recordings made by Yngvar Engebretsen)

oppose the misleading, unrealistic and destructive global net-zero CO_2-policy ('NetZero'). Instead, they promote climate adaptation policies that show a high benefit-cost ratio.

Being concrete, scientific organizations should openly address uncertainties and exaggerations in their predictions of global warming, while governments should dispassionately count the real costs as well as the imagined benefits of their policy measures. It is being summarized in CLINTEL's World Climate Declaration (WCD), consisting of seven fundamental statements. The WCD formulates a strong wake-up call for scientific organizations and world leaders and it functions as an inspirational guidance for the young

Statements in the WCD

I. Natural as well as anthropogenic factors cause warming

The geological archive reveals that the Earth's climate has varied as long as the planet has existed, with natural cold and warm phases. The Little Ice Age ended as recent as 1850. Therefore, it is no surprise that we now are experiencing a period of warming. Observations indicate that anthropogenic factors yield only modest contributions to the current global warming period.

II. Warming is far much slower than predicted

The world has warmed significantly less than predicted by the Intergovernmental Panel on Climate Change (IPCC) on the basis of modeled anthropogenic forcing. The large gap between the real world and the modeled world tells us that we are far from understanding climate change. The science is far from settled.

III. Climate policy relies on inadequate models

Climate models have many shortcomings and are not remotely plausible as global policy tools. They consistently blow up the effect of greenhouse gases such as CO_2 , leading to large discrepancies with observations.

IV. CO_2 is plant food, the basis of all life on Earth

CO_2 is not a pollutant. It is essential to all life on Earth. Photosynthesis is a blessing. More CO_2 is beneficial for nature, greening the Earth: additional CO_2 in the air has promoted growth in global plant biomass. It is also good for agriculture, increasing the yields of crops worldwide.

V. Global warming has not increased natural disasters

There is no statistical evidence that global warming is intensifying hurricanes, floods, droughts and suchlike natural disasters, or making them more frequent. However, there is ample evidence that CO_2-mitigation measures are as damaging as they are costly.

VI. Increase of sea levels is steady for the past 150 years

The mean global sea level shows considerable spatial variations due to differences in the Earth's gravity field and spatial variations in the water temperature and salinity. Estimates of average global sea level changes are about 1.5 – 3.5 mm per year. Despite the increasing CO_2-levels, there is no evidence of any sea level rise crisis.

VII. Climate policy must respect scientific and economic realities

There is no climate crisis. Therefore, there is no cause for panic and alarm. We strongly oppose the harmful and unrealistic net-zero CO_2-policy proposed for 2050. Until better approaches are effective, and they are on the horizon, we have ample time to reflect and adapt.

Heads of governments must dispense with their frightening narrative that climate change causes a "Existential Crisis". Don't link extreme weather to human-caused CO_2-emission and stop spreading disinformation on impending global warming and global sea level rise disasters! Instead, spread hope and truth. In the following we show what the WCD means for scientific organizations, world leaders and young generations.

Meaning of the WCD for scientific organizations

Scientific organizations serve society by fostering, creating and passing on new scientific knowledge through research and teaching. Today, quality universities have become a primary source of prosperity in the area where they are located. The higher the scientific level realized, the greater the contribution to prosperity. Universities, therefore, should promote excellence at all times. This means that they should not settle for followership, but aim for leadership in their scientific fields. It also means that universities are communities without ideological and political purposes. And above all, at universities the principle of *Freedom of Speech and Inquiry* are by no means negotiable. The meaning of the WCD for scientific organizations is summarized by the following fundamental items:

- *The complexity of multi-factor, multi-scale systems – such as the Earth's climate – demands close co-operation between a wide range of scientific fields and disciplines*

Climate change has a wide variety of causes, natural as well as anthropogenic. Integration of knowledge from many scientific fields, such as astronomy, geophysics, geology, archaeology, meteorology, oceanography and biology, is indispensable to a full understanding of the complex causal relationships underlying climate change. At the same time, the integration of theoretical knowledge with measurement technologies should have high priority. This is hardly the case in today's mainstream climate research. Early-stage models are claimed as being 'settled science'.

- *Sound scientific research is open-minded and is characterized by a wide variety of viewpoints without dogmas and prejudices*

Within the established climate science, curiosity and diversity are being suppressed and the 'Catastrophic Anthropogenic Global Warming' (CAGW) dogma is ruthlessly enforced. However, science is neither a religion nor a political faction. Science advances not by chanting "We believe" but by asking "I wonder". Funding for CAGW-critical research is non-existent today. Censorship complicates and all too often prevents the publication of critical articles in mainstream peer-reviewed scientific journals. Again, the CAGW-models are considered to be the truth and fit for climate policy making.

- *Faith in scientific models is faith in the underlying assumptions; only correct assumptions can lead to correct answers*

What computer models tell us depends entirely on what is input by the model-makers: hypotheses, relationships, parameterizations, arithmetical simplifications, boundary conditions, etc. Unfortunately, mainstream climatologists seldom discuss these choices in their complex algorithms. For

instance, how sensing results to the biased assumptions or to the coarse arithmetic grids? We still hear very little about it.

- *With enough model parameters it is always possible to reconstruct recorded measurements in a relatively small observation window*

Parametric tuning says. The famous mathematician John von Neumann (1903 – 1957) said: "With four parameters I can fit an elephant; with five I can make him wiggle his trunk." A critical and most valuable test is whether a model can accurately predict future measurements. That is precisely where climate models are going wrong. For 40 years, the IPCC has falsely predicted alarming high temperatures in its reports. Actually, their level of alarm increased overtime ("It is five minutes to midnight").

- *The history of science shows that new insights do not come from followers but from dissenters; doubters and dissenters make history in science*

Copernicus, Galilei, Newton, Gauss, Curie, Einstein, Watson, Crick, Wilkins and Hawking all looked critically at the prevailing consensus and dared to take a different path. Progress would not have been possible without them. In contrast, the mainstream climate community has contributed embarrassingly little headway. They have been transmogrified into a media campaign to sell the CAGW-hypothesis. Doubters and dissenters are excommunicated.

- *Academies of Sciences have a moral responsibility to warn society of irresponsible conclusions that follow from a naive belief in immature scientific models*

So far, climate models have proven their inability to make reliable predictions of global warming. Therefore, their predictions are the wrong basis for making government policy. Bear in mind that the National Academies of Sciences see themselves as guardians of science. If so, should they not at last creak into action?

Already in 2015, Academies should have given an abundantly clear warning to world leaders that the climate science is still in its infancy. By their negligence, the Academies made themselves complicit in the absurdity of the Paris Agreement and everything that followed.

Meaning of the WCD for World Leaders

Encouraged by a scientific community that profits by exaggerating the imagined threat from a mildly warming global climate, the message of world leaders is that "to go beyond a rise of 1.5 ºC would unleash catastrophes, including extreme sea level rises, crippling droughts, monstrous storms and wildfires far worse than those the world is already suffering".

But is this scaremongering story true? The WCD implies the following thought-provoking messages for world leaders:

• *What is the problem with the current global warming?*

Yes, the climate is changing – as it always has – but there is NO 'climate crises.' The crisis comes from extreme scenarios. And the 1.5 ºC crisis limit for global warming is a political invention. While CO_2-concentration has continued to increase, there has been negligible global warming in the past decade. We even may be at the very beginning of a cooling period.

• *Supply-driven energy sources are a big mistake*!

Supply-driven energy sources are unreliable, unaffordable and destabilize electricity supply. Similarly, calling the destruction of ecosystems for wood burning a clean and sustainable solution is irresponsible.

• *For affordability and security of supply society needs multiple energy sources*

Coal, gas and nuclear power should all be used. Coal is the cheapest of all and – with modern technology – much cleaner than wood burning; gas is the cleanest fossil fuel, easy to transport and store; nuclear stations require high upfront investments, but they emit no CO_2, deliver their power continuously and have a long lifetime. Today we see that energy policies lead to rising energy prices and rising energy prices lead to an acceleration in inflation.

• *Please, prioritize the development of concrete climate adaptation plans*

Global mitigation policies cost an exorbitant amount of money and they have never saved one life. National adaptation plans work, whatever the cause of climate change. In addition, adaptation plans are needed to protect us from extreme weather. Head of governments, please look at the costs and benefits of your policies.

In conclusion, the big climate picture tells world leaders that we may slowly move via ups and downs to the next global cooling period. The recovery from the Little Ice Age has been very beneficial for mankind and nature. Enjoy today's relatively benign climate! Sometime in the future we will again move to a colder phase and ultimately into the next ice age.

Wind- and solar energy can play only a modest role in the energy transition. Please, use clean fossil fuel power for the increasing energy needs, particularly in developing countries. Meanwhile, cooperate worldwide to develop the nuclear power plants of the future, together with new energy storage and transportation technologies. It will result in prosperity for all.

Meaning of the WCD for the young generation

Climate alarmists are telling the youngsters that the older generation has caused catastrophic global warming (CAGW) by emitting too much CO_2. They also led them to believe that if they do not reverse what the "industrial oldies" have brought about, our planet will soon become uninhabitable for people and animals. No time to lose, we are in the middle of a climate crisis! But is this scaremongering story true? The WCD has the following instructive and hopeful message for all of the young people:

• *Don't act like a parrot*

Be critical against the many false prophets who are trying to take advantage of you and set you up against what your parents and grandparents have achieved. The information these prophets tell you is one-sided and misleading. Their information comes from faulty science, wrong model predictions and extreme scenarios.

• *Deepen your knowledge on the facts of our climate*

By doing so, you will discover that there is no evidence that points to a climate crisis. Yes, climate change exists and is of all times. But don't worry, the current global warming is gentle (ca. 0.14 ºC per decade) and has already made many positive contributions to the quality of your life. Think about that while you are protesting.

• *CO_2 is the molecule of life*

Did your teachers ever tell you that CO_2 is a blessing for everything that lives on our planet? Far from being pollution, CO_2 is the molecule of life, providing food for plants. Without plants there would be very little animal life and no human life at all. Think about that as well, while you are protesting.

• *Don't confuse climate change with environmental pollution*

These are two completely different phenomena. Climate change is largely caused by the primordial natural forces and environmental pollution is largely caused by human behavior. Climate change requires clever adaptation measures and environmental pollution asks for clever clean production technologies.

• *Don't waste your life by solving a problem that does not exist*

Instead, put all your talents and energy in developing a productive circular economy. Only then can you realize enough financial means to increase the standard of living beyond the basic needs. When you go back to the unproductive past and make yourself poor, you are no longer in control of your future!

Finally, for all of you who have been influenced by fear of things to come, forget the dodgy preachers of doom and gloom; they ruin your future by destroying everything your parents and grandparents have built. Look at the positive times ahead of you, and consider the above challenges as your mission in life.

Conclusions

1. CO_2 budgets are not based on science, but they are based on fear. They limit human rights, feed extremism and push mankind into a deep physical, mental and financial crisis. It is clear that citizens throughout the world don't want to become poor and, above all, they don't want to live in a culture of fear.
2. History shows that living on planet Earth requires adaptation all the time. If we continue to advance science and technology, we generate new capabilities to adapt to climate change, to protect our natural environment, to end hunger and poverty, to take care of one another and to conquer the universe. Intelligent adaptation is the formula for creating a better world.
3. Head of governments, look at the real costs as well as the imagined benefits of your policy measures. Instead of squandering trillions to a problem that does not exist, release people from hunger and poverty, solve global health issues, invest more in science and education and, above all, take better care of all life on our unique planet.

Epilogue

The World Climate Declaration (WCD) has brought a large variety of competent scientists and engineers together from all over the world. At the moment around 1500 professionals have signed and combine forces. The considerable knowledge and experience of this scientific group is indispensable in reaching a balanced, dispassionate and competent view of climate.

Literature

Battagglia, Franco 2021, *There Is No Climate Emergency*, 75 pages, 21mo Secola

Furfari, S., Clerici, A., 2021, *Green hydrogen: the crucial performance of electrolysers fed by variable and intermittent renewable electricity*, Eur. Phys. J. Plus 136, 509

Goklany, Indur M., 2021**,** *Impacts of Climate Change, Perception and Reality*, Global Warming Policy Foundation, Report 46

Koonin, Steven E. 2021, *Unsettled: What Climate Science Tells Us, What It Doesn't, and Why It Matters*, 309 pages, BenBella Books

Koutsoyiannis, D 2021, *Rethinking climate, climate change, and their relationship with water*, Water, 13 (6), 849, 2021

Lindzen, Richard 2011, *Dynamics in Atmospheric Physics*, 324 pages, Cambridge University Press

Lomborg, Bjørn 2020, *False Alarm*, 323 pages, Hachette Book Group

Monckton of Brenchley, Christopher 2021, What is science and what is not? Sci. Clim. Change 1(1), 14-53.

Plimer, Ian 2021, *Green Murder*, 598 pages, Connor Court Publishing

van Wijngaarden, W. A. and Happer, W 2020, ***Dependence of Earth's Thermal Radiation on Five Most Abundant Greenhouse Gases****,* preprint, physics.ao-ph
https://arxiv.org/abs/2006.03098

,

Correspondence to editor@scienceofclimatechange.org

Vol. 2.1 (2022)

pp. 48-53

The Gulf Stream Beat[1]

Nils Axel Mörner[†2]

Institute of Paleogeoophysics & Geodynamics, Stockholm, Sweden

Abstract

This talk is devoted to the science of the Oceans with special reference to the Gulf Stream Beat. Forcing of the ocean circulation system is controlled by the planetary beat on the Sun, Moon, and the Earth. The sea is not at all in a rapidly rising mode.

Submitted 20-12-2021, Accepted 30-12-2021. DOI: https://doi.org/10.53234/scc202203/14

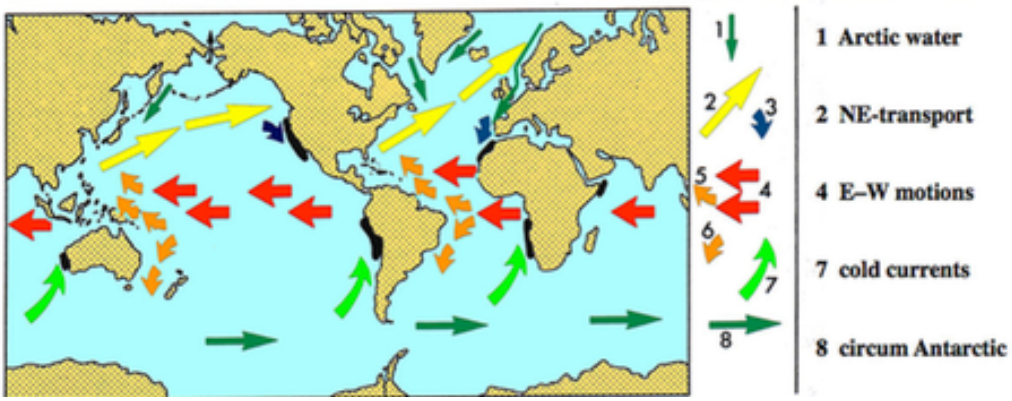

Figure 1. Main global ocean surface circulation patterns: The main equatorial currents are lagging the Earth's rotation. The Kuroshio and Gulf Stream systems bring warm equatorial water to mid and high latitudes, and the circum Antarctic currents bring cold water to low latitudes and are responsible for significant coastal upwelling.

1. Ocean circulation changes

The ocean circulation can be simplified in 8 dominant systems and their directions of motions (Figure 1). The system is supersensitive to changes in Earth's rate of rotation in a feedback-coupling and interchange of angular momentum (Mörner, 1984, 1996, 2019). The most dominant system is the equatorial system that moves from East to West, in the opposite direction of the Earth's rotation. If rotation changes, this will have an immediate response in the current system.

The Gulf stream and the Kuroshio stream brings equatorial warm water to the north and make livable conditions at our northern latitudes. On the figure we also see the costal upwellings of nutrient rich waters which are extremely productive for marine life.

[1] . The talk can be seen here: https://www.youtube.com/watch?v=g_n2bzjQetM (Recorded by Yngvar Engebretsen

[2] Nils-Axel Mörner died in Oct. 2020. The talk is transcribed by Jan-Erik Solheim

.

2. The Gulf Stream Beat

The Gulf stream is divided into a northern (NB) and southern branch (SB) as shown in Figure 2. The volume of water flowing in the two branches changes with the Earth's rate of rotation. When one is

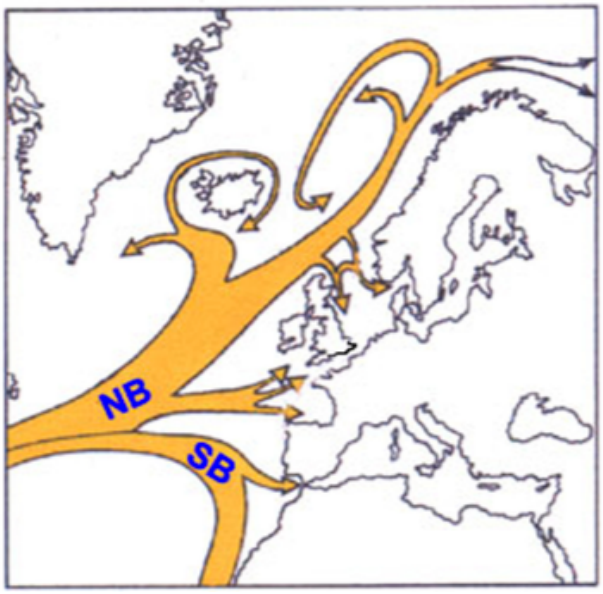

Figure 2. The Gulf Stream and its division into a Northern (NB) and a Southern branch (SB).

strong - the other is weak. This is what we call the Gulf Stream Beat (GSB). Since this is a result of changes in the Earth's rate of rotation, we observe similar beats in other currents worldwide. It is a global phenomenon.

An example of the GSB is demonstrated in Figure 3 for the period 1672-1702, which was the coldest part of the Little Ice Age. Then the SB became stronger, while the NB is weaker. The upper left panel shows 8 red dots from the Baltic to North Africa. In the right panel we have temperature graphs showing warm periods in yellow and blue periods in blue. Observations show how it gets colder at locations 1-7, and warmer at location 8 which is off the coast of North Africa. My interpretation is that cold surface water from the Arctic is flowing far south by the western coast of Europe. This was the coldest part of the little ice age. During this period the solar activity was extremely low. Very few spots were observed on the Sun during the period 1640-1720, which was named the Maunder grand solar minimum (Usoskin 2007).

A similar beat was observed 1435-1460 during the Spörer minimum, and 1808-1821 during the Dalton minimum. The Nordic inhabitants of Greenland got problems with ice and agriculture during the deep Wolf minimum 1270-1340 and had to change the sailing routes from Iceland and Norway.

After 1900 we have had a long period of high solar activity and the NB has been strong. An example of the difference in NB and SB was observed between 1930 and 1940 when a warm period developed in the North while the south was cooling.

After 2000 the solar activity is decreasing and we observe decreasing temperatures in Circum-Arctic Oceans, while the equatorial surface water is warming up as shown in Figure 4. This may be the indication of a coming Gulf Stream beat development.

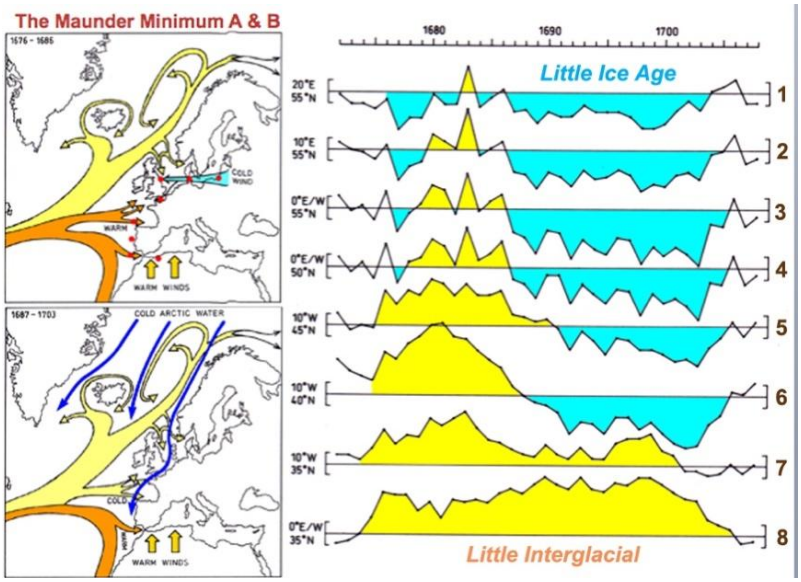

Figure 3. An example of GSB during the period 1672-1708. The left panels show ocean currents, Orange is strong, yellow is weak, and blue is cold. The right panels show temperature variations, where yellow is warm and blue is cold.

The observed temperature record from Mallorca provides an interesting documentation of the N–S anti-correlations in temperature due to the Gulf Stream beat.

So, what did the IPCC proponents do? They did *data adjustment.* Now the official temperature record for Mallorca shows increasing temperature from 1880 until 2000, just as shown by models. *And by that they killed the dynamics of climate change and ocean circulation.*

3. Sea level beats during Grand Solar Minima and Minima

Oceanographers say that the ocean currents are forced by thermohaline circulation. That is explained as heavy salt water downwelling in cold regions of the North Atlantic and in the Antarctic Current. When the Gulf Stream runs by the coast of Svalbard its heavy salt water is forced down by fresh water from Russian rivers and melting ice on top of it. The warm water that enters the Arctic from the south pushes cold water out through the Fram strait down the East coast of Greenland (Mörner et al. 2020).

Based on my own observations in many regions of the world, I claim that the Earth's rotation also changes the sea level (Mörner 2013a, 2019). During grand solar maxima the North Atlantic current is slightly stronger and sea level is a little higher. In North Africa the sea level is slightly lower and the sea a little colder. The most notable difference takes place around the coasts of India and in Polynesia where the sea level can be 60-70 cm lower. According to models the sea level should now be high because of ice melting. *This is not observed*.

At grand solar minima the SB is strengthening. Sea level is lower in the north and slightly higher at the coast of North Africa. However, around India and in Polynesia we observe an increase in the sea level of the order 60-70 cm.

The sea surface is irregular, it is not flat and parallel like a perfect globe. I will give you an example: The sea-level at Tenerife was stable before 1940, then rising 1945-1960, falling 1970-2000, and now rising after 1995.

4. The forcing function behind the Gulf Stream Beat

The GSB is a function of changes in the Earth's rate of rotation. This can be forced by external and internal forcing as shown in figure 4 (Mörner et al. 2020). The solar wind controls the Earth's shielding and controls Grand Solar Cycles in rotational eustacy and GSB. The solar wind consists of electric charged particles which carry a magnetic field with it. With a strong and steady solar wind the Earth's rotation will slow down by the pressure on the ocean surface and the magnetic torque on the Earth's magnetic core (Solheim et al. 2021).

The periodic variation in the solar wind generates the main 60-year geomagnetic cycles we observe in Earth's rotation and climate (PDO, NAO, etc.) and the integrated effect in the sea level and ocean oscillations.

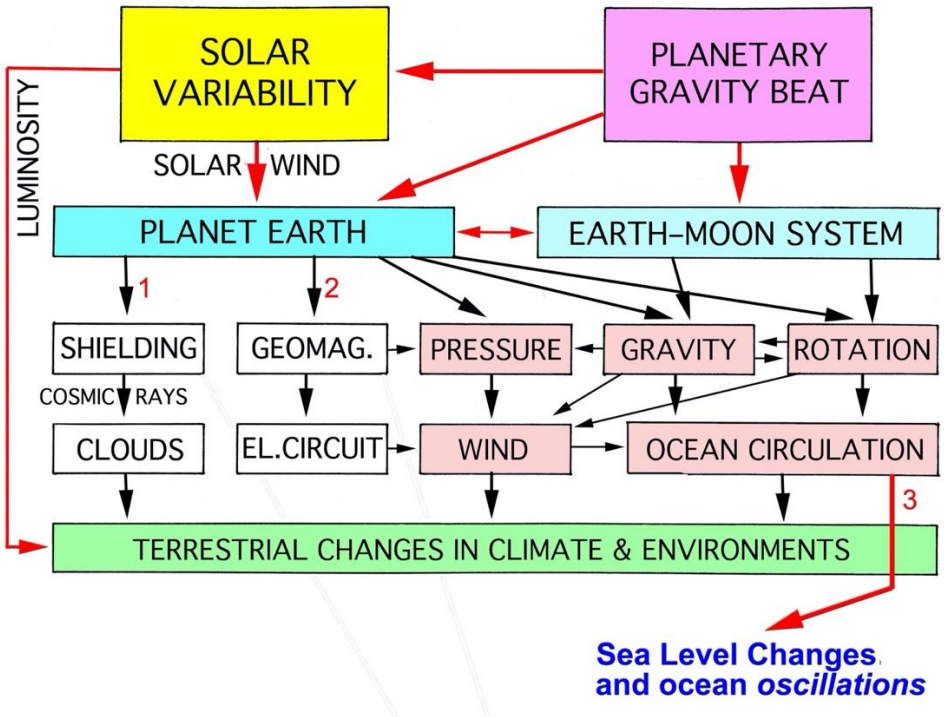

Figure 4. Integrated effects of the planetary beat on solar variability and, via the solar wind, on a number of fundamental terrestrial processes, and, via direct effects on the Earth-Moon system, on gravity, rotation, wind, ocean circulation, sea level changes, and oceanic oscillation systems (Mörner, 2013a, 2020).

The solar wind varies as a function of soler internal variability, which again is forced by the beat of the planets which modulate the solar energy production and the solar magnetic field variations (Mörner 2013b). The planets move in elliptical orbits as discovered by Johannes Kepler. The combined action of the planets forces the Sun into a very complicated orbit around the barycenter of the solar system. The main players are the large planets Jupiter and Saturn. They are in the same direction seen from the Sun every 20 years and are back at the same place relative to the stars after 60 years. This gives us the 60-year cycle.

The GSB is a function of the magnetic shielding of the Earth, which varies with the solar wind which carries a magnetic field with it. With a strong and steady wind the Earth's rotation will slow down by the pressure on the ocean surface and the magnetic torque on the Earth's magnetic core. This happens during Grand Solar Maxima. During Minima the Earth rotates faster, and the Gulf streams northern branch weakens while the soutern branch strengthen (Mörner 2010).

The planetary forcing also includes effects of the distance from the Sun, orbital velocity, angular momentum and electromagnetic field variations. Since the planets orbits are stable over millenia and millions of years, even small periodic variations will be amplified and lead to observable effects in the climate system. The Earth's climate experience both direct forcing from variation sin solar irradiance (TSI) (Connolly et al. 2021) and in magnetospheric shielding which controls the galactic cosmic ray flux and its subsequend cloud production (Svensmark et al. 2017).

There are signs that we are entering a Grand Solar Minimum in this century (Abdussamatov 2016, Miyahara 2021). This will most likely start during the coming decades and last for the rest of the century. How deep it will be, can only be guessed. Some scientists find it most likely that it will match the Maunder Minimum (1640-1720), while I find it to be somewhat less severe, like the Dalton minimum and with a GSB with cold Arctic water all the way down to Lisbon in 2030-2050 (Mörner 2010).

5. Global Sea level and the absence of a flooding treat

The integrated effect from changes in the Earth's rotation as a function of the magnetic shielding conrolled by the solar wind is observed in the sea level changes during the last 500 years. The eustatic sea level of the Equatorial oceans (i.e below ±30 deg latitude) has been stable for the last 50 years. It changed of the order. +70 cm around 1800, -140 cm around 1700, and probably +70 cm about 1550. In NW Europe a small rise of the order 1.1 mm/year has taken place since 1800. This follows the general climatic changes quite well and hence seems to be dominated by glacial eustasy. The equatorial changes are in opposite modes and have oscillations of much higher amplitudes, indicating that they are dominated by other forcing functions, viz. rotational eustasy. At the moment there is no treat of a flooding disaster.

6. Conclusion

1. The Gulf Stream Beat is a function of the planetary beat on the Sun, the Earth and the Earth-Moon system.

2. Sea level is not in a rapidly rising mode, and there is not a single point on Earth where a true acceleration in sea level has been observed.

3. The changes in sea level show an opposed trend between the northern hemisphere and the equatorial region on the Grand Solar cycle and the 60-year cycle.

4. Let us forget all the trouble about CO_2, which has:
   – no effects on ocean circulation
   – no effect on sea level
   – hardly any effect on temperature

References

Abdussamatov H 2016, *The New Little Ice Age Has Started.* In: Easterbrook, D J., Ed., *Evidence-Based Climate Change*, Second Edition, Elsevier, Amsterdam: 307-328. https://doi.org/10.1016/B978-0-12-804588-6.00017-3

Connolly R et al. 2021, *How much has the Sun influenced Northern Hemisphere temperature trends? An ongoing debate.* Research in Astronomy and Astrophysics, 21, No 6:131 (68p) https://doi.org/10.1088/1674-4527/21/6/131

Humlum O 2018, www.climate4you.com

Miyahara H et al. 2021, *Gradual onset of the Maunder Minimum revealed by high-precision carbon-14 analysis,* Nature Scientific Reports, 11:5482, https://doi.org/10.1038/s41598-021-84830-5

Mörner N-A 1984**,** *Planetary, Solar, Atmospheric, Hydrospheric and Endogene Processes as Origin of Climatic Changes on the Earth.* In: Mörner, N-A and Karlén, W., Eds., *Climate Change on a Yearly to Millennial Basis*, Wiley & Sons, Christchurch:483-507. https://doi.org/10.1007/978-94-015-7692-5_48

Mörner N-A 1996*, Global Change and Interaction of Earth Rotation Ocean Circulation and Paleoclimate.* Annals of the Brazilian Academy of Sciences, 68:77-94.

Mörner N-A 2010, *Solar Minima, Earth's Rotation and Little Ice Ages in the Past and in the Future the North Atlantic-European Case*. Global and Planetary Change, 72: 282-293. https://doi.org/10.1016/j.gloplacha.2010.01.004

Mörner N-A 2013a, *Planetary Beat and Solar-Terrestrial Responses*. Pattern Recognition in Physics*,* 1: 107-116. https://doi.org/10.5194/prp-1-107-2013

Mörner N.-A 2013b, Solar Wind, *Earth's Rotation and Changes in Terrestrial Climate*. Physical Review & Research International, 3, 117-136.

Mörner N-A 2019, *Rotational Eustasy as Understood in Physics*. Int. J. of Geosciences, 10: 709-723. https://doi.org/10.4236/ijg.2019.106040

Mörner N-A, Solheim J-E, Humlum O and Falk-Petersen S 2020, *Changes in Barents Sea ice Edge Positions in the Last 440 years: A Review of Possible Driving Forces*. Int. J. of Astronomy and Astrophysics*,* 10: 97-164. https://doi.org/10.4236/ijaa.2020.102008

Solheim J-E, Falk-Petersen S, Humlum O. and Mörner N-A 2021, *Changes in Barents Sea Ice Edge Positions in the Last 442 Years, Part 2: Sun, Moon and Planets.* Int. J. of Astronomy and Astrophysics, *11: 279-341, https://doi.org/10.4236/ijaa.2021.112015*

Svensmark H, Enghoff M B, Shaviv N J & Svensmark J 2017*, Increased ionization supports growth of aerosols into cloudcondensation nuclei.* Nature Communications, 8: 2199. https://doi.org/10.1038/s41467-017-02082-2

Usoskin I G, Solanki S K and Kovaltsov G A 2007, *Grand Minima and Maxima of Solar Activity: New Observational Constraints***.** Astronomy and Astrophysics, 471: 301-309. https://doi.org/10.1051/0004-6361:20077704

Snow, Ice and Temperature Trends in the Arctic and Antarctic[1]

Correspondence to ronanconnolly@yahoo.ie

Vol. 2.1 (2022) pp. 54-57

Ronan Connolly

Center for Environmental Research and Earth Sciences, Dublin, Ireland

Submitted 19-12-2021, Accepted 30-12-2021. https://doi.org/10.53234/scc202203/15

1. Introduction

The term "cryosphere" refers to the frozen water regions on the Earth: e.g., glaciers, snow-covered regions, sea ice and permafrost regions. Glaciologists define an "ice age" for the Earth as periods where permanent ice sheets are present in both hemispheres. Therefore, technically, since there are permanent ice sheets in Greenland and Antarctica, we are currently in an ice age. However, fortunately, we are in an "interglacial" period of this ice age – much milder than the glacial period that ended 10-15,000 years ago.

Many people rely on the UN's Intergovernmental Panel on Climate Change (IPCC)'s Assessment Reports for evaluating trends in the cryosphere. These IPCC reports tend to describe quite accurately all those trends related to the cryosphere that imply "the ice is melting dramatically" (IPCC, 2014; 2019). However, they tend to downplay or overlook those trends which contradict this narrative. If we are interested in studying climate change, it is important to consider all the relevant trends – not simply the ones that agree with our chosen narrative. Therefore, in this talk (and accompanying abstract), I will briefly summarize the current scientific understanding of what we know about cryosphere trends and highlight some of the key observations that have been overlooked or downplayed by recent IPCC reports.

In the talk, I summarize the key trends associated with each aspect of the cryosphere (glaciers, ice sheets/ice shelves, sea ice, permafrost, and snow cover) and compare these trends to those described by the IPCC reports and the "hindcasted" trends that the global climate models (GCMs) used for the IPCC reports argue should have occurred. There, I demonstrate that the GCM hindcasts fail to replicate many of the observed trends, and that the IPCC reports are remarkably selective in which trends they report on. However, for brevity, in this extended abstract, I will mostly focus on the trends themselves.

2. Arctic sea-ice

Observations show that Arctic sea-ice has declined since satellite records began in 1978. But this long-term decline is more chaotic and intermittent than continual year-on-year decline the GCM hindcasts expect should have occurred. Also, in Connolly et al. (2017), we showed that 1978 coincidentally marked the end of roughly three decades of Arctic cooling (and increasing sea ice extent) since the 1940s. In Connolly et al. (2017), we compiled multiple pre-satellite era estimates of Arctic sea-ice extent from a range of different sources, e.g., ship measurements and aerial reconnaissance. However, because each source only covered a relatively short time period and was regional in nature, they were not always directly comparable with each other. Therefore, we used the corresponding regional surface air temperature trends to recalibrate each sea-ice estimate into a common format.

[1] The talk can be seen here: https://www.youtube.com/watch?v=YJbnBFsEDYw (Recorded by Yngvar Engebretsen)

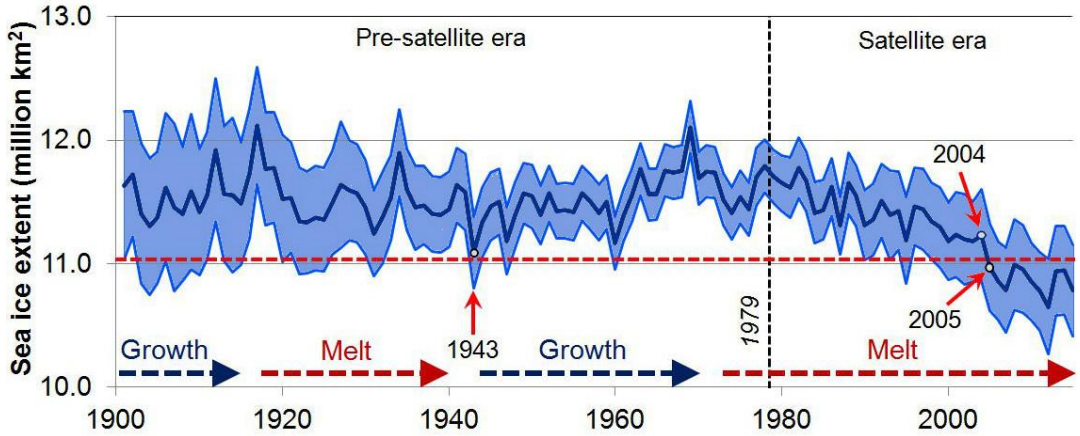

Figure 1. Annual trends of Arctic sea-ice (Connolly, Connolly and Soon 2017). The shaded area shows the uncertainty.

These recalibrated estimates could then be directly composited together to generate continuous time series from 1901-2016. In Figure 1, this recalibration of the amount of Arctic sea-ice back to the year 1901 is shown. We see a general growth in ice until 1920s, a decline 1920-1940s, growth 1940s-1970s, and then decline.

Stein et al. (2017) have used sediment core samples to estimate periods of permanent ice, seasonal ice, and ice-free areas for four different Arctic regions far back in time. According to these estimates, all four of the investigated areas (Chukchi, East Siberian and Laptev Seas and the Fram Strait) were "mostly ice-free" 6000 B.C. In the Bronze age, the cores imply there was "seasonal ice" in the Fram Strait and Laptev Sea while Chukchi and East Siberian Seas were "mostly ice-free". At present, only the Fram Strait is "mostly ice-free".

3. Snow cover

The IPCC reports only mention the Northern Hemisphere spring snow cover, which has been declining from 1967 – the start of the satellite records. They did not mention that the autumn and winter snow cover have generally increased over the period of this satellite record. Nor did they highlight the fact that the GCM hindcasts have predicted that snow cover should have been continually decreasing for all four seasons (Connolly et al. 2019).

4. Arctic temperature trends

As part of our analysis for Connolly et al. (2017), we also estimated Arctic temperature variations. This estimate was an update of a similar analysis we described in Soon et al. (2015). The estimate is shown in Figure 2. It can be seen that Arctic temperatures have gone through multiple multi-decadal periods of warming and cooling: an Arctic warming 1900s-1940s, an Arctic cooling 1940s to 1970s, and then another period of Arctic warming (1980s to present).

The warming before 1940 is very unlikely to be related to increasing greenhouse gases, since atmospheric concentrations of CO_2 and other greenhouse gases were still relatively close to pre-industrial concentrations according to the estimates favored by the IPCC. Therefore, current GCMs are unable to explain it satisfactorily, since the current GCMs assume that greenhouse gases are the main climatic driver. However, given that this early 20th century Arctic warming is qualitatively quite similar to the current Arctic warming, it is plausible that whatever caused it might also be involved in the current warming. With that in mind, in Soon et al. (2015), we showed that if you used a different estimate of solar activity than the ones considered by the

GCM hindcasts submitted to the IPCC reports, you can explain much of the early and current Arctic warming as well as the cooling from the 1940s-1970s in terms of changes in solar activity.

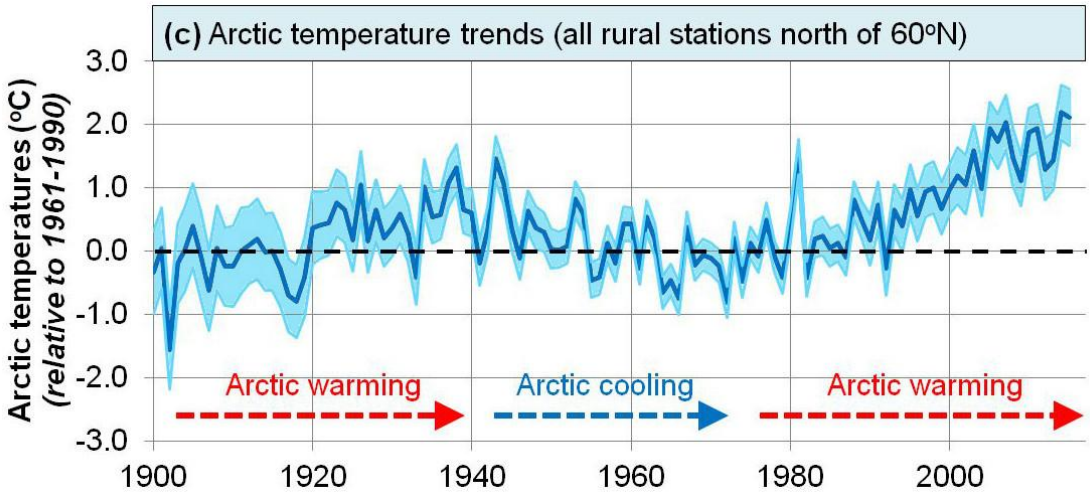

Figure 2. Arctic temperature trends (Connolly and Connolly 2015).

5. Antarctic

During the satellite era, the Antarctic sea -ice has mostly been increasing, not decreasing as expected by the GCM hindcasts.

In terms of Antarctic temperatures, the available temperature records are very limited before 1957/58, i.e., the International Geophysical Year) and are still quite limited post-1958. Nonetheless, Steig et al. (2009) applied statistical interpolation techniques to this limited data and calculated a general warming for the entire continent since 1957. However, O'Donnell et al. (2011) later reanalyzed Steig et al. (2009)'s data and discovered that their interpolation techniques had inadvertently blended conflicting trends for different regions of the continent. O'Donnell et al. (2011)'s analysis revealed that while the West Antarctic Peninsula has warmed considerably since 1957, large sections of the much bigger East Antarctica have generally cooled.

6. Summary

- The UN IPCC is great at identifying any "warming trends", but they seem to have a blind spot for anything else
- Current Global Climate Models blame almost all their "melting ice" on human-caused greenhouse gas emissions
- But, the Global Climate Models are doing an awful job of "hindcasting" the observed cryosphere trend
- The Arctic seems to alternate between multidecadal periods of warming and cooling
- Recent Antarctic trends have been the opposite to Arctic, but:
    - Some localized warming (the West Antarctic Peninsula)
    - Data is very limited before 1957
- For the future: Plan for warming **or** cooling

References

Connolly R., Connolly M. and Soon W, 2017. *Re-calibration of Arctic sea ice extent datasets using Arctic surface air temperature records,* Hydrological Sciences Journal, Vol. 62, pp1317-1340, https://doi.org/10.1080/02626667.2017.1324974

Connolly R., Connolly M., Soon W., et al., 2019. *Northern Hemisphere Snow-Cover Trends (1967–2018): A Comparison between Climate Models and Observations.* Geosciences, Vol. 9, Issue 3. https://doi.org/10.3390/geosciences9030135

IPCC, 2014. *IPCC Fifth Assessment Report (AR5), Climate Change, The Physical Science Basis,* T. F. Stocker T F, D. Qin D, G.-K. Plattner G-K et al., Eds., Cambridge University Press, New York, NY, USA. https://www.ipcc.ch/

IPCC, 2019, *The Ocean and Cryosphere in a Changing Climate, Summary for Policymakers*. https://www.ipcc.ch/

O'Donnell R., Lewis N., McIntyre S. and Condon, J., 2011. *Improved methods for PCA-based reconstructions: Case study using the Steig et al. (2009) Antarctic temperature reconstruction*. Journal of Climate, Vol. 24, pp2099-2115 https://doi.org/10.1175/2010JCLI3656.1

Soon W., Connolly R. and Connolly M, 2015. *Re-evaluating the role of solar variability on Northern Hemisphere temperature trends since the 19th century.* Earth-Science Reviews. Vol. 150, pp409-452, https://doi.org/10.1016/j.earscirev.2015.08.010

Steig E.J., Schneider D.P., Rutherford S.D. et al., 2009. *Warming of the Antarctic ice-sheet surface since the 1957 International Geophysical Year.* Nature, Vol. 457, 459-462, https://doi.org/10.1038/nature07669

Stein R., Fahl K., Schade I., et al., 2017. *Holocene variability in sea ice cover, primary production, and Pacific-water inflow and climate change in the Chukchi and East Siberian Seas (Arctic Ocean).* Journal of Quaternary Sciences. Vol. 32, pp362-379. https://doi.org/10.1002/jqs.2929

See www.ronanconnollyscience.com for more

Useful Lessons from Earth's Past Climate[1]

Ole Humlum

Arctic Historical Educational and Research Organisation (ArcticHERO), Svalbard, Norway

Correspondence to ole.humlum@gmail.com

Vol. 2.1 (2022) pp. 58-65

Submitted 17-11-2021, Accepted 29 -12-2021. https://doi.org/10.53234/scc202203/16

1. Evidence for past climatic changes

Outlining a few past geological events is useful to clarify the overall importance of climatic variations, and to place our perception of modern changes in a broader context.

During an interglacial-glacial cycle, lasting for about 100 ka (kilo-years) years and occurring with fairly regular periodicity since mid-Quaternary about 800 ka ago (Lowe and Walker, 1997), polar regions have acted as ice-sheet nucleation areas during glaciations. The formation of high latitude ice sheets during the Quaternary (last 2.8 million years) has repeatedly led to fundamental shifts in the global climate system, caused by increased planetary albedo and globally altered planetary wave structure (see, e.g., Forman et al., 2002). In turn, 120-130 m global sea-level changes, caused by water exchange between ice sheets and oceans, affected both global ocean circulation and the bathymetry of the vast continental shelf seas that border northern Eurasia and Beringia (Weaver, 1995). Land bridges formed across sounds and between islands, in turn affecting ocean surface currents, shallow-sea life and productivity, and opening and closing routes of migration for plants and animals. The Bering land bridge, existing due to lowering of sea level during the last glaciation, made possible the spread of humans from Asia to North America, as well as spread of large mammals like the woolly mammoth to the Siberian islands (Mandryk et al., 2001). The Quaternary Eurasian ice sheets terminated in the Russian-Siberian lowlands and on the adjacent shallow continental shelf, modulating freshwater flux into the global ocean through blockage of two of the ten largest river systems in the world, the Ob and Yenisei rivers (Rudoy and Baker, 1993). Continental-scale proglacial lakes that may have formed with ice sheet damming of drainages in northern Siberia (Mangerud et al., 2001), rerouted fresh water from the Arctic Ocean to lower latitude seas, potentially impacting North Atlantic deep-water formation (Weaver, 1995), affecting temperatures and precipitation at lower latitudes.

Following the termination of the last glaciation about 11.7 cal. ka BP (calendar years before present), comparatively warm conditions have characterised the global climate, but especially near the poles. Several important climatic variations, however, played out during the entire Holocene. These variations were superimposed upon initially a warm period, followed by a long-term cooling trend from about 5 ka BP.

In Iceland the birch woodland therefore began retreating from 4 cal. ka BP, the mountain tree line fell, and heaths and peatlands expanded, indicating cooler and wetter climate (Hallsdóttir, 1995). Glaciers reformed and started expanding already by 5 cal. ka BP, but generally reached their Holocene maximum extension during the Little Ice Age in the later part of the 19th century (Gudmundsson, 1997). In Svalbard, permafrost near sea level was reforming shortly before 3

[1] The talk can be seen here: https://www.youtube.com/watch?v=g2m0_w2kttc (Recorded by Yngvar Engebretsen)

cal. ka BP (Humlum et al., 2003). In Greenland, a late Holocene period of glacier growth was initiated 3.5-3 cal. ka BP, followed by major advances around 2 cal. ka BP (Kelly, 1980). In NE Greenland Hjort (1997) documented those fjords being ice-free during the early and mid-Holocene, became ice-covered after 5.7 cal. ka BP.

In western Norway, Nesje (1992) found that valley and cirque glaciers in the Jostedalsbre region reached their greatest Neoglacial extent during the mid-18th century, during the so-called Little Ice Age. Elven (1978) demonstrated that the glacier Omsbreen in southern central Norway most likely began growing from almost nothing around 550 BP, reached its maximum size (14 km^2) during the 18th century, and underwent significant retreat during the 20th century. Grove (1972) examined historical documents from western Norway to assess the extent of landslides, rock-slides, avalanches, and floods during the Little Ice Age. The study indicates that during the 17th and 18th centuries there was a much higher incidence of disastrous land, rock and snow slides/avalanches as well as more intensive flooding than was observed during previous and later warmer periods.

The terms "Medieval Warm Period" and "Little Ice Age" have been used to describe two late Holocene climate epochs with ample historical documentation, covering roughly the period from AD (after birth of Christ) 900 to AD 1200 and AD 1300 to AD 1900, respectively. The exact timing of these relative warm and cold periods, however, vary somewhat from region to region. Apparently, the onset of the Little Ice Age was comparatively early in Greenland and at high latitudes, and somewhat later at lower latitudes. Conversely, the termination of the Little Ice Age was relatively late in high latitudes (around AD 1920), and early (around AD 1860) at mid latitudes. Neither of these periods were characterised by continuous relative warm or cold conditions. Both were interrupted by a number of periods with opposite temperature trends, and their relative 'warmth' or 'cold' derives from the dominating climatic situation.

Arguments against continuing usage of the terms "Medieval Warm Period" and "Little Ice Age" have been presented by Crowley and Lowery (2000) and by Jones and Briffa (2001), suggesting that current evidence does not support globally synchronous periods of anomalous warmth or cold over these timeframes. Considered as periods with general climatic characteristics such as outlined above, however, there is overwhelming evidence for the "Medieval Warm Period" (MWP) and the "Little Ice Age" (LIA) representing roughly globally synchronous climate periods, superimposed upon a general late Holocene cooling. Also, the Summit (Greenland Ice Sheet) reconstruction of Holocene temperatures clearly shows both the MWP and the LIA periods (Dahl-Jensen et al., 1998).

Ambrosiani (1984) examined how climatic change affected settlement patterns in Scandinavia during the mid- and late-Holocene, using multiple lines of evidence. Apparently tremendous agricultural production during the Medieval Warm Period led to population explosion and ultimately the expansion of farms to marginal highland areas. The climatic decline associated with the Little Ice Age (LIA) resulted in a decline in agricultural production, which led to the collapse of many agrarian communities, and increased starvation among Scandinavian people living in marginal environments.

Lamb (1979) evaluated a variety of historical documents, including cod fishery and sea-ice reports from the Northeast Atlantic for the 17th and 18th centuries, in conjunction with the results of the CLIMAP analysis of deep-sea cores recovered from the North Atlantic and records of sea surface temperature (from AD 1867 onwards), to identify periods when winds were anomalously high and temperature anomalously low. The various lines of evidence indicate there was an enhanced thermal gradient between 55 and 65^{o}N during the Little Ice Age, and that these conditions effected torrential windstorms along the European coastline; sea surface temperature was 3 to 5 ^{o}C below the modern mean and Arctic sea-ice penetrated south beyond its normal extent.

Figure 1.Danish frigate Højendal in icebound Copenhagen Harbour, surrounded by Swedish cavalry on 11. February 1658. During the preceding week the Swedish army commanded by King Karl X Gustav marched across the sea-ice from Jutland in western Denmark, to the the island Funen, and then via the islands Langeland, Lolland and Falster to Zealand and the capital Copenhagen. By fully exploiting the tactical possibilities offered by an extraordinary cold winter the Swedish army successfully carried out a swift campaign (later known as Blitzkrieg), changing the political situation in northern Europe completely

Lamb (1984) also examined historical documents from northern Europe, Iceland, and Greenland to identify how people living in marginal environments responded to climatic change during the Medieval Warm Period and the Little Ice Age. During the MWP, farmers were able to expand their agricultural fields to higher elevations and latitudes, and the northern fishing industry became very prosperous. In contrast, during the LIA, many farmers had to retreat from lands they were cultivating because the fields were overrun by glaciers. Many gave up farming and began working for shipping companies or fisheries to make a living. In AD 1690, however, also the fishing industry declined due to changes in oceanic circulation. Historical records also document more outbreaks of disease, possibly due to undernourishment.

2. Perception of climatic changes

Most likely people have long been aware of ongoing climatic variations. Whether such changes were interpreted as manmade or natural depended on the general philosophy of the time (Storch and Stehr, 2000). In Medieval time, change was seen as a natural process, the systematic deterioration of a living, and thus ageing, world. By the eighteenth and nineteenth centuries, interest focused on the effects of deforestation and other changes in land use. As an example, the colonies of North America were thought to have become more temperate as a result of deforestation during colonization. The modern concern about carbon dioxide as an agent of anthropogenic climate change can be traced back to the nineteenth century and French scientist Jean Baptiste Joseph Fourier (today best known for his Fourier series) and the Swedish chemist Svante Ar-

rhenius. In the 1920s the increasing concentration of atmospheric greenhouse gases (especially CO_2) was suggested as being the cause of atmospheric warming registered at that time, and future global warming was expected to follow. Contemporary studies suggested that from year 1850 to 1940, the mean thickness of sea ice in the Arctic Ocean had decreased by about 30 % and the surface extent by as much as 15 %. The Arctic Ocean was expected to be virtually ice free within a foreseeable future.

Back in the 1960s and early 1970s, the timeframe of most scientists was still retrospective, rather than prospective (Oldfield, 1993). However, the revived notion of the Milankovitch theory then suddenly offered the new possibility of actual climate prediction. At that time there was relatively little emphasis on potential or actual 'global warming', and the idea was virtually unknown to popular consciousness. Indeed, a widespread belief at that time was that the planet was heading for a new ice age, fuelled by acceptance of the Milankovitch theory and new knowledge gained from isotope analysis of Greenland ice cores (Dansgaard et al., 1970, 1971). Hays et al. (1976) suggested that the observed orbital-climate relationships predict that the long-term trend over the next several thousand years would be toward extensive Northern Hemisphere glaciation. This period of global cooling in the early 1970s, thought to be the first indication of a new ice age, was seen as being accelerated by aerosols from industrial pollution blocking out sunlight. Such concerns in the mid-1970s brought together atmospheric scientists and the US Central Intelligence Agency (CIA) in an attempt to determine the geopolitical consequences of a sudden onset of global cooling.

Late 20th century concerns about the future climatic development mainly stem from the increasing concentration of greenhouse gasses in the atmosphere. According to current GCM's global climate should since year 1850 be experiencing man-induced increased greenhouse warming, foreseen to continue in the future. What can be learned from such profound and recurrent changes in scientific perception related to the climate issue? Apparently, climate science has limited inertia and is exposed to rapid paradigm-like shifts in common notion, in concert with observed 10–60-year surface air temperature variations (Chambers and Brain, 2002). All climate hypotheses, including the present one focusing on atmospheric greenhouse gasses, are by nature highly vulnerable to new trends in the observational evidence. Additionally, part of the reason for the lack of longevity of different 20th century climatic hypotheses may be the fact that climate science and climatology traditionally was considered a scientific backwater, with few eminent scientists such as Hubert Lamb (UK) and Christian Phister (Switzerland) as outstanding exceptions. Since about 1990, however, an increasing number of scientists, often without formal meteorological or climatologically training, oceanographers, hydrologists, biologists, etc., have all been redefined as climate scientists. More than anything, this indicates the degree to which the main research-agenda and -funding now is hitched to the political side of the climate issue.

3. From empirical science to modelling

Numerical models are increasingly used as tools for predicting how the global climate will respond to changes in atmospheric composition and land surface albedo. Such numerical models are typically developed only to reproduce the characteristics of modern climate and its inherent variability during a short period with relatively modest climate change. Using numerical models for projections of future climate therefore always involves extrapolation beyond the time range for which the models have been developed and tested. This contrasts with the prudence by which numerical models are applied in other and less complicated frameworks, e.g., engineering. In addition, even state-of-the-art GCMs only incorporate the theoretical effects of a limited number of well understood climatic forcing factors, while other potential, but less well understood drivers such as solar and cosmic rays effects are downplayed or left out. This is disturbing, as geological knowledge suggests that the celestial forcing represents a primary global climate driver on most time scales. In addition, the economic projections used in the IPCC emis-

sions scenarios are based on models for population- and economic growth, which themselves are subject to debate and potential fallacious assumptions.

Will improved understanding of theoretic greenhouse radiational effects effectively address the global climate change issue? Most likely the answer is no. No matter how firm our theoretical knowledge of greenhouse effects becomes, there is no way in which we can effectively 'multiply-up' or extrapolate that knowledge to address megascale, complex issues such as the dynamics of the Earth's atmosphere. The atmospheric greenhouse radiative effects may be amenable to sophisticated instrumental and theoretical research, but the possible derived macroscale result (future global climate change) is not. Overwhelmingly, the published work on future climate change takes one process (greenhouse radiative effects) and the ensuing result (global warming) as unquestionable.

This obviously represents an appropriate moment at which to invoke the ideas forwarded by Platt (1964). Modern climate modelling becomes an illustration of what Platt would state characterizes a discipline that is not robust and vigorous. Clearly what is needed in this instance is to scrutinize, challenge, and investigate the basic concepts rather than accept them as given. Such scepticism can conflict with other important features of science, such as the need for creativity and for conviction in arguing a given position. But organized and searching scepticism as well as openness to new ideas is essential to guard against the intrusion of dogma or collective bias into scientific results. Failure to adopt this sceptical approach, may have the consequence that a numerical model for future climate development will not serve as a test vehicle, but as a 'regulative principle' (von Engelhardt and Zimmermann, 1988).

Improved empirical knowledge (field and lab. data) and techniques offer the prospect of enormously expanding our knowledge of global climate change, past and present. We cannot afford to put our scientific faith in improved modelling abilities alone. It will never be possible to span the full range of climatic spatial and temporal scales by merely multiplying-up our instrumented process research, because, as Church (1996) have noted, theoretical integration across many scales seems infeasible. What we do need to do is to focus our growing instrumental and modelling capacities on critical, sharply defined problems that are within the appropriate time- and scale range. We will serve ourselves poorly as scientists if we produce a climate science dominated by instrumentation and computer models, unrestrained by data or rigour.

The focus on climate research over the last 20-25 years have resulted in an increased awareness that climate is not as constant as it may have previously appeared. In this context, even the most extreme and divergent forecasts of future climate may have done some good. This is, however, a situation that should not continue much longer, as it tends to confuse political decision-makers and the general public about the asserted extraordinariness of modern climate changes.

4. Conclusion

Today, the immediate need for science is to improve empirical knowledge on climate change, past and present, and to understand the limitations of each kind of approach to forecasting. Such accumulated knowledge is the very basis for improving the quality of computer-based modelling attempts. For the decision-makers the lesson is to allow wider margins for future climatic change, cooler as well as warmer, wetter as well as drier, windier as well as less windy, etc. Climate science remains a highly complex issue where simplification tends to lead to confusion, and where understanding requires knowledge, openness to new hypotheses, thought and effort.

References

Ambrosiani, B. 1984**.** *Settlement expansion - settlement contraction: a question of war, plaque, ecology or climate?* In Climatic Changes on Millenial Basis: Geological, Historical and Instrumental Records. Edited by Mörner, N.-A., and W. Karlen, 241-248. D. Reidel: Dordrecht. https://doi.org/10.1007/978-94-015-7692-5_25

Chambers, F.M. and Brain, S.A. 2002. *Paradigm shifts in late-Holocene climatology***?** The Holocene 12, 239-249. https://doi.org/10.1191/0959683602hl540fa

Church, M.J. 1996. *Space, time, and the mountain—how do we order what we see?* In The Scientific Nature of Geomorphology, Rhoads, B.L. and Thorn, C.E (eds), 147-179, Wiley: Chichester. http://www.geoinfo.amu.edu.pl/wpk/natgeo/chapt6.pdf

Crowley, T. J. and T. Lowery, 2000. ***How warm was the Medieval warm period?*** Ambio 29, 51-54. https://doi.org/10.1579/0044-7447-29.1.51

Dahl-Jensen, D., Mosegaard, K., Gundestrup, N., Clow, G.D., Johnsen, S.J., Hansen, A.W. and Balling, N. 1998. *Past Temperatures Directly from the Greenland Ice Sheet***.** Science 282, 268-271. https://doi.org/10.1126/science.282.5387.268

Dansgaard, W., Johnsen, S.J. and Clausen, H.B. 1970. *Vi går mot bistra tider***.** Forskning och Framsteg 8:7, 11-15.

Dansgaard, W., Johnsen, S., Clausen, H.B. and Langway, C.C., Jr. 1971. *Climatic record revealed by the Camp Century ice core***.** In: K.K. Turekian (ed.), *Late Cenozoic glacial ages*, 31-56, Yale Univ. Press, New Haven and London.

Elven, R. 1978. *Subglacial plant remains from the Omsbreen glacier area, south Norway.* *Boreas* 7, 83-89. https://doi.org/10.1111/j.1502-3885.1978.tb00266.x

Forman S.L, Ingólfsson Ó, Gataullin V, Manley W.F and Lokrantz H. 2002. *Late Quaternary stratigraphy, glacial limits and paleoenvironments of the Marresale area, western Yamal Peninsula, Russia.* Quaternary Research 57, 355-370. https://doi.org/10.1006/qres.2002.2322

Grove, J.M. 1972. *The incidence of landslides, avalanches, and floods in western Norway during the Little Ice Age***.** Arctic and Alpine Research, 4:2, 131-138. https://doi.org/10.1080/00040851.1972.12003633

Gudmundsson, H. 1997. *A review of the Holocene environmental history of Iceland*. Quaternary Science Reviews 16, 81-92. https://doi.org/10.1016/S0277-3791(96)00043-1

Hays, J.D., Imbrie, J. and Shackleton, N.J. 1976. *Variations in the Earth's orbit: pacemaker of the ice ages.* Science 194, 1121-1132. https://doi.org/10.1126/science.194.4270.1121

Hallsdóttir, M. 1995. *On the pre-settlement history of Icelandic vegetation***.** Icelandic Agricultural Science 9, 17-29.

Hjort, C. 1997. *Glaciation, climate history, changing marine levels and the evolution of the Northeast Water Polynia***.** Journal of Marine Systems 10, 23-33. https://doi.org/10.1016/S0924-7963(96)00068-1

Humlum, O., Instanes, A. and Sollid, J.L. 2003. *Permafrost in Svalbard; a review of research history, climatic background and engineering challenges.* Polar Research 22:2, 191-215. https://doi.org/10.3402/polar.v22i2.6455

Jones, P.D. and Briffa, K.R. 2001**.** *The "Little Ice Age"; local and global perspectives*. Climate Change 48, 5-8. https://doi.org/10.1023/A:1005670904293

Kelly, M. 1980. *The status of the Neoglacial in western Greenland***.** The Geological Survey of Greenland, Report 96, 24 pp.

Lamb, H.H. 1979**.** *Climatic variation and changes in the wind and ocean circulation: the Little Ice Age in the Northeast Atlantic.* Quaternary Research 11, 1-20. https://doi.org/10.1016/0033-5894(79)90067-X

Lamb, H.H. 1984. *Climate and history in northern Europe and elsewhere*. In Climatic Changes on Millenial Basis: Geological, Historical and Instrumental Records. Edited by Mörner, N.-A., and Karlen, 225-240. W. D. Reidel, Dordrecht. https://doi.org/10.1007/978-94-015-7692-5_24

Lowe J.J. and Walker M.J.C. 1997. *Reconstructing Quaternary Environments*. 446 pp. Longman: Harlow. https://doi.org/10.4324/9781315797496

Mangerud J, Astakhov VI, Murray A, Svendsen JI. 2001. *The chronology of a large ice-dammed lake and the Barents-Kara Ice Sheet advances, Northern Russia***.** Global and Planetary Change 31, 321-336. https://doi.org/10.1016/S0921-8181(01)00127-8

Mandryk, C.A.S., Josenhans, H., Fedje, D.W. and Mathews, R.W. 2001. *Late Quaternary paleoenvironments of Northwestern North Americe: implications for inland versus coastal migration routes.* Quaternary Science Reviews 20, 301-314. https://doi.org/10.1016/S0277-3791(00)00115-3

Nesje, A. 1992. *Younger Dryas and Holocene glacier fluctuations and equilibrium-line altitude variations in the Jostedalsbre region, western Norway.* Climate Dynamics 63:3-4, 221-227. https://doi.org/10.1007/BF00193534

Oldfield, F. 1993. *Forward to the past: changing approaches to Quaternary palaeoecology.* In Chambers, F.M. (ed.), Climate change and human impact on the landscape, 3-9. Chapman and Hall, London. https://doi.org/10.1007/978-94-010-9176-3_2

Platt, J.R. 1964. *Strong Inference*. Science 146, 347–353. https://doi.org/10.1126/science.146.3642.347

Rudoy, A.N. and Baker, V.R. 1993. *Sedimentary effects of cataclysmic late Pleistocene glacial outburst flooding, Altay Mountains, Siberia.* Sedimentary Geology 85, 53-62. https://doi.org/10.1016/0037-0738(93)90075-G

Storch, H.von and Stehr, N. 2000. *Climate change in perspective.* Nature 405, 615. https://doi.org/10.1038/35015179

Von Engelhardt, W. and Zimmermann, J. 1988. *Theory of Earth Science*. Translated by Fischer L (first published in German in 1982). Cambridge University Press: Cambridge.

Weaver, A.J. 1995. *Driving the ocean conveyor***.** Nature 378, 135-136. https://doi.org/10.1038/378135a0

Wegener, A. 1924. *The origins of continents and oceans*. Translated by J. Skarl, from third German Edition. Methuen. London.

Correspondence to
copenhagenrock-
shop@outlook.com
Vol. 2.1 (2022)
pp. 66-68

Temperature at the Coast and Inlands

Frank Lansner

Fredensborg, Denmark

Submitted 18 -12 - 2021, Accepted 29 -12-2021. https://doi.org/10.53234/scc202203/17

We can divide the land climate in two categories: the continental climate with warm summers and cold winters, and the maritime climate with cool summers and mild winters. This is a report of a project where we have analyzed temperature data 1900-2010 from many (thousand) meteorological stations across the world, to figure out the difference between maritime and continental stations. We have found that we can divide the stations into two types: The ocean air affected (OAA) areas and the ocean air sheltered (OAS) areas. The latter are found in valleys which are sheltered from wind from the oceans as shown in Figure 1 as blue areas.

Since OAA and OAS areas often are located nearby, we have not included OAA/OAS border areas. We have also excluded areas which behave as OAS at certain wind directions, and like OAA stations at other directions. We have analyzed 16 geographical areas, and the result for 10 of those are presented in our first publication (Lansner and Pedersen 2018). The rest will be published later (Lansner and Pedersen, in progress).

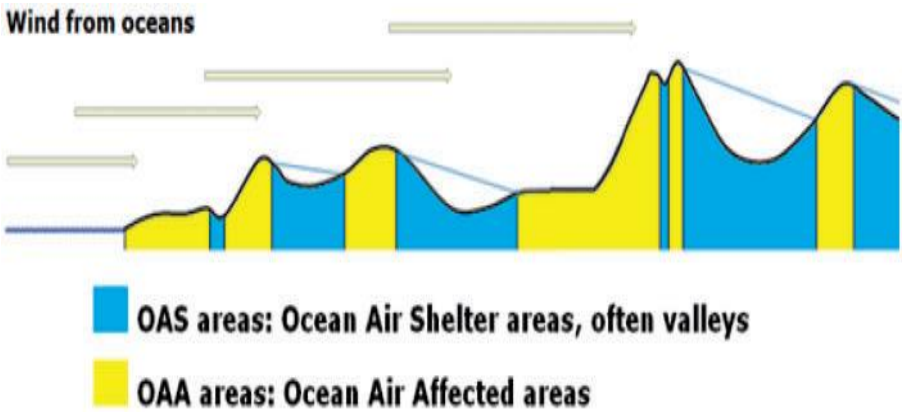

Figure 1. OAA and OAS locations with respect to dominating wind direction

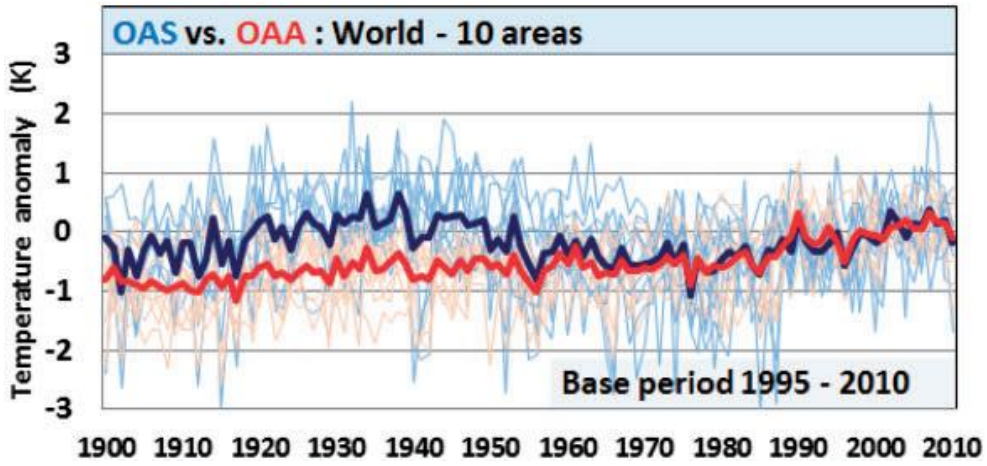

Figure 2. Global averages for OAS temperatures (blue) compared with OAA (red).

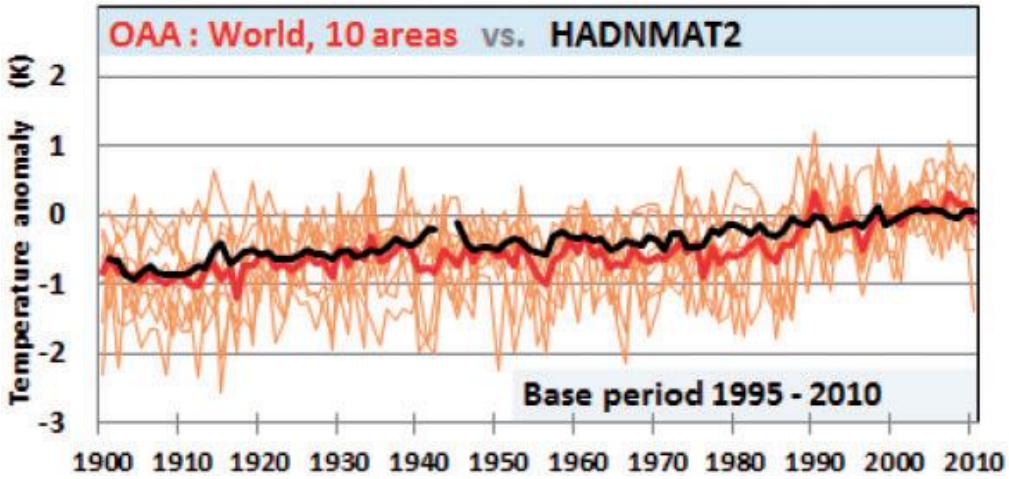

Figure 2. Sea surface temperature (HADMAT2) compared with OA

All areas analyzed show the same pattern: OAS series show a sine wave with a peak heating event 1930-1950, which is not seen in the ocean data. Another heating peak appears 2000-2010 in the OAS series. This has the same or lower amplitude. The OAA data have an almost linear trend 1900-2010 and the two series follow each other closely from 1950. This is demonstrated in Figure 2.

The ocean data does not show the heating waves, just slowly increasing temperature of the surface layer. This is demonstrated in Figure 3, where the OAA series (red) is compared with the HadCRUT sea-surface temperature (HADNMAT2(black)). The linear trend for the HADMAT2 series 1900-2010 is 0.71K/century, while we find for the OAA set a slope of 0.78K/century. Therefore, they are close.

Comparing OAS areas, we see larger variations in areas closer to the Arctic, but the same trend as in other areas. The same with the OAA data. This is a result of the Arctic amplification. For the North, Central and South Americas, the trends are the same, but in the OAS data, the 1930-ties are considerably warmer than the peak at the end of the century.

The OAS and OAA data from an area are always from the same source, so the differences we find are not due to different sources. The sources of data used are Meteorological Yearbooks (Europe), NOAH GHCN v2.raw, National Archives, Nordclim, Tutiempo, World weather records and statistical yearbooks.

We have also compared our results with "corrected" data series and find that they assume a trend and correct the data to fit the expected trend. The BEST collaboration even states this clearly: They adjust the data to follow the "expected trend". This is clearly wrong. All land areas have two correct temperature trends. Temperature corrections fails by ignoring this.

Examples can be found in the Alps, where OAS data are ignored, and only one trend is assumed to exist. Data from mountain peaks are accepted. They look like OAA data and are not changed. The same happens for Scandinavia. Comparing the original data sets with the European Center data sets, we found that data before 1950 were missing. The same with continental Europe data. The result is that the warm peak in the 1930-ties is only seen in the original data. Extreme examples are from Hungary where most stations have a temperature drop of 1.5K in the period 1934-1980 which is not seen in the adjusted data sets.

Conclusion

Any land area has two different, but correct, temperature trends (+ intermediate trends). In contrast, all official institutions are adjusting or homogenizing the data expecting one trend, not two. To decide on the amount of warming due to CO_2, one should compare with OAS stations, which show little or no warming after 1950, just the same or a smaller cycle than in the 1930ies.

Why do we need a large extra CO_2 heating after 1950 to explain "no extra heating after 1950?". The CO_2 emissions, exploding after 1950, seem to have no effect on the temperature when we delete the ocean noise.

Reference

Lansner, F. and Pedersen, J.O.P. 2018, *Temperature trends with reduced impact of ocean air temperature*, Energy and Environment, 29, 613-632.
https://doi.org/10.1177/0958305X18756670

Correspondence to
janesol@online.no

Vol. 2.1 (2022)
pp. 69-73

The Barents Sea Ice Edge During the Last Centuries[1]

Jan-Erik Solheim

Independent Scientist, Bærum, Norway

Submitted 08-11-2021, Accepted 29-12-2021. https://doi.org/10.53234/scc2022203/18

1. Introduction

To figure out what is driving the climate change it is vital to observe long climate series.
In this contribution I will report about data collection and analysis of a climate series covering the position of the Ice Edge in the Barents Sea for more than 440 years. A clear sign of planetary forcing is detected, and a model involving the solar wind is suggested. I will present a project where we use a long series of estimates of the position of the ice edge in the Barents Sea to investigate indications of planetary beat. At the conference in October 2019, only provisional results were shown, but since then we have two publications on the topic (Mörner et al. 2020 and Solheim et al. 2021). In the following I will present the data and some results from the analysis together with a simple harmonic model and suggested physical explanation.

1. The dance of the Sun conducted by planets

In the talk of Niklas Mörner (this proceedings) we learned about the Gulf Stream Beat, which changes the stream from a strong Northern Branch to a weaker and at the same time from a weak to a stronger Southern Branch, and how this may be the result of changes in Earth's rotation or length of day. He showed that this beat also exists in sea level changes in equatorial regions and in climate changes as the Little Ice Age and the warm recent era. He explained the changes in rotation as due to variations in the solar wind, which again varies with the solar activity, which is in some way related to the Sun's complicated orbit around our planetary systems center of mass as shown in Figure 1. He concluded forcefully that averages taken over the whole planet, kill the dynamicity, and destroys the information about our planet *which changes on all timescales*.

I have the deepest respect for the great observer of the orbits of the Moon and the planet Mars, Tycho Brahe (1546-1601), from his observatory on Ven between Denmark and Sweden, and the great mathematician Johannes Kepler (1571-1630) who discovered the planets elliptical orbits. The orbital periods of Jupiter are 11.9 years and Saturn 29.5 years. They meet in the sky every 19.9 years. When Jupiter has done 5 revolutions Saturn has done two and they are back in the same direction. This may be the origin of the 60-year cycle seen in many climate series.

The complicated pattern of the solar orbit (Figure 1) was first calculated by Jose (1965), who also related it with sunspot variations. He found that the pattern repeated approximately after about 179 years. This is called the Jose cycle. Charvátová and Hejeda (2014) showed that the solar orbit could be classified in regular (trefoil) periods which lasted about 50 years containing periods of high solar activity, and irregular periods which contain periods of deep minima. We

[1] The talk can be seen here: https://www.youtube.com/watch?v=oH8eYysz8lA (Recorded by Yngvar Engebretsen).

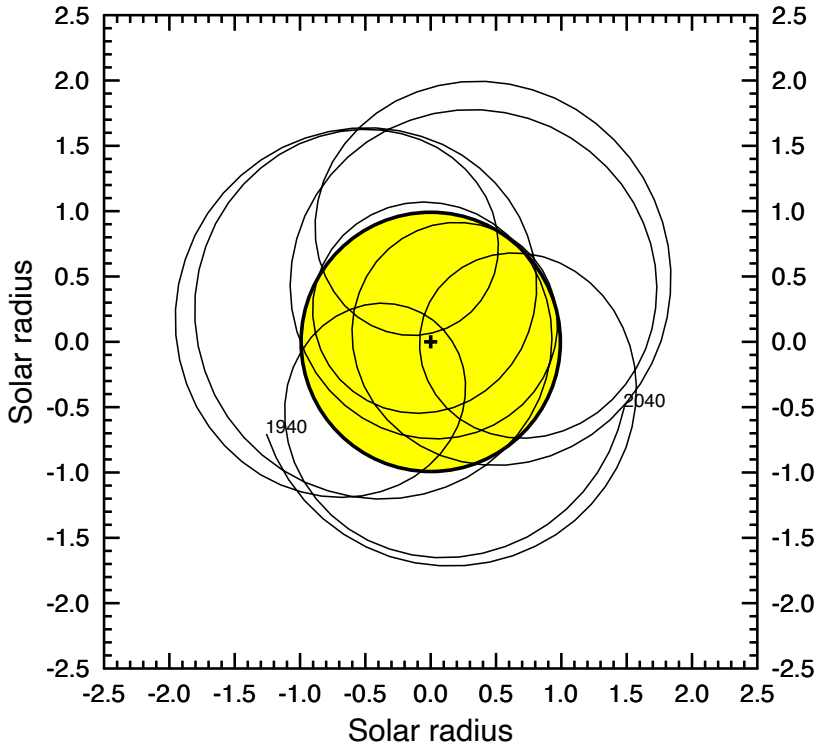

Figure 1, The orbit of the Sun relative to its orbital plane 1940-2040. The solar system barycenter is marked with a cross (+). The size of the sun is indicated by the yellow circle

are now in an irregular period which will last until 2040. Figure 4 in Mörner (2022) shows how planetary beats can lead to climate variations.

2. North Atlantic sea-ice

The west coast of Svalbard was "discovered" by Willem Barents in 1596 who reported rich stocks of seal and whales near the ice edge. A whaling industry started, first with land stations on Svalbard, later pelagic. When the whales went extinct around 1830, seal hunting along the ice edge became the main occupation. The English Muscovy Company operated a trade route to Archangel from 1553. From the hunting, trading, and Arctic explorers, a climatic map is constructed by Ole Humlum (2000) shown as Figure 2. This map shows the maximum sea-ice extent in various periods in addition to climatic events. Special cases aree the period 1660-1720 with ice almost to Scotland and 1769 with maximum ice limit north of Svalbard. Years of extreme weather events and crosses when species disappeared are also shown in the map.

A pioneering work was done by Torgny Vinje (1999) to create a 400-year long time series of the position of the ice edge in the Barents Sea between Svalbard and Frans Josefs Land, later updated by Norwegian Polar Institute (Falk-Petersen et al. 2015 and Solheim et al. 2021). The position is estimated for the two last weeks of August, from ship logs, expedition reports, and in recent time from airplanes and satellites. The completeness of the time series varies from 34 per cent the first 100 years (1579-1678) to 100 % after 1979 with satellite data. The Barents Sea Ice Edge (BIE) position had a southernly position (around 76 °N) in the period 1625-1680 and 1784-1830 and a nearly linear speed north 1890-2020 with 0.035°N per year.

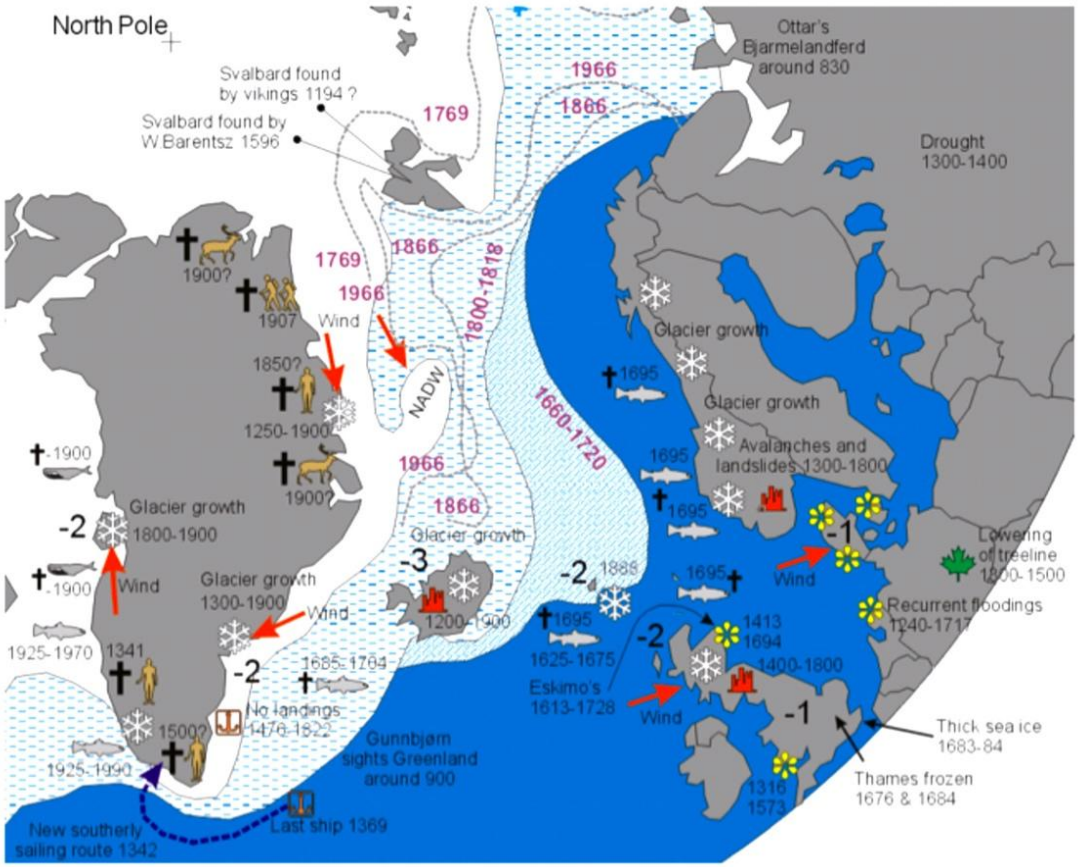

Figure 2. Climate history of Northwestern Europe – with maximum ice cover in certain periods (Humlum 2000).

3. The ice edge position – sign of planetary periods

We have correlated the BIE position series with other climate series for the North Atlantic and northern hemisphere, solar variations, both local and global, and effects integrated in the Earth's rotation. We find that most of the series are correlated. In the longer BIE-series we find planetary orbit fingerprints.

This is shown in Figure 3, where the dots are BIE positions and the red curve is a 4-period harmonic simulation with periods 3, 3/2, 4/5 times the Jose period, plus a 84 year period related to the planet Uranus. Since the periods of the planets are constant over millennia, it means that even small forcings with these periods will repeat for a long time and can create forced oscillations. In addition, some weaker, non-significant shorter periods are shown in black. They are the 60-year and 19.7-year Jupiter-Saturn periods and a 14-year period of unknown origin.

This simple harmonic model explains the almost linear trend since 1890, and a maximum in the 4 periods around 2010. In the following decades this model shows BIE moving south to about 79°N, signaling a colder climate around the North Atlantic. In Figure 3 we have also shown periods when the Gulf Stream beats (GSB) from a strong northern to a strong southern branch (see Mörner's contribution Figure 2). That happens during or after extreme low positions of BIE, which will not take place this century.

4. A suggested relation between solar activity and the BIE position

In Mörner et al. (2020) we suggested that the solar wind can change the Earth's rotation, which again acts on ocean currents which brings heat to the Arctic regions. The solar wind can work directly by pressure slowing the Earth's rotation, or by changing the Earth's shielding capacity

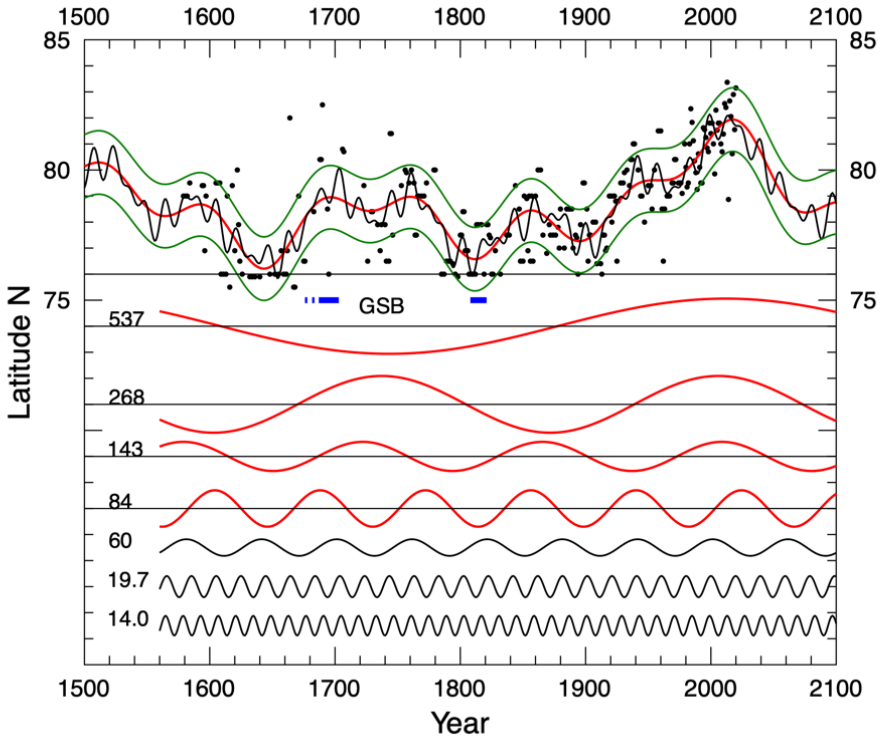

Figure 3.BIE positions with a 4-parameters harmonic model based on planetary periods (red) with uncertainty interval (green). In addition, three weaker periods are shown in black. The various components are shown separately in the lower panel

which protects the Earth against cosmic rays which can increase cloud formation. We also found that electric charges carried with the solar wind can magnetize our planet's iron core and slow the Earth's rotation. This is also modulated with the Jose period (Duhau and de Jager 2012), but with a delay of 94 years.

5. Conclusions

We have analyzed a long series of estimated the ice edge positions in the Barents Sea and found it's variations can be explained by stationary cycles which originate in the planetary system. This may explain the apparent warmer climate the last century and indicates that a change to a colder climate will take place this century.

References

Charvátová I and Hejeda P 2014, *Responses of the basic cycles of 178.7 and 2402 yr in solar-terrestrial phenomena during the Holocene*, Pattern Recogn. Phys. 2, 21-26. https://doi.org/10.5194/prp-2-21-2014

Duhau S and de Jager C 2012, *On the Origin of the Bi-Decadal and the Semi-Secular Oscillations in the Length of the Day*, in S. Kenyon et al. (eds), Geodesy for Planet Earth, International Association of Geodesy Symposia 136, Springer -Verlag Berlin Heidelberg, pp. 507-51. http://dx.doi.org/10.1007/978-3-642-20338-1_61

Falk-Petersen S, Pavlov V, Berge J, Cottier F, Kovacs K M and Lydersen C 2015**,** *At the Rainbow's End: High Productivity Fueled by Winter Upwelling along an Arctic Shelf*, Polar Biology, 38, 5-11. https://doi.org/10.1007/s00300-014-1482-1

Humlum O 2000, *Grønland i Nordatlanteren*, In: Atlas over Grønland, Royal Danish Geographical Society, Copenhagen, p. 8-9.

Jose P D 1965, *Sun's motion and sunspots*, Astron. J., 70, 193-200. https://doi.org/10.1086/109714

Mörner N-A, 2022, *The Gulf Stream Beat*, Scienc ot Climate Change, 2, 47-52 https://doi.org/10.53234/scc202112/xxx

Mörner N-A, Solheim J-E, Humlum O and Falk-Petersen S 2020, *Changes in Barents Sea ice Edge Positions in the Last 440 years: A Review of Possible Driving Forces***,** Int. J. of Astronomy and Astrophysics ,10, 97-164. https://doi.org/10.4236/ijaa.2020.102008

Solheim J-E, Falk-Petersen S, Humlum O and Mörner N-A 2021, *Changes in Barents Sea Ice Edge Positions in the Last 442 Years, Part 2: Sun, Moon and Planets*, Int. J. of Astronomy and Astrophysics, 11, 279-341, *https://doi.org/10.4236/ijaa.2021.112015*

Vinje T 1999, *Barents Sea Ice Edge Variation Over the Past 400 Years*. Proceedings of the Workshop on Sea-Ice Charts of the Arctic. Seattle, WA, USA, 5-7 August 1998, World Meteorological Organization, WMO/TD No. 949, 4-6.

Correspondence to har-ald.yndestad@ntnu.no
Vol. 2.1 (2022)
pp. 74-77

Lunar-driven Control of Climate and Barents Sea Eco-systems[1]

Harald Yndestad

Norwegian University of Science and Technology, Aalesund, Norway

Keywords: Lunar nodal tide; Lunar forced climate variability; Marine ecosystem variability; Eco system resonance; Biomass collapse

Submitted 14-12-2021, Accepted 29-12-2021. https://doi.org/10.53234/scc202203/19

1. Introduction

Herring periods and cod periods along the Norwegian coast have been known for more than 1000 years. Periods of growth in the fisheries, have formed the basis for settlement, industrialization, economic growth, and wealth. Periods, when the fish disappeared, led to emigration, hunger, and poverty. Over the years, one has questioned whether good years, or bad years, were accidental, or ruled by higher powers. The fish stock grew during the 1940s. After 1945, a new fishing fleet was built, which had good years in the 1950s and 1960s. In the 1970s, the herring stock and the cod stock disappeared. Questions were then asked about possible causes. Was there a lack of scientific management, overfishing, or was there something unknown phenomenon in nature, which led to the fish stocks disappearing. This presentation is a summary of a doctoral dissertation in which this topic was studied.

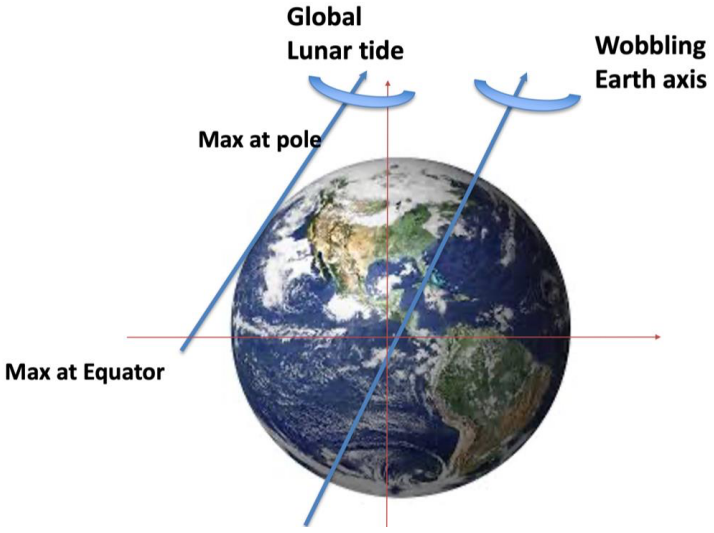

Figure 1. The Earth axis and the lunar nodal tide wave.

[1] The talk can be seen here: https://www.youtube.com/watch?v=EN1WwV9TZ7Y. (Recorded by Yngvar Engebretsen)

The 18.6-year cycle

Gravity between the Earth, the Sun, and the Moon, cause the Earth's axis to change direction, in a period of 18.6 years. The earth's axis nutation period introduces a standing lunar nodal tidal wave, between the pole and the equator, with a period of 18.6 years. The tidal wave has a maximum amplitude at the poles and the equator and a node at about 35 degrees in the orbital plane.

The tidal wave of 18.6 years leads to a vertical mixing of between cold and warm temperature layers. The result of vertical mixing is that the surface water has a periodic change of 18.6 years, which follows the ocean currents northwards, and affects the climate. The tidal wave has a $\pi/2$ (rad) phase lag from the earth's axis nutation period. The lunar forced temperature period has a $\pi/2$ (rad) phase lag from the 18.6-year lunar nodal tide. Over time, a set of lunar forced temperature periods of 18.6 years is produced, which gives periodic spectrum of [1, 2, 3, 4 ...]*18.6 years. Coincidences in the lunar forced temperature spectrum give climate periods up to 75, 223 and 446 years. A wavelet spectrum analysis of data series has identified periods of [1/2, 1, 4]*18.6 years in the inflow of North Atlantic water to the Norwegian Sea, Barents Sea, the NAO index, land surface temperature and rainfall along the Norwegian coastline. Arctic ice extent from 1570, has periodic variations in periods of [1, 4, 12]*18.6 years. Greenland temperature has periods of [1, 4, 12, 24]*18.6 years.

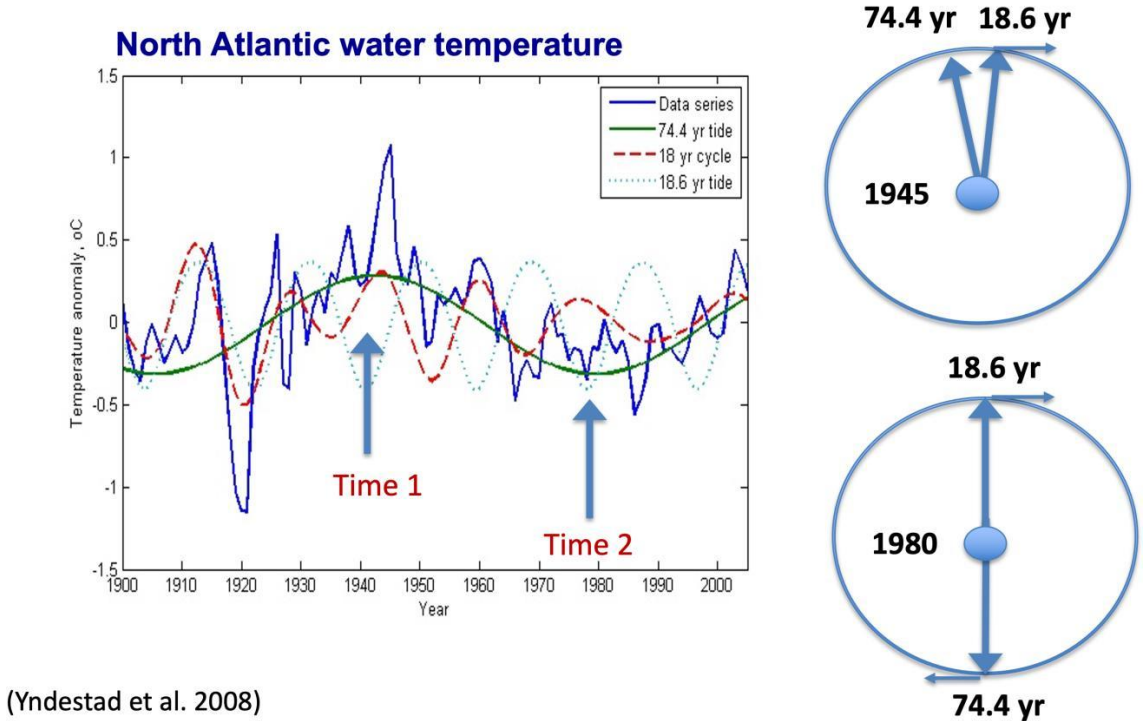

Figure 2. The North Atlantic water temperature cycle

2. The effect of the cycle on the fisheries

A study of Barents Sea ecosystems shows that green algae, plankton, herring, capelin, and cod follow a periodic variation of [1/2, 1, 3, 4]*18.6 years. The capelin stock recruits in periods of (18.6/2)/3 years, which optimizes the capelin stock over a period of 18.6/2 years. The cod stock recruits in periods of 18.6/3 years, which optimizes the stock's growth over 18.6 years. The cod stock period of 18.6 years, at the same time follows the temperature variations of 3*18.6 years and 4*18.6 years, which has an average period of (3 + 4)18.6/2 = 65 years. Herring periods follow cod stock periods. The explanation for good fishery periods and bad fishery periods, is

recruitment, growth, and mortality, adapted to sea temperature variations of [1/2, 1, 2, 3, 4, ...]*18.6 years. The explanation for the biomass collapse, is allocation of catch quotas, which do not follow period phase-variations from sea temperature variations of [1/2, 1, 2, 3, 4, ...]*18.6 years.

References

Yndestad, H 1996, *System Dynamics of North Arctic Cod*, The 84'th international ICES Annual Science Conference, Hydrography Committee, Iceland, October 1996.

Yndestad, H 1997. *Systems Dynamics in the Fisheries of Northeast Arctic Cod*. 15th International System Dynamics Conference (ISDC ´97), August 1997, Istanbul.

Yndestad, H 2000. *The predestined fate. The Earth nutation as a forced oscillator on management of Northeast Arctic cod.* The 18th International Conference of The System Dynamics Society. Aug. 6-10, 2000, Bergen, Norway.

Yndestad, H 2001a**.** *Earth nutation influence on Northeast Arctic cod management.* ICES Journal of Marine Science, 58, 799-805.

Yndestad H and Stene A 2002. *Systems Dynamics of Barents Sea Capelin.* ICES Journal of Marine Science, 59, 1155-1166.

Yndestad H 2002. *The Code of Norwegian spring spawning herring Long-term cycles*. ICES Annual Science Conference, Oct. 2002, Copenhagen.

Yndestad H 2003a. *A Lunar nodal spectrum in Arctic time series***.** ICES Annual Science Conference, Sept. 2003. Tallinn. ICES CM 2003/T.

Yndestad H, Turrell W R and Ozhigin V 2004. *Temporal linkages between the Faro-Shetland time series and the Kola section time series.* ICES Annual Science Conference, Vigo. Sept. 2004. Theme Session M. Regime Shifts in the North Atlantic Ocean: Coherent or Chaotic?

Yndestad H. 2004. *The cause of Barents Sea biomass dynamics*. Journal of Marine Systems.

Yndestad, H. Dr.philos. Thesis. 2004:132. *The Lunar nodal cycle influence on the Barents Sea.* Norges teknisk-naturvitenskapelige universitet, NTNU. Trondheim.

Yndestad, H 2006*. The Arctic Ocean as a coupled oscillating system to the forced 18.6 yr lunar nodal cycle.* 20 Years of Nonlinear Dynamics in Geosciences. American Meteorological Society & European Geosciences Union, June 11-16, 2006, Rhodes, Greece.

Yndestad, H 2006. *The influence of the lunar nodal cycle on Arctic climate.* ICES Journal of Marine Science, 63:3, 401–420. http://doi.org/10.1016/j.icesjms.2005.07.015.

Yndestad, H 2006. *Possible Lunar tide effects on climate and the ecosystem variability in the Nordic Seas and the Barents Sea.* ICES annual conference. Session ICES CM 2006/C: Climatic variability in the ICES area 2000-2005 in relation to previous decades: physical and biological consequences 19-23 sept. 2006, Maastricht, Netherland.

Yndestad, H 2007. *Long tides influence on the climate dynamics and the ecosystem dynamics in the Barents Sea.* Symposium on Ecosystem Dynamics in the Norwegian Sea and the Bar-

ents Sea. Theme session: Climatic effects on food webs. Tromsø. Norway 12-15 March 2007.

Yndestad, H 2008. *The Barents Sea ecosystem dynamics as a coupled oscillator to long tides.* Annual Science conference 22-26 Sept. 2008, Theme Session Coupled physical and biological models: parameterization, validation and application. *ICES CM 2008/L:01*

Yndestad, H, Turrell W R and Ozhigin, V 2008. *Lunar nodal tide effects on variability of sea level, temperature, and salinity in the Faroe-Shetland Channel and the Barents Sea.* Deep-Sea Research I: Oceanographic Research Papers, 55:10, 1201–1217. http://doi.org/10.1016/j.dsr.2008.06.003

Yndestad H 2009. *The influence of long tides on ecosystem dynamics in the Barents Sea. Deep-Sea Research II. (2009) 2108-2116.* Deep-Sea Research II, 56, 2108-2116. http://doi.org/10.1016/j.dsr2.2008.11.022

Yndestad, H 2021. *Barents Sea Ice Edge Position Variability 1579-2020*, Report no TN210214, NTNU-Ålesund. May 2021. http://doi.org/10.13140/RG.2.2.16122.41928.

Correspondence to peter-ridd@yahoo.com

Vol. 2.1 (2022)

pp. 78-82

Is the Great Barrier Reef Threatened?[1]

Peter Ridd

Independent scientist, Australia

Submitted 19-12-2021, Accepted 29-12-2021. https://doi.org/10.53234/scc202203/20

The popular news media have in recent years been deluged with stories claiming that the Great Barrier Reef (GBR) is severely damaged and has a very poor outlook for the future[2]. Major threats to the reef supposedly include rising temperatures, ocean 'acidification', and pollution (sediment fertiliser and pesticides) from agriculture on the adjacent coast.

Government regulations aimed to 'save the reef' now affect every major industry in north Queensland - mining, sugar, beef cattle and others[3]. In addition, bad publicity about the reef affects the tourist industry because Queensland's biggest tourist attraction, the Great Barrier Reef, is constantly maligned in the media.

In fact, the outlook for the Great Barrier Reef, and its present condition, is far more encouraging than the public has been led to believe.

A good indication of the condition of the reef is the fraction of the reef that is covered by living coral, which has been surveyed by the Australian Institute of Marine Science (AIMS) each year since the mid 1980s (Figure 1). The quantity of coral fluctuates dramatically from year to year, falling mainly due to hurricanes, the waves of which smash large amounts of coral. Hot water events, and crown of thorns starfish plagues also periodically kill large amounts of coral. The latest data shows that the amount of coral has never been higher despite the reef supposedly having three unprecedented bleaching events in the last five years.

The other important statistic about the health of the reef is the coral calcification data. This is effectively the rate at which coral grows. Large corals have growth rings similar to tree rings, and thus drilling a core into the coral gives a record of its growth. Very large, and therefore old, corals record their growth rate back a few centuries. AIMS has collected this data and claimed that the coral growth rates suddenly started to decline in about 1990 (Figure 2). However, this has been disputed by Ridd et al (2013) who demonstrated instrumental measurement errors in the AIMS measurements. In addition, AIMS made a methodology change in 1990 changing from sampling only large corals to including mainly small corals from 1990-2005. Correcting these errors shows that coral growth rates have not reduced over the last century. AIMS has not

[1] The talk can be seen here: https://www.youtube.com/watch?v=gSSNXjPbpOY (Recorded by Yngvar Engebretsen).

[2] https://www.bbc.com/news/world-australia-57938858

[3] https://www.legislation.qld.gov.au/view/html/bill.first/bill-2018-008/lh

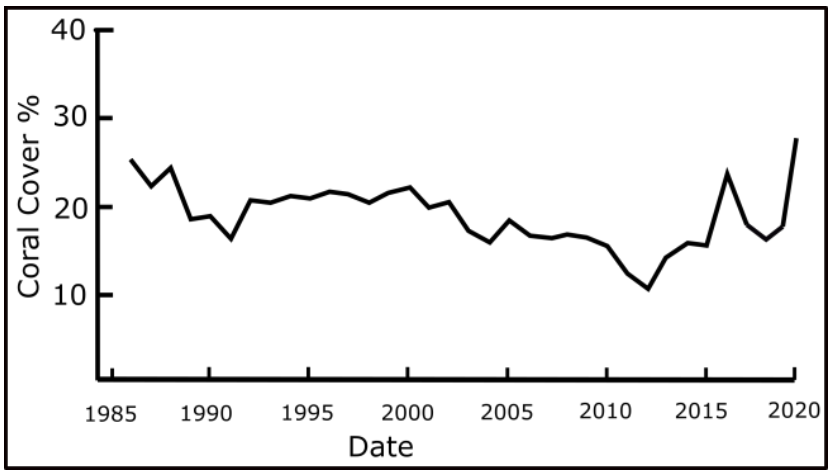

Figure 1. Coral cover for the Great Barrier Reef compiled from AIMS long term monitoring data. Note that this has been updated since the conference, which was in 2019, and the figure shows the updated data. Data was weighted from the three major regions of the reef according to the number of reefs surveys in each region

produced any data of the average reef growth rate since 2005. This is a serious oversight which needs to be remedied as soon as possible.

The influence of sediment (mud), fertilizers and pesticides from farms has also been demonstrated to be completely insignificant. For example, mud from farms almost never reaches the Great Barrier Reef because the reefs are mostly between 30 and 100 kilometres from the cost (Larcombe and Ridd, 2015). The white coralline sand on all the reefs (see Figure 3) is

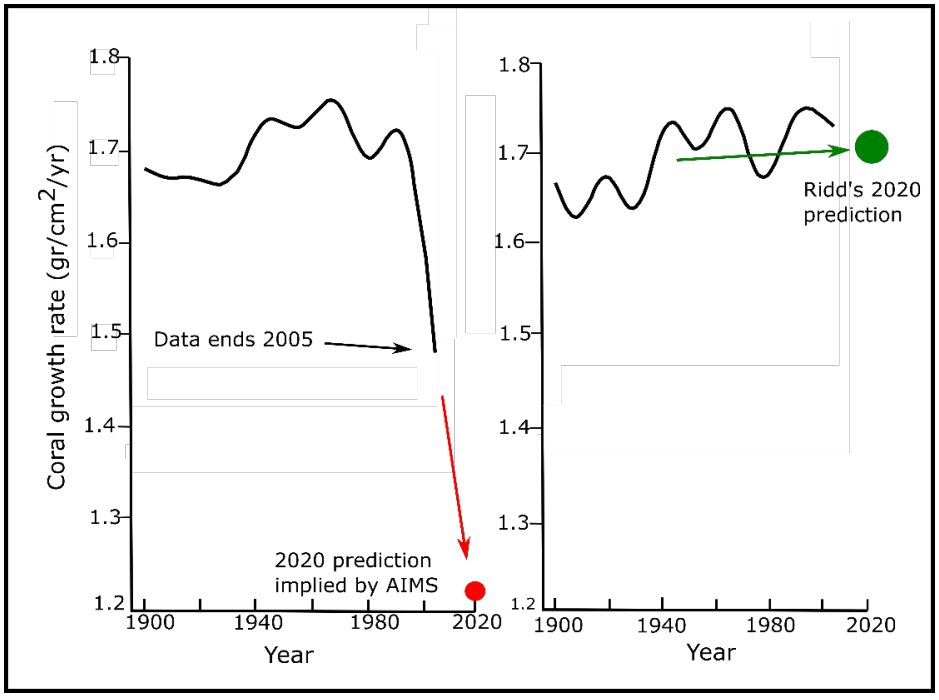

Figure 2.Coral growth rate (calcification rate) on the GBR for the 20th century. (Left) Calculated by De'ath et al. (2009) showing drastic reduction after 1990 and prediction (red dot) for 2020 implied by the Australian Institute of Marine Science. (Right) Reanal Reanalysed to account for measurement errors and sampling problems (Ridd et al., 2013). Green dot is the alternative prediction for 2020. ***Note****: There is no data of the GBR-average growth rate since 2005.*

Figure 3.White sand typical of all 3000 of the reefs of the Great Barrier Reef. This demonstrates that sediment from land has no effect on the reef, as would be expected as the reef is 30 to 100 km from the coast.

composed almost entirely of calcium carbonate sand which is derived from broken coral that lived and died over millennia. Sediment from the land, which has a completely different chemical composition, is almost entirely absent. It is thus inconceivable that the Great Barrier Reef is being directly affected by mud from farms.

Close to the coast adjacent to the Great Barrier Reef, and therefore a long distance from the reef, pesticides are almost always in extremely small concentrations and have never been detected in concentrations harmful to biota (Gallen et al., 2019). On the Great Barrier Reef, measurements are rarely even attempted as concentrations are so low that they cannot be detected with even the most sensitive scientific equipment.

Climate Change

Although it is often claimed that coral reefs are very susceptible to a warming climate, corals are a species that grows faster in warmer climates. (see Figure 4). Corals growing in the colder waters south of the Great Barrier Reef, such as in Moreton Bay, are far smaller than those of the Great Barrier Reef and grow relatively slowly. They are regularly stressed by a water temperature which is far colder than the ideal conditions for coral.

There is no doubt, however, that on occasions large amounts of coral are killed in years when the water temperature is well above average. Under such conditions, corals 'bleach" – they eject the symbiotic algae, called zooxanthellae, that lives inside them. The zooxanthellae give the coral energy via photosynthesis. Most corals that bleach do NOT die (Marshall and Schuttenberg, 2006).

The following is a useful summary of facts about the bleaching process (Baker et al., 2003; Buddemeier and Fautin, 1993; Guest et al., 2003; Marshall and Baird, 2000)

- With high temperature and light, photo-systems in the Zooxanthellae break down.
- Zooxanthellae leaves or is ejected by the coral.
- Bleaching is not a death sentence it is a strategy for life – it will usually stop the coral from dying.
- A rough analogy is some arid-zone trees that lose leaves during a drought to save water.

- Bleaching occurs when the water temperatures is higher than usual.
- A species of coral that might bleach at 28 °C in one location may not bleach until a much higher temperature is reached if it lives in a warmer climate. The *change* in temperature from average is important, not the absolute temperature.
- Infant corals have no zooxanthellae - they are captured from the water and surroundings.
- By changing zooxanthellae, corals can adapt extremely quickly to changing temperatures – they do this by bleaching.
- After a coral bleaches, it may take on a different species of zooxanthellae which will make it less susceptible to bleaching in the future
- Different species of zooxanthellae affect coral growth rates and susceptibility to bleaching.
- Some "low octane" species of zooxanthellae will give resistance to bleaching but the coral will grow slowly.
- "High octane" zooxanthellae will allow the coral to grow quickly but a hotter-than-average year will cause bleaching and possible death of the coral.
- There is no hard threshold temperature. The same coral will bleach at different temperatures with different zooxanthellae.

The proposition that most corals on earth are very close to their upper thermal limit, and are extremely sensitive to small changes in climate is not supported by data. In fact, corals are among the best adapted species to changing temperature because of their ability to change zooxanthellae with bleaching.

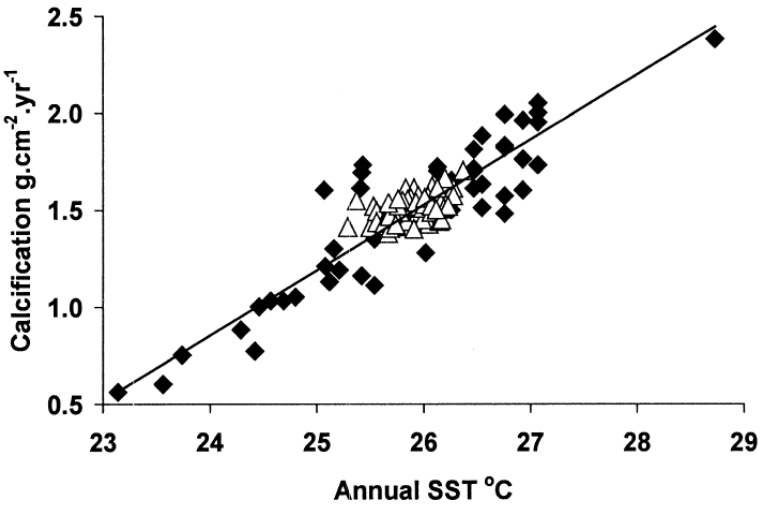

Figure 4. Coral calcification rate (growth rate) as a function of temperature. (after Lough and Barnes (2000)). Solid diamonds - Indo-Pacific reef data. Open triangles – Great Barrer Reef data. Corals grow faster in hotter water.

References

AIMS (2021) https://www.aims.gov.au/docs/research/monitoring/reef/latest-surveys.html

Baker, A.C. 2003. *Flexibility and Specificity in Coral-Algal Symbiosis: Diversity, Ecology, and Biogeography of Symbiodinium.* Annual Review of Ecology, Evolution, and Systematics, 34:1, pp.661–689.

Buddemeier, R.W. and Fautin, D.G. 1993. *Coral Bleaching as an Adaptive Mechanism.* BioScience, 43:5, pp.320–326.

De'ath, G., Lough, J.M. and Fabricius, K.E. 2009. *Declining Coral Calcification on the Great Barrier Reef.* Science, 323:5910, pp.116–119.

Gallen, C., Thai, P., Paxman, C., Prasad, P., Elisei, G., Reeks, T., Eagleham, G., Yeh, R., Tracey, D., Grant, S. and Mueller, J. 2019. *Marine Monitoring Program. Annual Report for inshore pesticide monitoring 2017–18. Report for the Great Barrier Reef Marine Park Authority,* Townsville: Great Barrier Reef Marine Park Authority, p.118.

Guest, J.R., Baird, A.H., Maynard, J.A., Muttaqin, E., Edwards, A.J., Campbell, S.J., Yewdall, K., Affendi, Y.A. and Chou, L.M. 2012. *Contrasting Patterns of Coral Bleaching Susceptibility in 2010 Suggest an Adaptive Response to Thermal Stress.* PLoS ONE, 7:3, p.e33353.

Larcombe, P. and Ridd, P. 2015. *The Sedimentary Geoscience of the Great Barrier Reef Shelf - context for Management of Dredge Material.* Brisbane: Queensland Port Association.

Lough, J.M. and Barnes, D.J. 2000. *Environmental controls on growth of the massive coral Porites.* Journal of Experimental Marine Biology and Ecology, 245:2, pp.225–243.

Marshall, P.A. and Baird, A.H. 2000. *Bleaching of corals on the Great Barrier Reef: differential susceptibilities among taxa.* Coral Reefs, 19:2, pp.155–163.

Marshall, P. and Schuttenberg, H. 2006. *A Reef Manager's Guide to Coral Bleaching.* Townsville, Australia, Great Barrier Reef Marine Park Authority

Ridd, P.V., Da Silva, E.T. and Stieglitz, T. 2013. *Have coral calcification rates slowed in the last twenty years?* Marine Geology, 346, pp.392–399.

Is Life on Earth Really Dying?[1]

Morten Jødal[†2]

Bærum, Norway

Correspondence to editor@science-ofcli-matechange.org

Vol. 2.1 (2022) pp. 83-86

Abstract

We are told about a 6th mass extinction of species and disappearance of the biological diversity. Facts contradict these claims. We know only a few species going extinct since 1500. The extinction rate is going down. All humans on Earth experience a larger diversity in their natural local surroundings. Most species have a better life in a slightly warmer climate. There is no reason to panic about the life on Earth.

Submitted 18-11-2021, Accepted 29-12-2021. https://doi.org/10.53234/scc202203/21

1. What we are told

There exists a parallel institution to IPCC called IPBES (Intergovernmental Science-Policy Platform on Biodiversity and Ecosystem Services). They too love hockeystics. Their scary message is that the cumulative number of extinctions since 1500 is dramatically increasing (Figure 1).

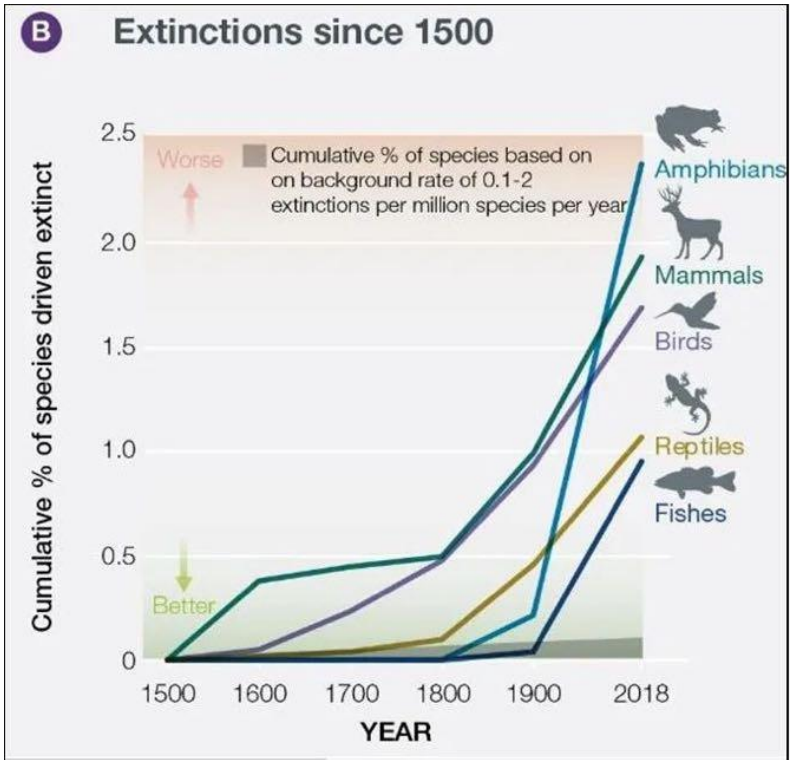

Figure 1. The scary story of IBES: The number of extinctions of species are increasing exponentially.

[1] The talk can be seen here: https://www.youtube.com/watch?v=bocF5yzMF1k (Recorded by Yngvar Engebretsen).

[2] Morten Jødal died in September 2021. The talk is transcribed by Jan-Erik Solheim

The story started with Norman Myers book (1979) where it was told that 40 000 species go extinct per year. Another number from EU and Germany presented in 2008, was that 3 species go extinct pr hour, or 26 280 species per year. In 2018 we were told that insects are going extinct and this year (2019) the Amazon Forest is burning, and species will go extinct. But Myers number of 40 000 species per year was based on a remark from a conference in 1974 where a lecturer guessed that one million species will go extinct in 25 years. This is completely wrong.

2. The reality

In the same building in Switzerland where IPBES is situated, we find another agency, International Union for Conservation of Nature (IUCN) which keeps tracks of endangered and extinct species. Their Red List of all extinct species by decade since 1500 is shown in Figure 2. There was an increase in the extinction rate between 1800 and 1900, but from then on the extinction rate is going down dramatically. During the last 10 years zero extinctions have been found. Since 1500 in total 860 species have gone extinct according to IPBES.

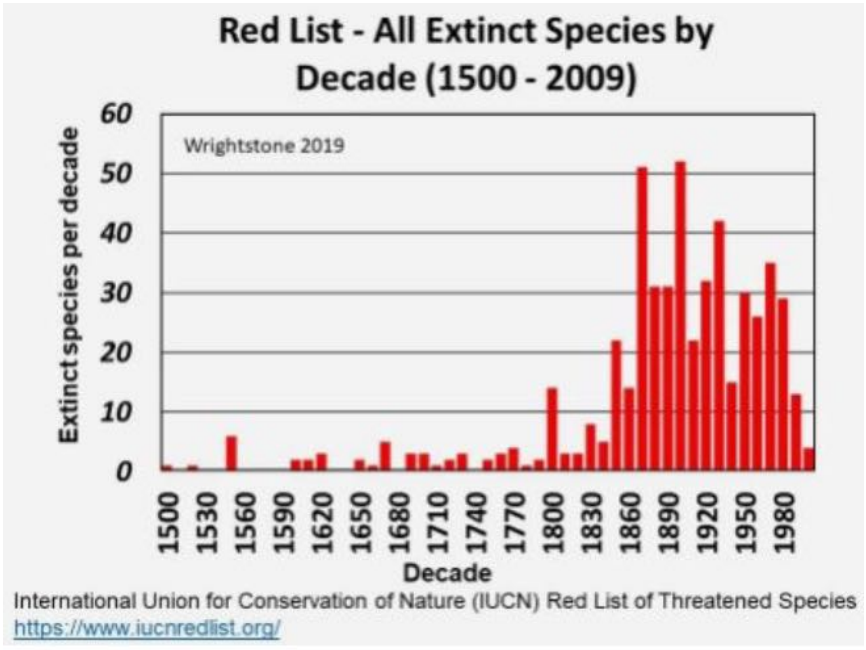

Figure 2. The number of species extinct per decade (from IUCN).

In addition, there are about 65 species not living in nature, but are still alive in zoos. There is a big difference between the number 40 000 per year and 860 per 500 years. The reality in the red list is 1.7 species per year or 0.004 % of the IPBES claim.

Table 1: Species going extinct since 1500 according to IPBE

Group	Extinct
Mammals	83
Birds	156
Fish	63
Reptiles	27
Amphibians	33
Anthropods	81
Molluscs	297
Other animals	4
Plants	116
All	**860**

3. The main threats

- Loss of habitat: Agriculture is most important, but since 1960 we need 68 % less area to produce the same amount of food. Most species have gone extinct on islands.
- Introducing species: Especially islands are vulnerable. The cat and the rat are good examples on predators destroying island habitats
- Hunting
- Pollution
- Climate change – NO: Life is normally restricted by cold weather. But on mountain tops in the Alps the number of plant species has increased by more than 138 % in 100 years.

4. New plants introduced by humans

On nearly all islands we find a perfect relationship between native and introduced species. In Europe more than 12 000 new plant species have been introduced the last 500 years. We are experiencing a much larger biological diversity than our great-great-great-grandmother.

And now they tell us: If we lose a few species, the ecosystem will collapse. Gro Harlem Brundtland was wrong when she said: "Everything is connected to everything". That is not correct anymore. This is not good biology.

5. The real problems

The real extinctions are small but are in many cases mixed up with reduced population sizes – which is a problem for some species. We hear all the time that something is unnatural. The nature changes dynamically. It changes all the time. We like the losers, not the winners. One example is the King Crab, introduces by Russians, which is doing very well – giving good income for the fisheries. It has come to stay. We absolutely want the white mountain fox, a beautiful animal. Large resources are allocated to save and increase the population. But the raccoon dog, which is numerous in Sweden – is blacklisted and hunted without restrictions in Norway. However, there are species in danger of extinction. Table 2 shows the full red list:

Table 2. The red list in categories

Category	Abr	Numbers IUCN	Numbers Norway
Extinct	EX	860	114
Extinct in wild		68	
Critically endangered	CR	5210	241
Endangered	EN	7781	879
Vulnerable	VU	11316	1235
Near Threatened	NT	5736	1235
Least Concern	LC	40920	16477

A problem with this list is that most of the species listed, are regionally at the edge of their distribution. The species have not gone extinct, but individuals have died. We have many such examples in Norway and Sweden of species listed as threatened, which live quite well in Russia and in the rest of Europe

6. A new biological Pangea – never mentioned in media.

Pangea was a supercontinent which allowed species to move across all land areas on the Earth. When the continents separated, this movement became restricted. We got isolated habitats and evolution in different directions.

Figure 3. A new biological Pangea is created.

The increased travel between continents by humans has created a new biological Pangea as shown in Figure 3. The result is that new species are created all the time by hybridization, by geographical isolation in new areas, and by new ecological niches. And the process of creating new species has become much shorter because of how humans move plants and species with them. An example is an apple tree brought in from abroad. With the tree comes insects, fungus, birds, and predators – and the habitat is changed in a few years.

My best rough guess: In one million years the Earth will have a double number of species.

Which means a new genesis.

We are not in the 6th extinction – it is really the opposite.

References

Norman Myers 1979. *The Sinking Ark. A New Look at the Problem of Disappearing Species.* Pergamon press.

Morten Jødal 2017. *Miljømytene – står vi framfor verdens undergang?* 448 p. (in Norwegian), Klimarealistene, ISBN 978-82-999196-2-3

Correspondence
sjcrock@shaw.ca

Vol. 2.1 (2022)

pp.87-92

The Polar Bear Catastrophe that Never Happened[1]

Susan J. Crockford

Victoria B.C. Canada

Submitted 14-11-2021, Accepted 29-12-2021. https://doi.org/10.53234/scc202203/22

Figure 1. A sow and her half-grown male cub feed on the ice near Svalbard, Norway. Courtesy Shutterstock.

Since the start of this century, polar bears have been an icon for all that's worrisome about human-caused global warming. Polar bears are the most-used example to try and convince the public that burning fossil fuels already has had - and will continue to have - a harmful effect on the planet. As we are told the Arctic is warming twice as fast as the rest of the planet, the polar bear is often called the 'canary in the coal mine' for climate change (Linden 2000; Richardson 2020; Siegle 2018).

Polar bears have gone from being threatened with (or 'vulnerable to') extinction by overhunting in 1973, saved in 1996, and threatened by climate change in 2006. The scientists who make up the Polar Bear Specialist Group (PBSG) of the International Union for the Conservation of Nature (IUCN) were pivotal to these conservation decisions (Crockford 2017, 2019).

In 2006, the opinion of PBSG members was that polar bear numbers would decline by 30 % or more within the next 45 years because of predicted future declines in summer sea ice (ACIA 2005; Aars et al.

[1] Lecture https://www.youtube.com/watch?v=FaayfgFLnb8 (Recorded by Yngvar Engebretsen).

2006; Hassol 2004). This was the first time that future threats based on climate models had been used to declare a species vulnerable to extinction by the IUCN: it was a watershed moment for animal conservation.

By 2007, American biologists at the US Geological Survey (USGS) folded suit (Adler 2008). The USGS used computer models that depended on the opinion of just one biologist – Steven Amstrup – regarding how polar bears would respond to projected summer sea ice changes. The focus was on summer ice because spring, fall and winter ice model projections showed no significant change by mid-century while those for summer ice showed a dramatic decline (Amstrup et al. 2007; Durner et al. 2007; Holland et al. 2007).

USGS biologists concluded that if summer sea ice declined as rapidly as predicted by mid century and stayed that low for at least eight out of ten years, a massive decline in polar bear numbers was inevitable. By 2050, summer sea ice was expected to drop 42 % below 1979 levels (i.e. less than about 5 million square km and a loss of 2/3 of the world's polar bears was anticipated (Amstrup et al. 2007; Courtland 2008; Hunter et al. 2007; USGS 2007). Given their starting estimate of about 24,500 bears, that meant only 8,100 were expected to survive: fewer bears than were thought by experts at the time to have existed in the late 1960s (Crockford 2019).

Unfortunately,, summer sea ice unexpectedly dropped in September 2007 to less than 4 Mkm^2 (million square km,) a level that had not been predicted to occur until mid-century (Amstrup et al. 2008). USGS lead author Amstrup knew this fateful news by the time his report was published in early September (Amstrup et al. 2007) and explained that since the sea ice loss was worse than anyone had expected, the predictions he and his colleagues had made about polar bears were probably overly conservative: polar bear populations would likely decline sooner, or numbers drop even more dramatically than their models had predicted. Suddenly, the catastrophe was imminent, not decades away. Two years later, sea ice researchers stated summer sea ice loss was "at least 30 years" ahead of model predictions and concluded an ice-free Arctic by 2040 was quite likely (Wang and Overland 2009; see also Stroeve et al. 2007). In contrast, ice models used by polar bear biologists did not expect an ice-free Arctic until 2100 (Durner et al. 2007, 2009).

Contrary to expectations, however, the decline of summer ice did not get steadily worse: it stabilized (Swart et al. 2015). With the exception of two years when the September minimum was slightly above 5 Mkm^2, sea ice between 2007 and 2016 remained between 3 and 5 Mkm^2 (and indeed has remained in that range up to 2021) (NSIDC 2019, 2021). In other words, the dreaded mid-century threshold of sea ice levels – reached in at least eight out of ten years – had arrived decades before it was anticipated.

This set the stage for a hypothesis test. You don't have to put a collar on a polar bear to assess whether a prediction published in 2007 matched documented observations published in the scientific literature. While I explored whether the profound loss of summer sea ice in eight out of ten years had indeed caused a 67 % decline in polar bear numbers and the extirpation of more than half of all subpopulations, USGS polar bear biologists instead continued to promote a subsequent model projection that suggested the anticipated polar bear catastrophe could be avoided through a dramatic reduction of global greenhouse gas emissions (Amstrup et al. 2010).

I wrote a scientific paper showing that the global polar bear population had not declined in size – in fact it grew from about 24,500 in 2005 to about 28,500 in 2015 – an apparent 16 % increase despite the sudden and dramatic sea ice loss. Not a single subpopulation had been wiped out. The global population size increases (which grew further to about 30,000 in 2020) may not be statistically significant because of differences in methodology over time (both within and between subpopulation estimates), but there was certainly not a 67 % decline in polar bear numbers (Crockford 2017, 2019, 2021; Crockford and Geist 2018). Both the Arctic sea-ice and polar bear survival models were spectacularly wrong.

Today, there are fat healthy polar bears throughout the Arctic despite almost 50 % less ice than there was in 1979 (NOAA Oceans Today 2012; Scott and Hansen 2016; NSIDC 2021). For example, recent studies have shown that Chukchi Sea bears are in very good condition and reproducing well (Rode et al. 2014, 2018) and the population size was recently estimated at about 3,000: far higher than the estimate of 2,000 used for the 2015 IUCN assessment (Regehr et al. 2018; Wiig et al. 2015). Similarly, in the Barents Sea – where summer sea ice loss has been six times more pronounced than in Western Hudson Bay – polar bears in the late 2010s were found to be in better condition than they had been in the late 1990s and were reproducing well with good cub survival (Aars and Andersen 2021; Lippold et al. 2019; Regehr et al.

2016). Western Barents Sea polar bear numbers increased 42% between 2005 and 2015 but this was deemed 'statistically insignificant' (Aars et al. 2017).

Why were the USGS models so wrong? It came down to false assumptions and previously known facts that were ignored (Crockford 2017, 2019). For example, although spring sea ice conditions are much more important than summer, the predictive models did not include a provision for the population size effects of periodic thick spring ice conditions, such as has been documented in the Southern Beaufort Sea and Hudson Bay. Also, we know from Western and Southern Hudson Bay data that bears well-fed in spring easily survive a 5-month summer fast, which means bears elsewhere in the Arctic must also have this capability whether they retreat to land or stay on the sea ice during the summer.

However, this was not information PBSG scientists wanted the public to know. In response, renowned Canadian polar bear specialist Ian Stirling, former USGS biologist Steven Amstrup (whose opinions about polar bear survival formed the basis of the 2007 prediction of catastrophe) teamed up with American climate scientist Michael Mann, Australian psychologist Stephan Lewandowsky, Dutch ecologist Jeff Harvey and nine other people to publish a defamatory paper denouncing my work (Harvey et al. 2018). Three press releases were issued, and the story was taken up by media outlets around the world, including the New York Times (Crockford 2018; Laframbroise 2018). It was an organized attempt to silence legitimate scientific criticism.

The paper contained many egregious errors, and no effort was made to address any of the criticisms I had advanced regarding polar bear conservation: it accused me, through my popular blog (www.polarbearscience), of publishing misleading or error-filled information. Although the paper denigrated online blogs in general, it was a vindictive attack meant to publicly discredit me in particular. Judith Curry, Emeritus Professor of Earth and Atmospheric Sciences at Georgia Institute of Technology, spoke for many when she proclaimed it "...absolutely the stupidest paper I have ever seen published" (Curry 2017).

Meanwhile, my university was busy doing some silencing of its own. By the time the Harvey paper came out, I had already been expelled from the university's Speakers Bureau based on a single complaint about my presentations to local schools in 2016. There was no right of appeal. Then, in late spring of 2019, my university department refused to renew my unpaid adjunct professor status, a position I had held for 15 years. The university has refused to answer any questions about these actions against me (Laframbroise 2018, 2019; Laframboise and Crockford 2020): it was an academic hanging without a trial, conducted behind closed doors. Although their actions were entirely legal, it was nevertheless an unethical attack on my academic freedom.

Despite these setbacks, I continue to provide critical commentary regarding the biological health and conservation status of polar bears with regard to changing sea ice conditions (e.g. Crockford 2020, 2021).

Of particular concern is the continued obfuscation of global polar bear population sizes. Polar bear specialists suggest that polar bear numbers doubled between the late 1960s and 1996 but have stayed the same since. However, no other overhunted species has failed to continually increase its population size once protection from over-hunting was provided. I suggest numbers have continued to climb and that a plausible scientific estimate of the global total at 2018 was 39,000, with a range of 26,000-58,000 (Crockford 2017, 2019). Consider that in 1986, Canadian biologist Ian Stirling proposed there were probably about 40,000 polar bears in the world when he took into account areas without data, which included all of Russia (Crockford 2019:106). If that was true in 1986, 39,000 as an average in 2018, with a potential for 58,000 maximum, is likely a conservative estimate after more than 30 years of protection.

In conclusion, it is apparent that summer sea ice is not crucial for polar bear health and survival and that contrary to expectations, in some regions less summer ice than existed in the 1980s appears to be beneficial. Not only is there currently no 'climate emergency' for polar bears but the 'canary in the coal mine' of climate change turns out to be an outstanding survivor. No climate emergency for polar bears suggests there is no climate emergency period.

References

Aars, J. and Andersen, M. 2021**.** *Norwegian Polar Institute Environmental Monitoring of Svalbard and Jan Mayen, Polar bear. Last updated 8 September 2021* [accessed 29 November 2021], https://www.mosj.no/en/fauna/marine/polar-bear.html

Aars, J., Lunn, N. J. and Derocher, A.E. 2006. *Polar Bears: Proceedings of the 14th Working Meeting of the IUCN/SSC Polar Bear Specialist Group, Seattle, Washington, 20-24 June 2005,* IUCN, Gland, Switzerland, Occasional Paper of the IUCN Species Survival Commission 32.

Aars, J., Marques,T.A, Lone, K., Anderson, M., Wiig, Ø., Fløystad, I.M.B., Hagen, S.B. and Buckland, S.T. 2017. *The number and distribution of polar bears in the western Barents Sea***.** Polar Research, 36:1, 1374125. https://doi.org/10.1080/17518369.2017.1374125

ACIA 2005. *Arctic Climate Impact Assessment: Scientific Report. Cambridge University Press*.

Adler, J.H. 2008. *An animal to save the world: climate change and the polar bear*. The New Atlantis, 21, 111–115.

Amstrup, S.C., Marcot, B.G. and Douglas, D.C. 2007. *Forecasting the rangewide status of polar bears at selected times in the 21st century.* Administrative Report, US Geological Survey, Reston, Virginia,

Amstrup, S.C.,Marcot, B.G. and Douglas, D.C. 2008. *A Bayesian network modeling approach to forecasting the 21st century worldwide status of polar bears.* In: *Arctic Sea Ice Decline: Observations, Projections, Mechanisms, and Implications,* E.T. DeWeaver, C.M. Bitz and L.B. Tremblay (eds.), American Geophysical Union, Washington, D.C., Geophysical Monograph 180, 213-268. https://doi.org/10.1029/180GM14

Amstrup, S.C., DeWeaver, E.T., Douglas, D.C., et al. 2010. *Greenhouse gas mitigation can reduce sea-ice loss and increase polar bear persistence.* Nature, 468, 955–958. https://doi.org/10.1038/nature09653

Courtland, R. 2008. *Polar bear numbers set to fall.* Nature, 453, 432–433. https://doi.org/10.1038/453432a

Crockford, S.J. 2017. *Testing the hypothesis that routine sea ice coverage of 3-5 mkm2 results in a greater than 30% decline in population size of polar bears (Ursus maritimus).* PeerJ Preprints https://doi.org/10.7287/peerj.preprints.2737v3

Crockford, S.J. 2018. *Climate mauling, polar bears, and the self-inflicted wounds of the self-righteous.* PolarBearScience, 10 April. http://polarbearscience.com/2018/04/10/climate-mauling-polar-bears-and-the-self-inflicted-wounds-of-the-self-righteous/

Crockford, S.J. 2019. *The Polar Bear Catastrophe That Never Happened.* Global Warming Policy Foundation, London.

Crockford, S.J. 2020. ***State** of the Polar Bear Report 2019.* Global Warming Policy Foundation Report 39, London.

Crockford, S.J. 2021. *The State of the Polar Bear Report 2020*. Global Warming Policy Foundation Report 48, London.

Crockford, S.J. and Geist, V. 2018. *Conservation Fiasco.* Range Magazine, Winter 2017/2018, 26-27.

Curry, J. 2017. *This is absolutely the stupidest paper I have ever seen published: https://academic.oup.com/bioscience/article/68/4/281/4644513*. Twitter, 29 November, 1:27 PM, [accessed 29 November 2017]. https://twitter.com/curryja/status/935983612205326336?lang=en

Durner, G.M., Douglas, D.C., Nielson, R.M., et al. 2007. *Predicting 21st-century polar bear habitat distribution from global climate models.* Administrative Report, US Geological Survey, Reston, Virginia.

Durner, G.M., Douglas, D.C., Nielson, R.M., et al. 2009. *Predicting 21st-century polar bear habitat distribution from global climate models.* Ecological Monographs, 79, 25–58. https://doi.org/10.1890/07-2089.1

Harvey, J.A., van den Berg, D., Ellers, J., et al. 2018. *Internet blogs, polar bears, and climate-change denial by proxy.* Bioscience, 68, 281-287. [published online 29 November 2017] https://doi.org/10.1093/biosci/bix133

Hassol, S.J. 2004. *Impacts of a Warming Arctic: Arctic Climate Impact Assessment Synthesis Report.* Cambridge University Press, Cambridge UK.

Holland, M.M., C.M. Bitz, and B. Tremblay. 2006. *Future reductions in the summer Arctic sea ice.* Geophysical Research Letters, 33, L23503. https://doi.org/10.1029/2006GL028024

Hunter, C.M., Caswell, H., Runge, M.C., et al. 2007. *Polar bears in the Southern Beaufort Sea II: Demography and population growth in relation to sea ice conditions.* Administrative Report, US Geological Survey, Reston, Virginia.

LaFrambroise, D. 2018. *Polar bears and the sleazy New York Times. No Frakking Consensus,* 13 April. https://nofrakkingconsensus.com/2018/04/13/polar-bears-and-the-sleazy-new-york-times/

Laframboise, D. 2019. *Was this zoologist punished for telling school kids politically incorrect facts about polar bears? National Post (Canada),* 16 October. https://web.archive.org/web/20191017195343/https://business.financialpost.com/opinion/was-this-zoologist-punished-for-telling-school-kids-politicallyincorrect-facts-about-polar-bears

LaFrambroise, D. and Crockford, S.J. 2020. *Walruses, polar bears, and the fired professor***.** In: *Climate Change: The Facts 2020,* J. Marohasy (ed.), Institute of Public Affairs, Melbourne, Australia, 21-34.

Linden, E. 2000. *The Big Meltdown*, TIME Magazine, 156(10), 53-55.

Lippold, A., Bourgeon, S., Aars, J., et al. 2019. *Temporal trends of persistent organic pollutants in Barents Sea polar bears (Ursus maritimus) in relation to changes in feeding habits and body condition.* , Environmental Science and Technology 53:2, 984-995. https://doi.org/10.1021/acs.est.8b05416

National Snow and Ice Data Center (NSIDC). 2019. *Falling up*. 3 October [accessed 3 October 2019], https://nsidc.org/arcticseaicenews/2019/10/falling-up/

National Snow and Ice Data Center (NSIDC). 2021. *September turning.* 5 October [accessed 29 November 2021], http://nsidc.org/arcticseaicenews/2021/10/september-turning/

NOAA Oceans Today. 2012. *Happening now: Arctic sea ice sets record low.* NOAA September news report [accessed 6 December 2021]. https://oceantoday.noaa.gov/happennowarcticseaice/

Regehr, E.V., Hostetter, N.J., Wilson, R.R., et al. 2018. *Integrated population modeling provides the first empirical estimates of vital rates and abundance for polar bears in the Chukchi Sea. Nature* Scientific Reports, 8:1. https://doi.org/10.1038/s41598-018-34824-7

Regehr, E.V., Laidre, K.L, Akçakaya, H.R., et al. 2016. *Conservation status of polar bears (Ursus maritimus) in relation to projected sea-ice declines.* Biology Letters, 12, 20160556. https://doi.org/10.1098/rsbl.2016.0556

Richardson, E. 2020**.** *Polar bears: The very large canary in the coalmine for our generation. Environment and Climate Change Canada, 17 November* [accessed 20 November 2020] http://www.ic.gc.ca/eic/site/063.nsf/eng/98181.html

Rode, K.D., Regehr, E.V., Douglas, D., et al. 2014. *Variation in the response of an Arctic top predator experiencing habitat loss: feeding and reproductive ecology of two polar bear populations.* Global Change Biology 20, 76-88. https://doi.org/10.1111/gcb.12339

Rode, K. D., Wilson, R. R., Douglas, D.C. et al. 2018. *Spring fasting behavior in a marine apex predator provides an index of ecosystem productivity.* Global Change Biology, 24, 410-423. https://doi.org/10.1111/gcb.13933

Scott, M. and Hansen, K. 2016. *Sea Ice. NASA Earth Observatory Article, 16 September,* https://earthobservatory.nasa.gov/features/SeaIce [accessed 6 December 2021]

Siegel K. 2018. *Keeping fossil fuels in the ground is the only way to save polar bears ravaged by climate change.* The Hill, 26 May. http://thehill.com/opinion/energy-environment/389493-keeping-fossil-fuels-in-the-ground-is-the-only-way-to-save-polar.

Stroeve, J., Holland, M.M., Meier, W., et al. 2007. *Arctic sea ice decline: Faster than forecast.* Geophysical Research Letters, 34, L09501. https://doi.org/10.1029/2007GL029703

Swart, N.C., Fyfe, J.C., Hawkins, E., et al. 2015. *Influence of internal variability on Arctic sea ice trends.* Nature Climate Change, 5, 86-89. https://doi.org/10.1038/nclimate2483

US Geological Survey (USGS). 2007. *Executive Summary, USGS Science Strategy to Support U.S. Fish and Wildlife Service Polar Bear Listing Decision*. Administrative Report, US Geological Survey, Reston, Virginia.

Wang, M. and Overland, J.E. 2009. *A sea ice free summer Arctic within 30 years?* Geophysical Research Letters, 36, L07502. https://doi.org/10.1029/2009GL037820

Wiig, Ø., Amstrup, S., Atwood, T., et al. 2015. *Ursus maritimus. The IUCN Red List of Threatened Species 2015: e.T22823A14871490* [accessed Nov. 28, 2015, population figures in supplement], http://www.iucnredlist.org/details/22823/0

Correspondence to karliver@klimarealisme.dk
Vol. 2.1 (2022)
pp. 93-96

Mariculture: A Resource-efficient Food Production[1]

Karl Iver Dahl-Madsen

Copenhagen, Denmark

Abstract

Due to a resource-efficient food production – famine will be a thing of the past in our affluent society. Famine due to climate change is simply not true. We can easily feed everyone – even if we are more than ten billion people.

Submitted 26-12-2021, Accepted 30-12-2021. https://doi.org/10.53234/scc202203/23

1. Background

Most of the issues we have in the rich countries are small related to the problems in the developing world. The famine we sometimes observe is due to bad government – not related to climate change. The most important resource we have is the human being. Many books are written about that. The speaker especially recommended books by Julian Simon, Bjørn Lomborg, and Martin Ågerup (see the literature list).

In Martin Ågerup's book: *Doomsday is Cancelled*, or Dommedag *er aflyst* (Danish), we get a list of expected improvements in our near future:

- We are more: 10-15 billion
- We live longer, get richer: seven times per hundred years,
- We get well-fed
- We get energetic
- We get access to ample resources and water
- We get more peaceful
- We are solving nature, environmental, and climate challenges
- We will still be afraid – for good reasons: maybe richer people are more afraid of losing their valuable items?
- We will have an accelerating technological change

The myth of ecological doomsday is neither catastrophic nor existential. We enjoy large positive effects of the use of stored solar energy as cheap energy sources.

The speaker and Ngyen Thi Kim Oanh have concluded: It is evident that the proposed cure of excessive CO_2 emission reductions may well be far more costly than the disease of global warming.

[1] Lecture: https://www.youtube.com/watch?v=SPnbKiqgFPg (Recorded by Yngvvar Engebretsen).

2. The four beasts in the eye

1.The number of *wars, deaths and refuges* is declining. We never had such a peaceful decade as the last one.

2. *Pestilence*: deaths are manageable, thanks to modern vaccinees and health care.

3.*Deaths from extreme weather* is down from half a million per year 100 years ago to 20 000 per year with a larger population. The cost of damage is declining from 0.3 to 0.2 % of BNP.

4. *Famine:* The warm, wet, and CO_2-increasing world is better for plants. They are now starving for CO_2.

All the four beasts are less important now. We have managed to greatly reduce their importance, in particular due to the effect of cheap and easily available fossil fuel.

3. Improved agriculture

Man does much better than Nature in growing plants, through increasing the Nitrogen cycle. The table below shows the development of the grain-yield based on various techniques:

Table: Grain harvest with different techniques

Technique	**yield (ton/ha)**
Slash and burn	<1
Backbreaking hard labor	1-2
Global average today	4
Modern farmer	10
Iowa's best farmer	30
Future GMO/Crispr/seaweed	100
Lighted greenhouses	>1000

The lighted greenhouses are much more expensive today, but since we all get richer, we can afford it. Food cost is relatively less in the rich part of the world now than 50 years ago. The limiting factor is water, but cost of desalination is about 0.5$ per m^2. Today these doubles the price of grain. This is affordable in the rich part of the world. When we get richer this will also work in the rest of the world. Today we find 800 million people in hunger due to bad governance. This is not due to climate change.

It was long preached that food could only grow linearly, while the number of people grow exponentially. Now it is opposite. Food production grow exponentially and in line with the population. We are getting well-fed. There is no excuse for hunger in this world. We must get rid of the poverty. The endless whining of catastrophic famine due to increasing population is due to false prophets. In the real-world food production has tripled since 1960, and food prices have been falling since 1700 in deflated money value.

Thanks to the global supply chain and the ingenuity of farmers and agricultural research, there is a huge capacity potential. Farmers are clever. They adapt quickly to changing weather and climate, while the researchers behind IPCC think the farmers are stupid and stick to the old farming methods. But it is quite the opposite. It is the IPCC-researchers that are stupid, not thinking that farmers adapt. The speaker gave some examples. One is repeated here:

Sweden had a serious famine in 1867-1869. 1867 was very cold: 80-100 000 died, emigration to America skyrocket. Denmark had serious drought in 2018 with 23 % less grain and a huge (10 %) economic loss. This should be a catastrophe, but nobody died of hunger. In the supermarkets

there was no sign of food scarcity. In the modern resilient society – there is no feeling of disaster.

4. The future

More rich people will certainly result in an Increasing demand for meat. Meat is healthy and good for the soul. The Amish solution produces more obesity than hunger. We expect 35 % higher demand for animal protein in the next 20 years. Now we are reaching peak farmland, which is the maximum area used for farming. However, we will eventually use far less land for farming. Except if we change to organic farming. This is a disaster because of producing less on more land. This is a waste of good land.

The oceans have a great potential for food production. In practical terms the space and the quantity of water are unlimited. Small variations in salinity and temperature leads to stable production. This is the fastest growing food production field in the world.

The biggest fish farming catch volume is the freshwater fish carp. But in sea farming value, Norway is the Global front runner producing 1.4 million ton of salmon for a yearly revenue of 60 billion NOK. This is half the salmon produced in the world. The global market will be in the order of 10 million tons.

Resource efficiency (RE) is defined as the value added per unit of environmental impact.
Salmon is a high-value product with RE double of beef, because fish is cold blooded (poikilotherm) and need no energy for warming. They live in zero gravity and need minimal energy for moving around. The environmental impact of fish farming is low off-coast and offshore.

Then we hear about the insect eating craze. Insects and fish have more or less the same food conversion rate[2], but fish is much more in demand and valuable. We are now down to 1-2 kg wild fish per kg salmon. This is for the protein and Omega3 fatty acids. The rest comes from the land like soya etc. But in food production the future is GMO-plants and seaweeds.

Off-shore Agriculture is coming - pioneered by Norway. Seaweed production is increasing – here the whole plant can be used.

Conclusion

A sane world will never run out of food. We have an unlimited production capacity on land and sea together. Climate change will only be a minor factor. Production can always be moved to better places. A richer world can accept higher food prices. More CO_2 is better for the plants and the food production. The myth of ecological doomsday is neither catastrophic nor existential. We can praise the relatively large positive effects of the use of stored solar energy.

References to important books

Bjørn Lomborg, 2001, *The Skeptical Environmentalist*, Cambridge University Press.

Bjørn Lomborg, 2004, *Global Crises, Global Solutions*, Cambridge University Press (new edition in 2009).

Bjørn Lomborg, 2010, *Cool It*, Knopf Publishing Group.

[2] Food conversion rate (FCR) is the weight of feed intake divided by weight gained by the animal.

Bjørn Lomborg, 2020, *False Alarm*, Basic Books.

Julian L. Simon, 1981, *The Ultimate Resource*, Princeton University Press, 734p. ISBN 0-691-00381-5 (Revised 1996 edition, paperback).

Martin Ågerup, 1998, *Dommedag er aflyst - velstand og fremgang I det 21. Århundrede,* Gyldendal (in Danish).

The Replication Crisis[1]

Peter Ridd

Independent scientist, Australia

Correspondence to peterridd@yahoo.com.au

Vol. 2.1 (2022)
pp. 97-100

Submitted 01-11-2022, Accepted 16-12-2022. https://doi.org/10.53234/scc202203/24

1. Introduction

The replication crisis is a phenomenon widely accepted in major institutions of science (Ioannidis, 2005, 2014, Baker 2016). Roughly half of peer reviewed scientific literature is probably flawed or totally wrong. There are almost certainly problems in all fields of science. How did this problem develop? The inadequacies of the peer review system are largely to blame. The peer review process is a grossly deficient quality assurance process.

2. The peer review problem

Peer review as it works today:

- Peer review is a quick check by maybe a couple of "peers". It might take a just few hours.
- Peers never have time to do thorough checks or genuine replication of work.
- Peers might be the authors friends.
- The public is completely unaware of how pathetic the peer review process is, or its failure rate.
- Science institutions have deceived the public to think peer review is a far more robust and lengthy process than it actually is.
- Peer review makes group-think inevitable.

Examples of reliable science abound and are foundational to our civilization. It is massively replicated and often tested every day. Examples are Newtons laws of motion, Quantum Mechanics, Thermodynamics, Theory of Relativity, most of the medical sciences. You can stake your life on it. *In fact, you do so every day.*

Unfortunately, most of science is not replicated as much as it should be. This often does not matter, because most of this research is not used at all. For example, who cares about the feeding habits of an obscure insect? It has no consequences to anybody. If the research is wrong, it does not matter too much.

Science used for industry is at the other end of the spectrum. It is checked thoroughly before any production is started because it must work. We must rely on it (Figure 1). If it fails, people could die, or the company could go broke

But not so for governments, especially if the consequence of the research is an anticipated problem decades in the future as is the case for many environmental issues. The problem is made worse if an element of ideology is involved. We may ask: What are the quality assurance processes in environmental science?

Those skeptical of catastrophic anthropogenic climate change are generally excluded from major science institutions. It is dangerous to the career of a young researcher to challenge the

[1] Lecture at https://www.youtube.com/watch?v=nETKLfJyY9E (Recorded by Yngvar Engebretsen)

Figure 1: It would be disastrous if industry used the same quality assurance system as the environmental science with its 50 % rate of failure.

conventional wisdom. However, the problems of peer review, which have contributed extensively to dubious conclusions about the role of carbon dioxide on climate, is completely accepted by the mainstream. In order to challenge the conventional wisdom about climate, the problems of peer review, and the lack of decent quality assurance protocols in much of science, must be highlighted.

Richard Horton, UK, the editor in chief of The Lancet stated (Horton, 2000):

"we know that the system of peer review is biased, unjust, unaccountable, incomplete, easily fixed, often insulting, usually ignorant, occasionally foolish, and frequently wrong."

Although there is wide acceptance of the replication crisis, and the problems with peer review, institutions are largely in denial about the possible consequences of this to the scientific foundations of some elements of public policy.

3. The replication crisis

It is claimed that 50 per cent of the scientific literature in medicine is wrong. Prof John Ioannidis (Stanford University) wrote a famous paper: *"Why most published research findings are false*?" (Ioannidis, 2005). It is also claimed that 85 % of science resources are wasted, due to false or exaggerated findings in the literature (Chalmers and Glaszios, 2009). Funding bodies don't fund replication – even though it is fundamental to the scientific processes.

Another example is the experience of pharmaceutical companies. They routinely try to replicate original scientific published results. One company found that the science was wrong in 80 % of the time (Prinz et al, 2011).

In psychology there is an almost complete failure of replication of the scientific findings. There is definitively a confidence crisis (Wagenmakers 2012).

In marine science two very eminent scientists, Carlos Duarte and Howard Browman (Duarte et al, 2015; Browman, 2016) have posted a call for "organized skepticism" to improve the reliability of the environmental marine sciences: *"the scientific community concerned with problems in the marine ecosystem (should) undertake a rigorous and systematic audit of ocean calamities, with*

the aim of assessing their generality, severity, and immediacy. Such an audit of ocean calamities would involve a large contingent of scientists coordinated by a global program that assess ocean health."

What happens to people that speak up against the wrongdoing of the system? They are silenced, expelled, or lose their jobs. In many cases they have to wait until retirement age to speak up. That is why there is a majority of grey heads in this audience.

4. The legal system vs the scientific system

The scientific system is missing an important component. Let us compare it with the quality assurance of the legal system. *The system is set up to guarantee a debate.* In a legal system there will always be a defense mounted against the prosecution. Regardless of how obviously guilty the defendant is. The defendant will be defended, and the case shall be decided by an independent jury.

In the Great Barrier Reef (GBR) or climate science, we have a jury like the Intergovernmental Panel on Climate Change (IPCC). They have been instructed about what they shall find: CO_2 emission has been guilty since the 1992 treaty was signed. All other scientific results must be silenced. In Great Barrier Reef science there is a consensus committee doing this job. They consist of the same people that will act as the prosecutors, "defense", judge and jury. We can have no trust in such a system. It must be changed.

5. A revision is needed

We need more Quality Assurance (QA) than peer review with its 50 % failure rate. We are not careful enough with QA in our sciences. We would not accept to fly airplanes that crash half the time? How can we respect a system that comes up with the wrong answer half the time?

And how did we arrive in this messy situation?

Before 1960, science was mostly done by the military or industry. It was generally well tested before put in use. The bomb must explode - the machine must work. Peer review was supplemented by the ultimate tests. Did it work? Then came the soft sciences and environmental sciences. We got predictions of doom in 30 years with no consequences for the scientists if the prediction turned out to be wrong: DDT, CFC-ozone, climate, diesel particle emission etc. How do we tell they are real? In most cases they turned out to be wrong or exaggerating the effects.

The proposed solution is to establish an Office of Science Quality Assurance (QSQA). Not under the Ministry of Science, but run through the Auditor General's office. They don't know science, but they know the meaning of independency. If a scientist produces junk-science, it should have an effect on the reputation of the scientist.

If there is a replication problem, with wrong results more than half the time, and government bodies follow these results, then it is inevitable there will be major consequences for public policy. The cost for people and environment can be excessive.

6. Conclusions

- The replication crisis was inevitable with a system that uses peer review. One group got control and excluded contradicting views.
- There is a deficiency in our scientific institutions and systems.
- Stop focusing too much on the details of climate science and concentrate on establishing a decent system of replication, checking, and testing the science.
- **Make science work as it should.**

References

Baker, M., 2016.*1,500 scientists lift the lid on reproducibility*. Nature 533**,** 452–454. https://doi.org/10.1038/533452a

Browman, H.I., 2016. *Applying organised scepticism to ocean acidification research***.** ICES J. Mar. Sci. 73:3, 529–536. http://dx.doi.org/10.1093/icesjms/fsw010.

Chalmers, I., Glasziou, P., 2009. *Avoidable waste in the production and reporting of research evidence.* Lancet 374, 86–89.

Duarte, C.M., Fulweiler, R.W., Lovelock, C.E., Martinetto, P., Saunders, M.I., Pandolfi, J.M., Stefan, G., et al., 2015. *Reconsidering ocean calamities.* Bioscience 65, 130–139.

Ioannidis, J.P.A., 2005. *Why most published research findings are false.* PLoS Med. 2:8e124.. Retrieved from. http://www.plosmedicine.org/article/info: https://doi.org/10.1371/journal.pmed.0020124

Ioannidis, J.P.A., 2014**.** *How to make more published research true. PLoS Med.* 11:10.

Prinz, F., Schlange, T., Asadullah, K., 2011. *Believe it or not: how much can we rely on published data on potential drug targets?* Nat. Rev. Drug Discov. 10,712. https://doi.org/10.1038/nrd3439-c1

Wagenmakers, E.J., Wetzels, R., Borsboom, D., van der Maas, H.L.J., Kievit, R.A., 2012. *An agenda for purely confirmatory research*. Perspect. Psychol. Sci. 7, 632–638. https://doi.org/10.1177/1745691612463078

Correspondence to
author@email
Vol. 2.1 (2022)
pp. 101-104

Green Murder book review

Stein Storlie Bergsmark

Independent Scientist, Tvedestrand, Norway

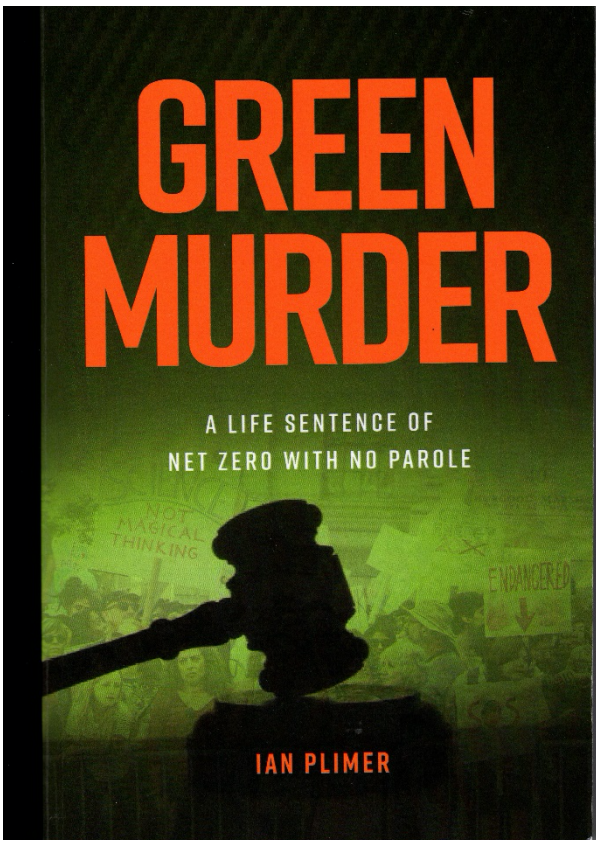

Green Murder
Ian Plimer
ISBN: 9781922449825 https://doi.org/10.53234/scc202203/25
Connor Court Publishing Pth Ltd, 2021

The book's main message is this: It has never been shown that human emission of the gas of life drives global warming. Large bodies of science that don't fit the narrative have been ignored by IPCC, COP and self-interested scientists paid by taxpayers. A huge subsidised industry of intermittent unreliable wind and solar electricity has been created, based on unsubstantiated science. The same hucksters now want subsidised hydrogen, costly inefficient EVs, subsidised mega-batteries and other horribly expensive tried and failed schemes to impoverish people, create unemployment, transfer wealth and enrich China.

Germany, Texas, California and the UK had a glimpse of Net Zero with blackouts, astronomically high electricity costs and hundreds of deaths. These countries once had reliable cheap electricity and now that governments have gone green, we are heading for hard economic times.

In this book the greens are charged with murder. They murder humans who are kept in eternal poverty without coal-fired electricity. They support slavery and early deaths of black child miners. They murder forests and their wildlife by clear felling for mining and wind turbines. They murder forests and wildlife with their bushfire policies. They murder economies producing unemployment, hopelessness, collapse of communities, disrupted social cohesion and suicide.

They murder free speech and freedoms and their takeover of the education system has ended up in the murdering of the intellectual and economic future of young people. They terrify children into mental illness with their apocalyptic death cult lies and exaggerations. They try to divide a nation. They are hypocrites and such angry ignorant people should never touch other people's money.

The greens are guilty of murder. The sentence is life with no parole in a cave in the bush enjoying the benefits of Net Zero.

Dr. Ian Plimer is Australia's best-known geologist. He is emeritus professor of Earth Sciences at the University of Melbourne, and has been serving at several other universities in Australia and Europe. He has many awards and has published more than 100 scientific papers on geology and has written eleven books for the general public. He spent much of his life in the zinc-lead-silver mining town of Broken Hill, Australia, working for North Broken Hill Ltd, and was a consultant to many major mining companies.

Through his new book, he covers all sides of the current climate debate, written in a clear and sharp, sometimes biting style, often in a black and white way. Climate history is covered, as is natural climate catastrophes, faulty climate modelling, temperature homogenization, 'Climategate', climate alarms, climate and energy policies, and the problems with renewables, with examples from Germany, US, France and other countries.

The book is an overwhelming and very useful source of information with its 597 pages and 1667 references. However, there is no index, so it is rather difficult to find the topic you are looking for.

In the introduction, he explains that if the green activists achieve their aims, the Third World will remain in poverty. It was coal that brought people out of grinding poverty and misery in the Industrial Revolution, and later hundreds of millions of Chinese out of crippling poverty. Policies of the greens would reverse such gains.

Abundant cheap reliable energy has solved global problems, it has led to great increase in health, diet, longevity, finances and leisure over the last five generations of humans. But one of the biggest social and human problems in the world today, is that globally, 1,3 billion people don't have access to electricity and 2,7 billion people rely on wood, twigs, leaves and dung for cooking and heating, which causes harmful indoor air pollution and death.

For more than 50 years, green activists made false and failed predictions about the end og the world, famine, health, pollution, sea level rise, ice sheet melting, extinction, global cooling, global warming and population, and they still do. If just one prediction was correct, we would not be here. The greens do not realize or will not admit, that by any measure, we live in the best of times, and not the worst of times. There should be street demonstrations thanking aspirational past generations for grinding through hardship to give us such a wonderful world.

It has never been shown that human emissions of carbon dioxide are the primary driver of global warming. Over the history of time, six of the six great ice ages started when there was more carbon dioxide in the atmosphere than now. Ice core measurements going back almost a million years show that temperature rises 650 to 1600 years before the carbon dioxide in the air rises.

Western countries try hard to cut carbon dioxide emissions. But in 1997, China was granted an exemption from any obligations to reduce emissions under the Kyoto Protocol, like India, on the ground that it was a 'developing nation'. China claims to be a Third World poverty- stricken backwater yet it has nuclear weapons, the world's largest army, the world's second largest economy and has landed rovers on the Moon and on Mars. China builds more coal-fired power than any other country on Earth and remains exempt from the demands of the Paris Agreement. India also has a space program, nuclear weapons and a large army, and builds coal-fired power on a large scale. We have been conned.

Current climate 'science' ignores the scientific method as does climate 'science' peer (or pal) review. 'Consensus' and 'settled science' are terms to enforce green activist and political certainty. These are not words of science. Climate science is not in accord with what is known from the geological past, archaeology, history and experiments. In the past, climate changed due to tectonic, galactic, orbital, solar, ocean and lunar cycles. Past climate changes were not driven by carbon dioxide. Nothing has changed.

The true nature of science is scepticism. Science encourages argument and dissent. Scientific evidence is derived from repeatable and reproducible observation and must be in accord with previous validated evidence. Much climate science research comprises a mathematical and computer model analysis of other peoples' data. In most cases the data cannot be independently validated by the modellers. Data for comparison has been 'homogenized', hence it is no surprise that models and measurements do not agree. Computer models are not evidence.

The greens claim that whatever happens today is unprecedented and can only be due to climate change. This is deliberate deceit. Chronicles of past catastrophic events such as bushfires can be found with a 30-second smartphone search. Green activists knowingly ignore information to pursue political rhetoric.

Drought is normal, the biggest droughts were before industry emitted carbon dioxide, and mega-droughts up to 300 years long changed human history. Floods inundate flood plains which are long-term sediment deposits from large floods. All of which exceeded anything experienced in your life. Modern catastrophic floods are inevitable and are unrelated to human-induced climate change.

A transition to a future running on renewable energy only, is a way to ruin a country. Renewables use concrete, metals, plastics and rare earth elements. Production of these commodities results in massive pollution and more carbon dioxide emitted into the atmosphere than renewables would save.

Coal or gas fired generators emitting carbon dioxide must operate 24/7 as backup for renewables, when the sun does not shine or the wind is not blowing. This results in very little reduction of carbon dioxide emissions. Wind turbines change local weather, change rainfall, destroy bird and bat population, start bushfires, damage human health and don't produce electricity when needed. Turbine blades and solar panels are dumped after their short life, resulting in heavy metals and toxins leaking into the soil, water and air. Forests have been clear felled and food-producing land has been sterilized for wind and solar generation.

Streetwise renewable companies have conned naïve green bureaucrats and politicians with little live experience into long-term subsidies for inefficient, variable and expensive energy production based on weather. Renewable companies are in the business of making money, not saving the environment. Wind and solar energy are not free, they can only survive on generous subsidies and the increased energy costs cripple families, businesses and economies. Electricity prices in the greenest countries have tripled as a result of renewables, money from the poor has been transferred to the rich. The dash to renewables is the biggest financial scam in history. The world's largest emitter China is producing most of the renewable equipment, and is laughing all the way to the bank.

The manufacture and charging of electric vehicles produce up to 28 % more carbon dioxide than for an equivalent diesel vehicle, and the vehicles use far more metal and various minerals than conventional cars. Such vehicles are subsidized and are designed to run off subsidized electricity.

Get rid of subsidies and mandates and let the market do what is does best.